Functional Studies of Candidate Oncogenes in Non-Small Cell Lung Cancer

Functional Studies of Candidate Oncogenes in Non-Small Cell Lung Cancer

A dissertation presented

by

Rachel Grace Liao

to

The Program in Biological Sciences in Public Health

in partial fulfillment of the requirements

for the degree of

Doctor of Philosophy

in the subject of

Biological Sciences in Public Health

Harvard University

Cambridge, Massachusetts

August 2013

Dissertation Advisor: Professor Matthew L. Meyerson Rachel Grace Liao

Functional Studies of Candidate Oncogenes in Non-Small Cell Lung Cancer

ABSTRACT

Cancer is a set of complex genetic diseases driven by diverse genomic alterations. The genomic study of cancer has enabled the discovery of novel, targetable events in almost all cancer types and in turn, has led to the development of new, targeted cancer therapies benefiting patients; however, the recent explosion of genomic datasets has also resulted in huge lists of new oncogenic factors of unknown biological relevance, and uncertainty over how best to use the data appropriately to influence patient care. Some of the most pressing questions surround the use of statistical methods to identify actionable genomic alterations in cancer and the identification of driving oncogenes in the context of the genomic evolution of cancer cells, undergone before, during, and after prolonged treatment regimens.

Few cancers are in greater need of study than non-small cell lung cancer. Lung cancer is responsible for more deaths per year than any other cancer type in both men and women and in up to half of cases of non-small cell lung cancer, no driving alteration is known. Here, we describe approaches to identify new oncogenic targets in lung squamous cell carcinoma that did not rise to the level of statistical significance using standard algorithms but nonetheless represent a promising target for therapy in patients who present with this disease, and secondary drivers that arise when lung squamous cell carcinoma is treated with prolonged exposure to targeted therapy. In addition, we examine a statistically significant alteration in lung adenocarcinoma that did not validate as a likely driver in our functional studies, despite strong computational evidence

suggesting its role as a lung cancer target. These studies together demonstrate both the promise and limitations of *in silico* approaches to target identification in cancer and the need for functional validation of alterations in preclinical models to best inform the development of clinical trials and patient selection for targeted therapy. It is our hope that these studies will contribute to a more complete understanding of the complex use of cancer genome characterization data, as well as improved treatment options for patients who develop non-small cell lung cancer.

TABLE OF CONTENTS

APPENDIX

For Ted, who encourages me.

ACKNOWLEDGEMENTS

I have had a full and rewarding PhD experience, which would not have been possible without the support I received from my advisor, Matthew Meyerson. Not only did Matthew provide the space, resources, and datasets to pursue fascinating translational science, he also never hesitated to send me to conferences to present my work, and he allowed a flexibility of schedule that enabled me to take classes outside of my field and to get involved in student activities and extracurricular programs, both at the Broad Institute and at Harvard. All of these opportunities contributed to my development as a well-rounded and independent scientist.

Many members of Matthew's group have been invaluable resources during my graduate school years, but Peter Hammerman stands out among them. Despite his responsibilities to his own postdoctoral research and his patients, Peter consistently spent his time helping me with experiments and answering my many questions, as well as editing abstracts and manuscript drafts and answering emails with lightning speed. I have been able to accomplish as much as I have, in large part due to Peter's near-daily support.

I would also like to thank the members of my dissertation advisory committee, Dr. Brendan Manning, Dr. Lewis Cantley, and Dr. Marianne Wessling-Resnick. They were an excellent source of advice, ideas and support, and I'm grateful for the time they invested in me for the past three years. I'm also grateful to Drs. Brendan Manning, Zhi-Min Yuan, Wendy Garrett, and Pasi Jänne, for their willingness to serve on my defense committee.

Finally, I especially want to acknowledge my husband Ted, who has been a constant source of support during my PhD years, even while he pursues his own graduate degree. His love and care mean the world to me, and I could not have accomplished this without him.

CHAPTER 1

Introduction

SUMMARY

The completion of the Human Genome Project in 2003 permanently altered the way that disease research was performed. The project, and its counterpart from the Celera Corporation, physically mapped the ~21,000 genes in the human genome and enabled their systematic study for the first time, launching an area of research now formally referred to as the field of genomics. Within a few years, the cost of genome sequencing and characterization precipitously dropped, while at the same time, its speed and accuracy skyrocketed, enabling not only the routine sequencing of the genes and genomes of many people, and of many non-human organisms, but also the systematic genomic characterization of cancer compared to its corresponding normal tissue across populations of patients. The large datasets generated then enabled the use of statistical methods to identify significant events, a subset of which were driving, functional, targetable alterations.

These alterations spurred the development of targeted therapies, far superior to conventional therapies such as chemotherapy and radiation, for appropriately selected tumors in many tumor types. Patients who previously received dismal prognoses were living progression-free for months or years, with minimal side effects. However, as genome characterization became more sensitive to detect alterations, it became clear that many cancers are highly altered, and most alterations are likely non-functional passenger events that simply occur in the course of tumor evolution. Thus it has become necessary to study not just the genomes of cancer, but to evaluate candidate drivers functionally in the lab in order to identify those most likely to respond to targeted therapy. Here, we focus on functional genomic studies in lung adenocarcinoma and lung squamous cell carcinoma, two subtypes accounting for the majority of non-small cell lung cancer diagnoses. We will describe the identification and characterization of functional

candidates in these diseases, as well as clinical successes with targeted therapies and the development of resistance.

BACKGROUND

Lung cancer is a prevalent and deadly disease that accounts for more deaths per year than any other cancer type in both men and women in the United States (1). The most common subtype of lung cancer is non-small cell lung cancer (NSCLC), which accounts for ~85% of lung cancer diagnoses (1). This subtype can be further broken down into categories, lung adenocarcinomas, which are most common, lung squamous cell carcinomas, and large cell carcinomas of the lung (1). NSCLC is widely studied, and genomic analyses of both lung adenocarcinoma and lung squamous cell carcinoma have been undertaken in recent years, resulting simultaneously in an excess of candidate oncogenic events and a dearth of preclinical functional data that might recommend new drug development studies and clinical trials for patients harboring driving, targetable events (2-5). Thus, the functional study of candidate oncogenes, in both academia and industry, has become a sub-field in the study of almost every cancer type, and perhaps none more so than non-small cell lung cancer.

Clinical aspects of non-small cell lung cancer

Behavioral and environmental risk factors

It is well established that cigarette smoking directly causes many non-small cell lung cancers, with one recent study putting the proportion of current or former smokers diagnosed with NSCLC at 85% (6). It has also been demonstrated that second-hand smoke has a small causal role in lung cancer development (7), as does the smoking of pipes or cigars (8). Air

pollution is also correlated with increased development of lung cancer and other lung diseases (9).

Non-smokers who develop lung cancer very frequently develop lung adenocarcinoma (6). These individuals are more likely to be women and more likely to be of East Asian descent (10), and some of the risk has been attributed to frequent use of cooking oil in East Asian cooking (11). Population-based genetic studies have also identified risk loci that increase lung cancer risk irrespective of smoking status (12, 13).

Histology and staging

Lung adenocarcinoma arises peripherally from glands within the lobe of the lung. It tends to grow at a reduced rate compared to other subtypes of lung cancer, which makes it more likely to be diagnosed prior to metastasis, and its external location makes it amenable to surgical removal, particularly if identified early (14). In contrast, squamous cell carcinoma of the lung arises centrally, near the bronchial junction connecting the trachea to the lung. These tumors resemble squamous epithelia, similar to the epithelial layers lining the oral cavity and trachea, but cell of origin is unknown as no squamous epithelia is found in the normal lung. Squamous tumors metastasize more frequently than adenocarcinomas and are less amenable to surgical removal due to their central location in the lungs (15).

Both subtypes are staged using the TNM staging system (16). T indicates the size and spread of the tumor into immediately surrounding tissue. N indicates involvement of lymph nodes, a preliminary identifier of spreading disease, and M indicates metastasis, i.e. whether the tumor has been identified at distant sites (16). As expected, prognosis deteriorates as stages increase.

Conventional therapy

Standard of care for patients presenting with NSCLC varies with stage. For example, patients with T1 or T2 tumors, indicating a smaller tumor size, frequently benefit from surgical resection (17), while larger tumors, indicating more advanced disease, often recommend non-surgical treatment (18, 19). Primary radiation is the most beneficial option for patients with early stage, unresectable disease, and adjuvant chemotherapy is recommended for patients with stage II tumors in addition to surgery (17). Patients with stage III tumors are treated primarily with chemoradiation therapies (18), and for patients with stage IV tumors, treatments ranging from platinum-based chemotherapy regimens to immunotherapy are utilized, recognizing that such advanced tumors are treatable, but no therapy will be curative (19).

Genomics of non-small cell lung cancer

Lung adenocarcinoma

The first recurrent genomic alteration formally identified in lung adenocarcinoma was *KRAS* mutation (20), now known to occur at a 15-20% frequency (21). This remained the only known recurrent driver for more than 15 years, until the identification of *EGFR* mutations by several groups in 2004 (22-24). EGFR events occur preferentially in non-smokers at a rate of ~10% in tumors of Caucasian patients and up to more than half of lung cancer patients of East Asian decent (21). Since the identification of EGFR driving events, many large-scale genomic characterization studies have been performed in lung adenocarcinoma patients (2, 3, 5), enabling identification of many recurrent low-frequency oncogenic alterations such as mutations and amplifications in *ERBB2*, mutations in *BRAF, PIK3CA, AKT1, MEK1,* and *NRAS*, and fusions

and translocations activating *ALK*, *ROS,* and *RET* (21, 25). With the exception of alterations in *PIK3CA*, these events are very frequently found to be mutually exclusive (21).

Beyond kinase drivers, amplified transcription factors have also been implicated in driving lung adenocarcinoma. Predominant among these is *NKX2-1* (26), a lineage-specific transcription factor that directs alveolar development in the lung (27). Other amplified transcription factors include *MYC* (5, 26).

Genomic studies have also identified recurrent events in lung adenocarcinoma that are likely tumor suppressors. The most common alteration in lung adenocarcinoma is missense or nonsense mutation of *TP53* in more than 50% of cases (2, 5). Statistically significant alterations also occur in *CDKN2A/B, RB1, ATM, NF1*, and *U2AF1* in high percentages of tumors (2, 5, 26), demonstrating the frequent co-occurrence of gain-of-function and loss-of-function alterations.

Despite the identification of many driving events in lung adenocarcinoma, almost half of all diagnosed tumors are still considered "oncogene negative"—that is, they express no identified driving event (25). It has also been demonstrated that several receptor tyrosine kinases identified as significantly mutated in genomic studies of lung adenocarcinoma, including *FGFR4, EPHA3, ERBB4, NTRK2,* and *NTRK3*, do not score in assays designed to evaluate oncogenic potential (2, 28), supporting the suggestion that statistics alone are not sufficient to define oncogenic drivers in cancer. Thus, functional studies of alterations identified in genomic characterizations of lung adenocarcinoma are ongoing.

Lung squamous cell carcinoma

The first identification of a driving oncogene in NSCLC was in lung squamous cell carcinoma, when a patient's tumor was found to harbor a KRAS G12C mutation that was not

present in normal tissue (29). A study screening 15 squamous tumors several years later did not identify any *RAS* mutations (20), and it has since been demonstrated that lung squamous tumors rarely mutate *RAS* family members (30).

Genomic characterization in lung squamous cell carcinoma has not experienced the breakthrough discoveries observed in lung adenocarcinoma, such as identification of driving kinases like *EGFR* and *ALK*. The few that were known, such as *SOX2* amplification and *FGFR1* amplification (31-33), had little influence over treatment or prognosis, and with the exception of a case study implicating mutations in *DDR2* as drivers in up to 4% of squamous tumors (34), no kinases were known to be mutated in this disease.

This changed with the publication of research from The Cancer Genome Atlas in 2012 (4). This study identified kinase alterations including amplifications in *EGFR, ERBB2*, and *AKT3*, as well as mutations in *ERBB2-4, JAK2, ABL1, ABL2, MET,* and *FGFR2-3*. Many of these mutations occur in known cancer genes but at novel loci, thus requiring functional characterization in order to determine their contribution to oncogenesis in lung squamous cancers.

The analysis from TCGA also identified many non-kinase alterations in lung squamous cell carcinoma that likely contribute to tumor growth and progression. *TP53* mutation is observed in over 80% of tumors, and events in *CDKN2A, PTEN,* and *RB1* are also significant (4, 35). *SOX2* amplification was confirmed, as was *TP63* amplification, while NOTCH pathway family members were often mutated, indicating a role for squamous differentiation in oncogenesis (4). In as many as 34% of cases, amplifications or mutations were observed in *NFE2L2, KEAP1,* or *CUL3*—three proteins that form a complex to mediate the oxidative stress

response (36). Studies are ongoing to identify how the loss of the oxidative stress response might influence the development or sustain growth of lung squamous cancers.

Targeted therapy and successes with tyrosine kinase inhibitors in NSCLC

In contrast to surgery, radiotherapy, and chemotherapy, targeted therapy is most successful in patients with tumors in which a targetable genomic alteration has been identified and an appropriate clinical inhibitor of that target can be applied (37). For the percentage of patients whose tumors harbor a targetable alteration, these treatments can induce complete, if temporary, responses with minimal side effects in sensitive tumors (37).

In NSCLC, the therapeutic approach most often taken has been to target oncogenic receptor tyrosine kinases (RTKs) with chemical small molecules or monoclonal antibodies (35, 38). This is the case for two approved targeted therapies in lung adenocarcinoma, erlotinib targeting *EGFR* mutations and crizotinib targeting ALK translocations (38, 39). Other inhibitors are in clinical development or have shown promise for clinical development in lung adenocarcinoma, including targeting MAPK pathway genes such as MEK alone or in combination with PI3K inhibitors for *KRAS*-mutant tumors (40, 41), targeting *ROS* fusions (42), and targeting *ERBB2* mutations (28).

In lung squamous cell carcinoma, aside from the unexpected case study of *DDR2*-mutant tumors (34), no therapies targeting a known prognostic factor have shown benefit to patients; however, treatment with monoclonal antibody cetuximab in combination with chemotherapy did improve survival compared to chemotherapy alone (43). With the completion of the TCGA analysis, many more targets have been identified. Several of these targets have shown promise as targets in preclinical studies (4, 33, 35, 44, 45).

A visualization of observed NSCLC alterations for which inhibitors are already approved or in clinical development is presented in Figure 1-1 for lung adenocarcinoma and lung squamous cell carcinoma. It is the hope of this author that functional genomic validation will demonstrate that many putative drivers in these diseases are targetable using these and other targeted therapies.

Inhibitor resistance

It is an unfortunate fact, however, that a subset of tumors expressing demonstrated targetable events will not respond to targeted therapy, and even tumors that respond will eventually acquire resistance (46, 47). It is expected that any kinase targets in lung cancer will follow this universal trend, and it is of great clinical interest to study resistance in this context in order to improve quality of life and time to progression for patients diagnosed with this aggressive disease.

Resistance mediated by mutation of the original target kinase

Resistance to kinase inhibition generally arises in one of two ways. First, in the case of kinase inhibitors considered "ATP-competitive," i.e., inhibitors that bind to the ATP-binding pocket of the kinase domain, resistance can arise via mutation within the exonic sequence encoding the ATP-binding pocket such that the mutant protein product renders therapy ineffective (48, 49). This sort of mutation, colloquially referred to as the "gatekeeper" mutation, can arise especially in response to Type 1 kinase inhibitors, which are designed to bind to the active conformation of the kinase (48). Gatekeeper mutations have been identified that confer resistance in patient tumors in response to approved therapies for chronic myeloid leukemia

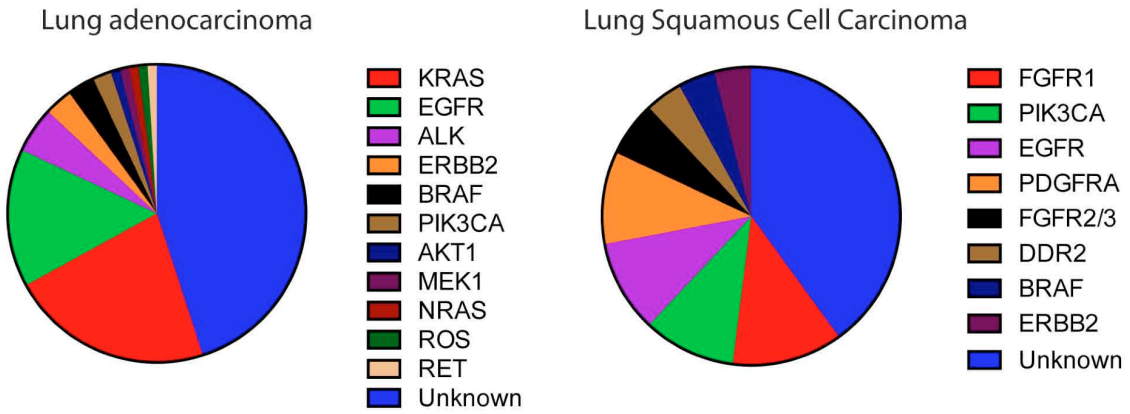

Figure 1-1. Genomic characterization identifies putative targetable alterations in non-small cell lung cancer.

Putative oncogenic drivers for which targeted therapies are available have been described in more than half of NSCLC cases. Approximate percentages of tumors observed with alterations in each potential target are shown for lung adenocarcinoma (left panel, adapted from (25)) and lung squamous cell carcinoma (right panel, adapted from (35)).

(CML) driven by the BCR-ABL translocation (50) and in some EGFR-driven lung adenocarcinomas (51), among others. In the case of CML, second line therapies designed to overcome gatekeeper-mediated resistance have been successful in the clinic (52, 53), and similar strides are being made against gatekeeper-mutated lung cancers driven by EGFR (54).

Not all kinases develop gatekeeper mutations in response to targeted therapy. A notable example is BRAF-driven melanoma, for which resistant gatekeeper mutants can be generated in the laboratory (55), but where extensive efforts to identify such mutations in clinical disease have failed to detect gatekeeper mutations when acquired resistance arises (56, 57). It therefore cannot be assumed *a priori* that kinases targeted by Type 1 kinase inhibitors will develop gatekeeper mutations to mediate acquired resistance.

Resistance mediated by alteration of a parallel effector to the original target kinase

The second common mechanism of resistance is the activation of another molecule whose signaling can replace or augment that of the original driving kinase. This is often accomplished through amplification, mutation, or other methods of activation of a kinase that can drive a signaling network parallel to that of the original target.

Amplification of a second factor as an acquired resistance response is observed in a subset of *EGFR*-mutant tumors that have developed resistance to EGFR inhibitors by amplification of *MET* and co-activation of ErbB3 in both lung adenocarcinoma and colorectal carcinoma (58, 59). In both cancer types, preclinical models and clinical tumors exhibiting this genotype respond to MET targeted therapy, suggesting that targeting resistance mechanisms driven by a secondary molecule might be a promising second-line strategy (58, 60).

Resistance driven by secondary mutation has been described to mediate acquired resistance in clinical samples of *BRAF*-mutant melanomas resistant to BRAF inhibitors by *NRAS* mutation (56). This is of particular interest because *NRAS* mutation is also identified as a primary driver of melanoma, indicating that it can contribute to the disease both as an original oncogenic factor as well as a mechanism of acquired resistance after BRAF inhibition (61). Melanomas driven by primary or acquired *NRAS* mutation have been targeted with inhibitors of downstream mitogen-activated protein kinase (MAPK) pathway signaling molecules such as MEK1, with some success (62).

Conclusions and context for the current work

With the generation of genomic datasets and suggestions of novel, targetable alterations, more validation of putative genomic targets is required for the treatment of non-small cell lung cancer. In the following work, we describe the successful characterization of oncogenic mutations in fibroblast growth factor receptors 2 and 3 (*FGFR2* and *FGFR3*) identified in genome sequencing data from lung squamous cell carcinoma, as well as their sensitivity to therapies targeting FGFR family members. We go on to describe acquired resistance that arises in fibroblast growth factor receptor 1 (*FGFR1*)-amplified lung squamous cell carcinoma after treatment with FGFR inhibitors that are currently seeing responses in patients enrolled in clinical trials. Finally, we demonstrate the necessity of functional characterization of statistically significant genomic alterations prior to their development as therapeutic targets with the preliminary characterization of *EphA3* mutations identified in lung adenocarcinoma genome sequencing data, which were not found to promote gain-of-function oncogenesis upon functional inquiry.

REFERENCES

1. Jemal A, Siegel R, Xu J, Ward E. Cancer statistics, 2010. CA Cancer J Clin. 2010;60(5):277-300.

2. Ding L, Getz G, Wheeler DA, Mardis ER, McLellan MD, Cibulskis K, et al. Somatic mutations affect key pathways in lung adenocarcinoma. Nature. 2008;455(7216):1069-75. PMCID: 2694412.

3. Govindan R, Ding L, Griffith M, Subramanian J, Dees ND, Kanchi KL, et al. Genomic landscape of non-small cell lung cancer in smokers and never-smokers. Cell. 2012;150(6):1121-34. PMCID: 3656590.

4. Hammerman PS, Lawrence MS, Voet D, Jing R, Cibulskis K, Sivachenko A, et al. Comprehensive genomic characterization of squamous cell lung cancers. Nature. 2012.

5. Imielinski M, Berger AH, Hammerman PS, Hernandez B, Pugh TJ, Hodis E, et al. Mapping the hallmarks of lung adenocarcinoma with massively parallel sequencing. Cell. 2012;150(6):1107-20. PMCID: 3557932.

6. Yang P, Allen MS, Aubry MC, Wampfler JA, Marks RS, Edell ES, et al. Clinical features of 5,628 primary lung cancer patients: experience at Mayo Clinic from 1997 to 2003. Chest. 2005;128(1):452-62.

7. Hackshaw AK, Law MR, Wald NJ. The accumulated evidence on lung cancer and environmental tobacco smoke. BMJ. 1997;315(7114):980-8. PMCID: 2127653.

8. Henley SJ, Thun MJ, Chao A, Calle EE. Association between exclusive pipe smoking and mortality from cancer and other diseases. J Natl Cancer Inst. 2004;96(11):853-61.

9. Vineis P, Husgafvel-Pursiainen K. Air pollution and cancer: biomarker studies in human populations. Carcinogenesis. 2005;26(11):1846-55.

10. Sun S, Schiller JH, Gazdar AF. Lung cancer in never smokers--a different disease. Nat Rev Cancer. 2007;7(10):778-90.

11. Ko YC, Cheng LS, Lee CH, Huang JJ, Huang MS, Kao EL, et al. Chinese food cooking and lung cancer in women nonsmokers. Am J Epidemiol. 2000;151(2):140-7.

12. Hung RJ, Boffetta P, Brockmoller J, Butkiewicz D, Cascorbi I, Clapper ML, et al. CYP1A1 and GSTM1 genetic polymorphisms and lung cancer risk in Caucasian non-smokers: a pooled analysis. Carcinogenesis. 2003;24(5):875-82.

13. Raimondi S, Boffetta P, Anttila S, Brockmoller J, Butkiewicz D, Cascorbi I, et al. Metabolic gene polymorphisms and lung cancer risk in non-smokers. An update of the GSEC study. Mutation research. 2005;592(1-2):45-57.

14. Harpole DH, Jr., Herndon JE, 2nd, Young WG, Jr., Wolfe WG, Sabiston DC, Jr. Stage I nonsmall cell lung cancer. A multivariate analysis of treatment methods and patterns of recurrence. Cancer. 1995;76(5):787-96.

15. Robinson LA, Ruckdeschel JC, Wagner H, Jr., Stevens CW. Treatment of non-small cell lung cancer-stage IIIA: ACCP evidence-based clinical practice guidelines (2nd edition). Chest. 2007;132(3 Suppl):243S-65S.

16. Detterbeck FC, Boffa DJ, Tanoue LT. The new lung cancer staging system. Chest. 2009;136(1):260-71.

17. Howington JA, Blum MG, Chang AC, Balekian AA, Murthy SC. Treatment of stage I and II non-small cell lung cancer: Diagnosis and management of lung cancer, 3rd ed: American College of Chest Physicians evidence-based clinical practice guidelines. Chest. 2013;143(5 Suppl):e278S-313S.

18. Ramnath N, Dilling TJ, Harris LJ, Kim AW, Michaud GC, Balekian AA, et al. Treatment of stage III non-small cell lung cancer: Diagnosis and management of lung cancer, 3rd ed: American College of Chest Physicians evidence-based clinical practice guidelines. Chest. 2013;143(5 Suppl):e314S-40S.

19. Socinski MA, Evans T, Gettinger S, Hensing TA, Sequist LV, Ireland B, et al. Treatment of stage IV non-small cell lung cancer: Diagnosis and management of lung cancer, 3rd ed: American College of Chest Physicians evidence-based clinical practice guidelines. Chest. 2013;143(5 Suppl):e341S-68S.

20. Rodenhuis S, van de Wetering ML, Mooi WJ, Evers SG, van Zandwijk N, Bos JL. Mutational activation of the K-ras oncogene. A possible pathogenetic factor in adenocarcinoma of the lung. The New England journal of medicine. 1987;317(15):929-35.

21. Pao W, Girard N. New driver mutations in non-small-cell lung cancer. Lancet Oncol. 2011;12(2):175-80.

22. Lynch TJ, Bell DW, Sordella R, Gurubhagavatula S, Okimoto RA, Brannigan BW, et al. Activating mutations in the epidermal growth factor receptor underlying responsiveness of non-small-cell lung cancer to gefitinib. The New England journal of medicine. 2004;350(21):2129-39.

23. Paez JG, Janne PA, Lee JC, Tracy S, Greulich H, Gabriel S, et al. EGFR mutations in lung cancer: correlation with clinical response to gefitinib therapy. Science. 2004;304(5676):1497-500.

24. Pao W, Miller V, Zakowski M, Doherty J, Politi K, Sarkaria I, et al. EGF receptor gene mutations are common in lung cancers from "never smokers" and are associated with sensitivity of tumors to gefitinib and erlotinib. Proceedings of the National Academy of Sciences of the United States of America. 2004;101(36):13306-11. PMCID: 516528.

25. Pao W, Hutchinson KE. Chipping away at the lung cancer genome. Nat Med. 2012;18(3):349-51.

26. Weir BA, Woo MS, Getz G, Perner S, Ding L, Beroukhim R, et al. Characterizing the cancer genome in lung adenocarcinoma. Nature. 2007;450(7171):893-8. PMCID: 2538683.

27. Ikeda K, Clark JC, Shaw-White JR, Stahlman MT, Boutell CJ, Whitsett JA. Gene structure and expression of human thyroid transcription factor-1 in respiratory epithelial cells. The Journal of biological chemistry. 1995;270(14):8108-14.

28. Greulich H, Kaplan B, Mertins P, Chen TH, Tanaka KE, Yun CH, et al. Functional analysis of receptor tyrosine kinase mutations in lung cancer identifies oncogenic extracellular domain mutations of ERBB2. Proceedings of the National Academy of Sciences of the United States of America. 2012;109(36):14476-81.

29. Santos E, Martin-Zanca D, Reddy EP, Pierotti MA, Della Porta G, Barbacid M. Malignant activation of a K-ras oncogene in lung carcinoma but not in normal tissue of the same patient. Science. 1984;223(4637):661-4.

30. Riely GJ, Marks J, Pao W. KRAS mutations in non-small cell lung cancer. Proc Am Thorac Soc. 2009;6(2):201-5.

31. Bass AJ, Watanabe H, Mermel CH, Yu S, Perner S, Verhaak RG, et al. SOX2 is an amplified lineage-survival oncogene in lung and esophageal squamous cell carcinomas. Nat Genet. 2009;41(11):1238-42. PMCID: 2783775.

32. Dutt A, Ramos AH, Hammerman PS, Mermel C, Cho J, Sharifnia T, et al. Inhibitor-sensitive FGFR1 amplification in human non-small cell lung cancer. PLoS ONE. 2011;6(6):e20351. PMCID: 3110189.

33. Weiss J, Sos ML, Seidel D, Peifer M, Zander T, Heuckmann JM, et al. Frequent and focal FGFR1 amplification associates with therapeutically tractable FGFR1 dependency in squamous cell lung cancer. Science translational medicine. 2010;2(62):62ra93.

34. Hammerman PS, Sos ML, Ramos AH, Xu C, Dutt A, Zhou W, et al. Mutations in the DDR2 kinase gene identify a novel therapeutic target in squamous cell lung cancer. Cancer discovery. 2011;1(1):78-89. PMCID: 3274752.

35. Liao RG WH, Meyerson M & Hammerman PS. Targeted therapy for squamous cell lung cancer. Lung Cancer Management. 2012;1(4):293-300.

36. Thimmulappa RK, Mai KH, Srisuma S, Kensler TW, Yamamoto M, Biswal S. Identification of Nrf2-regulated genes induced by the chemopreventive agent sulforaphane by oligonucleotide microarray. Cancer Res. 2002;62(18):5196-203.

37. Stegmeier F, Warmuth M, Sellers WR, Dorsch M. Targeted cancer therapies in the twenty-first century: lessons from imatinib. Clin Pharmacol Ther. 2010;87(5):543-52.

38. Janku F, Stewart DJ, Kurzrock R. Targeted therapy in non-small-cell lung cancer--is it becoming a reality? Nat Rev Clin Oncol. 2010;7(7):401-14.

39. Gandhi L, Janne PA. Crizotinib for ALK-rearranged non-small cell lung cancer: a new targeted therapy for a new target. Clinical cancer research : an official journal of the American Association for Cancer Research. 2012;18(14):3737-42.

40. Mahoney CL, Choudhury B, Davies H, Edkins S, Greenman C, Haaften G, et al. LKB1/KRAS mutant lung cancers constitute a genetic subset of NSCLC with increased sensitivity to MAPK and mTOR signalling inhibition. British journal of cancer. 2009;100(2):370-5. PMCID: 2634725.

41. Engelman JA, Chen L, Tan X, Crosby K, Guimaraes AR, Upadhyay R, et al. Effective use of PI3K and MEK inhibitors to treat mutant Kras G12D and PIK3CA H1047R murine lung cancers. Nat Med. 2008;14(12):1351-6. PMCID: 2683415.

42. Bergethon K, Shaw AT, Ou SH, Katayama R, Lovly CM, McDonald NT, et al. ROS1 rearrangements define a unique molecular class of lung cancers. Journal of clinical oncology : official journal of the American Society of Clinical Oncology. 2012;30(8):863-70. PMCID: 3295572.

43. Pirker R, Pereira JR, Szczesna A, von Pawel J, Krzakowski M, Ramlau R, et al. Cetuximab plus chemotherapy in patients with advanced non-small-cell lung cancer (FLEX): an open-label randomised phase III trial. Lancet. 2009;373(9674):1525-31.

44. Guagnano V, Kauffmann A, Wohrle S, Stamm C, Ito M, Barys L, et al. FGFR genetic alterations predict for sensitivity to NVP-BGJ398, a selective pan-FGFR inhibitor. Cancer discovery. 2012;2(12):1118-33.

45. Liao RG, Jung J, Tchaicha JH, Wilkerson MD, Sivachenko A, Beauchamp EM, et al. Inhibitor-sensitive FGFR2 and FGFR3 mutations in lung squamous cell carcinoma. Cancer Res. 2013.

46. Hammerman PS, Janne PA, Johnson BE. Resistance to Epidermal Growth Factor Receptor Tyrosine Kinase Inhibitors in Non-Small Cell Lung Cancer. Clinical cancer research : an official journal of the American Association for Cancer Research. 2009;15(24):7502-9.

47. Ellis LM, Hicklin DJ. Resistance to Targeted Therapies: Refining Anticancer Therapy in the Era of Molecular Oncology. Clinical cancer research : an official journal of the American Association for Cancer Research. 2009;15(24):7471-8.

48. Zhang J, Yang PL, Gray NS. Targeting cancer with small molecule kinase inhibitors. Nat Rev Cancer. 2009;9(1):28-39.

49. Carter TA, Wodicka LM, Shah NP, Velasco AM, Fabian MA, Treiber DK, et al. Inhibition of drug-resistant mutants of ABL, KIT, and EGF receptor kinases. Proceedings

of the National Academy of Sciences of the United States of America. 2005;102(31):11011-6. PMCID: 1180625.

50. Gorre ME, Mohammed M, Ellwood K, Hsu N, Paquette R, Rao PN, et al. Clinical resistance to STI-571 cancer therapy caused by BCR-ABL gene mutation or amplification. Science. 2001;293(5531):876-80.

51. Balak MN, Gong Y, Riely GJ, Somwar R, Li AR, Zakowski MF, et al. Novel D761Y and common secondary T790M mutations in epidermal growth factor receptor-mutant lung adenocarcinomas with acquired resistance to kinase inhibitors. Clinical cancer research : an official journal of the American Association for Cancer Research. 2006;12(21):6494-501.

52. Shah NP, Tran C, Lee FY, Chen P, Norris D, Sawyers CL. Overriding imatinib resistance with a novel ABL kinase inhibitor. Science. 2004;305(5682):399-401.

53. O'Hare T, Shakespeare WC, Zhu X, Eide CA, Rivera VM, Wang F, et al. AP24534, a pan-BCR-ABL inhibitor for chronic myeloid leukemia, potently inhibits the T315I mutant and overcomes mutation-based resistance. Cancer cell. 2009;16(5):401-12. PMCID: 2804470.

54. Engelman JA, Zejnullahu K, Gale CM, Lifshits E, Gonzales AJ, Shimamura T, et al. PF00299804, an irreversible pan-ERBB inhibitor, is effective in lung cancer models with EGFR and ERBB2 mutations that are resistant to gefitinib. Cancer Res. 2007;67(24):11924-32.

55. Whittaker S, Kirk R, Hayward R, Zambon A, Viros A, Cantarino N, et al. Gatekeeper mutations mediate resistance to BRAF-targeted therapies. Science translational medicine. 2010;2(35):35ra41.

56. Nazarian R, Shi H, Wang Q, Kong X, Koya RC, Lee H, et al. Melanomas acquire resistance to B-RAF(V600E) inhibition by RTK or N-RAS upregulation. Nature. 2010;468(7326):973-7. PMCID: 3143360.

57. Wagle N, Emery C, Berger MF, Davis MJ, Sawyer A, Pochanard P, et al. Dissecting therapeutic resistance to RAF inhibition in melanoma by tumor genomic profiling. Journal of clinical oncology : official journal of the American Society of Clinical Oncology. 2011;29(22):3085-96. PMCID: 3157968.

58. Bardelli A, Corso S, Bertotti A, Hobor S, Valtorta E, Siravegna G, et al. Amplification of the MET Receptor Drives Resistance to Anti-EGFR Therapies in Colorectal Cancer. Cancer discovery. 2013;3(6):658-73.

59. Engelman JA, Zejnullahu K, Mitsudomi T, Song Y, Hyland C, Park JO, et al. MET amplification leads to gefitinib resistance in lung cancer by activating ERBB3 signaling. Science. 2007;316(5827):1039-43.

60. Robinson KW, Sandler AB. The role of MET receptor tyrosine kinase in non-small cell lung cancer and clinical development of targeted anti-MET agents. Oncologist. 2013;18(2):115-22. PMCID: 3579594.

61. van 't Veer LJ, Burgering BM, Versteeg R, Boot AJ, Ruiter DJ, Osanto S, et al. N-ras mutations in human cutaneous melanoma from sun-exposed body sites. Molecular and cellular biology. 1989;9(7):3114-6. PMCID: 362784.

62. Ascierto PA, Schadendorf D, Berking C, Agarwala SS, van Herpen CM, Queirolo P, et al. MEK162 for patients with advanced melanoma harbouring NRAS or Val600 BRAF mutations: a non-randomised, open-label phase 2 study. Lancet Oncol. 2013;14(3):249-56.

CHAPTER 2

Inhibitor-sensitive FGFR2 and FGFR3 mutations in lung squamous cell carcinoma

Adapted from:

Rachel G. Liao[1,2], Joonil Jung[2,*], Jeremy Tchaicha[1,*], Matthew D. Wilkerson[3,*], Andrey Sivachenko[2], Ellen M. Beauchamp[1], Qingsong Liu[4], Trevor J. Pugh[1,2], Chandra Sekhar Pedamallu[1,2], D. Neil Hayes[3], Nathanael S. Gray[4], Gad Getz[2], Kwok-Kin Wong[1], Robert I. Haddad[1], Matthew Meyerson[1,2], and Peter S. Hammerman[1,2]. (2013). Inhibitor-sensitive FGFR2 and FGFR3 mutations in lung squamous cell carcinoma. *Cancer Res* 73(16): 5195-205.

[1]Department of Medical Oncology, Dana-Farber Cancer Institute, Boston, MA 02115

[2]The Broad Institute of Harvard and MIT, Cambridge, MA 02142

[3]Lineberger Comprehensive Cancer Center, University of North Carolina at Chapel Hill, Chapel Hill, NC 27599

[4]Department of Biological Chemistry and Molecular Pharmacology, Dana-Farber Cancer Institute, Boston, MA 02115

[*]These authors contributed equally

ATTRIBUTIONS

All experiments and analyses were performed by Rachel G. Liao except as follows:

Analysis in Figure 2-2 was performed by Matthew D. Wilkerson.

Analysis in Figure 2-3 was performed by Trevor J. Pugh.

Experiments and analysis in Figure 2-4B and 2-4C were performed by Jeremy H. Tchaicha.

Analysis in Figure 2-10B was performed by Joonil Jung and Chandra Sekhar Pedamallu.

Images in Figure 2-10C were obtained from Robert I. Haddad.

Chapter 2. Inhibitor-sensitive FGFR2 and FGFR3 mutations in lung squamous cell carcinoma

SUMMARY

A comprehensive description of genomic alterations in lung squamous cell carcinoma (lung SqCC) has recently been reported, enabling the identification of genomic events that potentially contribute to the oncogenesis of this disease. In lung SqCC, one of the most frequently altered receptor tyrosine kinase families is the fibroblast growth factor receptor (FGFR) family, with amplification or mutation observed in all four family members. Here, we describe the oncogenic nature of mutations observed in *FGFR2* and *FGFR3*, which are each observed in 3% of samples, for a mutation rate of 6% across both genes. Using cell culture and xenograft models, we show that several of these mutations drive cellular transformation. Transformation can be reversed by several small molecule FGFR inhibitors currently being developed for clinical use. We also show that mutations in the extracellular domains of *FGFR2* lead to constitutive FGFR dimerization. Additionally, we report a patient with an *FGFR2*-mutated oral squamous cell carcinoma who responded to the multi-targeted tyrosine kinase inhibitor pazopanib. These findings provide new insights into driving oncogenic events in a subset of lung squamous cancers, and recommend future clinical studies with FGFR inhibitors in patients with lung and head and neck SqCC.

BACKGROUND

Two goals of comprehensive next-generation sequencing studies of human cancers are to discover novel somatic alterations that can be targeted therapeutically and to identify new targets in cancers for which targeted therapies are already available. Genome-scale analyses of large cohorts of tumors representing many cancer types, including lung cancer, have been recently

completed (1-6), enabling the discovery of previously undetectable novel genomic alterations and identification of novel areas for application of targeted therapeutics.

Historically, targetable oncogenic alterations in cancer were discovered on an individual gene basis due to the prior inability to perform genome-scale analysis. This was the case for cancer-causing alterations observed in several tyrosine kinases, including *EGFR* and *ALK* in lung adenocarcinoma (7-9), *BRAF* in melanoma (10), *FGFR2* in endometrial carcinoma (11, 12), and *FGFR3* in urothelial carcinoma (13). These studies and others informed the global understanding of cancer genetics prior to the current genomics era and have led to several demonstrations of the successful application of targeted therapeutic agents and their superiority to conventional chemotherapy (14, 15). These studies have nominated a core set of somatic alterations which drive a fraction of cancers and thus have enabled prioritization of mutated genes from next-generation sequencing datasets for study as therapeutic targets.

Lung squamous cell carcinoma (lung SqCC) is a prevalent and deadly disease for which few targets are known and no targeted therapies are approved. Recent data reported by The Cancer Genome Atlas (TCGA) lung SqCC project ((4), tcga-data.nci.nih.gov/ and https://tcga-data.nci.nih.gov/docs/publications/lusc_2012/) demonstrated that the Fibroblast Growth Factor Receptor (FGFR) tyrosine kinases are one of the most frequently altered tyrosine kinase families in this disease. Amplification of *FGFR1* was observed, a finding in agreement with prior reports that identified focal amplification of *FGFR1* in approximately 10-20% of lung SqCC samples and demonstrated that *FGFR1* amplification is associated with *FGFR1* dependency in a subset of lung cancer cell lines (16, 17). Furthermore, mutations in all four *FGFR* kinases, and in particular *FGFR2* and *FGFR3,* were reported. While the frequency of these *FGFR* mutations did not reach statistical significance for enrichment at the cohort size examined by TCGA, several

features including recurrence, prior observation in other cancer types and congenital syndromes, and lack of other dominant oncogenic alterations in tumors with *FGFR* mutations, suggested they might be driving, targetable events in a subset of patients presenting with this disease.

Mutations in the FGFR tyrosine kinase family were described in human disease prior to being implicated in cancer, specifically in craniofacial and skeletal syndromes (18). Somatic point mutations identical to these germline events have also been observed in malignancies (19), confirming the importance of genomic alterations to this family in both germline and somatic disease. The FGFR family is made up of four active members and one member (FGFR5) without kinase activity, which is posited to be a negative regulator of the signaling pathway. FGFR1-4 each contain an extracellular domain (ECD) made up of two or three IG-like domains and a cytoplasmic kinase domain. Activation is stimulated by binding fibroblast growth factor (FGF) and heparan sulfate proteoglycan (HSPG) in the ECD, and subsequent dimerization of two receptor-ligand complexes, leading to transphosphorylation of the kinase domains of both receptors in the dimer. This leads to phosphorylation of intracellular binding partner FRS2 and downstream activation of Ras/MAPK and PI3K/AKT pathways, among others (20).

Alternative splicing regulates FGFR signaling through differential use of exons that alter the binding specificity of the third IG-like domain for its preferred FGF ligand. The FGF family is made up of more than 20 members, all of which retain specificities for both different FGFR family members and different transcript isoforms of each receptor (21). In addition, tissue types vary in which receptors, isoforms, and ligands are expressed, adding further levels of regulation and complexity to the system—and dysregulation can lead to oncogenesis, as has been shown with altered expression of receptors (16, 17, 22), altered isoform expression (23, 24), and altered ligand specificity (25) driven by somatic genomic events.

Aberrant FGFR signaling has been implicated in the development of several cancer types. In addition to lung SqCC, *FGFR1* amplification is observed in 10% of breast cancers (22) and risk alleles in *FGFR2* have been identified in genome-wide association studies of breast cancer patients (26). Oncogenic point mutations in *FGFR2* are observed in 12% of endometrial carcinomas (11) and mutations in *FGFR3* are observed in more than 30% of urothelial carcinomas (13). Furthermore, in multiple myeloma, t(4:14) translocations frequently fuse the IgH locus with *FGFR3*, resulting in an active overexpressed FGFR3 kinase domain, and in a subset of cases, FGFR3 also acquires an activating kinase domain mutation, rendering it an even more potent oncogene (27, 28). Cell lines harboring these events have demonstrated sensitivity to inhibition by FGFR small molecule inhibitors, and some clinical trials have begun to test FGFR inhibitors in patient populations harboring mutations or amplification of *FGFR* family members (19).

Here, we characterize *FGFR2* and *FGFR3* mutations observed in lung SqCC sequencing data and demonstrate the ability of these mutations to drive oncogenic proliferation using models of both transformation and dependency, thus establishing their role as putative oncogenes. We also demonstrate that cells harboring these mutations are sensitive to inhibition by several clinically relevant FGFR-specific and multi-kinase inhibitors. In addition, we report a first case of a patient with an *FGFR2*-mutated squamous cell carcinoma of the tongue, and who responded to pazopanib, an inhibitor of multiple tyrosine kinases, including the FGFR family. Together, these data identify a promising new therapeutic target for patients with lung SqCC and other squamous epithelial tumors.

RESULTS

FGFR2 and FGFR3 are recurrently mutated in lung squamous cell carcinoma

We analyzed solution-based hybrid capture (whole-exome sequencing) data generated by The Cancer Genome Atlas ((4), https://tcga-data.nci.nih.gov/docs/publications/lusc_2012/) for mutations in the *FGFR2* and *FGFR3* genes. We identified 5 *FGFR2* and 6 *FGFR3* mutations in analysis of exome sequencing data of 178 tumor/normal pairs, as well as an *FGFR2* K660N mutation in a sample that was excluded from the TCGA report due to poor RNA quality (TCGA-21-1083), for a total of 12 mutations. This number is slightly higher than the prevalence reported by the TCGA Network in the discussion of potential therapeutic targets because the TCGA restricted reporting of mutations to those detected by both exome and RNA sequencing of a given tumor. We also queried the data from the targeted hybrid-capture validation sequencing to identify *FGFR2* or *FGFR3* mutations that may have been missed in the original exome sequencing.

Patients in the reported TCGA cohort with *FGFR* mutations (n=10, as one subject had two *FGFR* mutations) ranged from 58 to 81 years old with a median age of 73. All patients were current or former smokers with a pack year history of 9 to 63 pack years (median 49). Tumors were obtained from resected specimens with a T stage of 1 (n=3) or 2 (n=7) and N stage of 0 (n=8) or 1 (n=2). More extensive patient data are available in Table 2-1 and complete data are available for download from the TCGA.

The observed mutations fell in both the extracellular domain and kinase domains of FGFR2 and FGFR3, and in codons in which mutations have been previously reported in endometrial carcinoma (11, 12) and urothelial carcinoma (13), and also at novel residues (Figure 2-1). In the samples containing *FGFR2* or *FGFR3* mutations, the IIIb isoforms of each protein were overexpressed compared to the IIIc isoforms (Figure 2-2) *FGFR* kinase alterations were

Table 2-1. Clinical characteristics of patients whose lung squamous tumors harbored *FGFR2* or *FGFR3* mutations.

Tumor ID	Sex	Age at diagnosis	T stage	N stage	M stage	Smoking Status	Pack years	FGFR2 Mutation	FGFR3 Mutation	Expression Subtype
LUSC-18-3419	MALE	73	T2	N1	M0	Current reformed smoker for < or = 15 years	50		p.S249C	Basal
LUSC-60-2710	FEMALE	67	T1	N1	M0	Current reformed smoker for < or = 15 years	63	p.W290C		Classical
LUSC-21-5782	FEMALE	68	T2	N0	M0	Current reformed smoker for < or = 15 years	48	p.T787K		Basal
LUSC-34-2600	FEMALE	76	T1	N0	M0	Current reformed smoker for < or = 15 years	50	p.S320C	p.S249C	Basal
LUSC-66-2780	MALE	65	T2	N0	M0	Current reformed smoker for > 15 years	28	p.K660N		Basal
LUSC-22-5482	MALE	81	T2a	N0	M0	Current reformed smoker for < or = 15 years	60	p.E471Q		Classical
LUSC-22-5485	FEMALE	58	T1a	N0	M0	Current smoker	60		p.S435C	Classical
LUSC-66-2770	MALE	79	T2	N0	M0	Current reformed smoker for > 15 years	25		p.S249C	Classical
LUSC-21-1078	MALE	77	T2	N0	M0	Current reformed smoker for < or = 15 years	9		p.R248C	Primitive
LUSC-51-4079	FEMALE	73	T2	N0	N/A	Current reformed smoker for < or = 15 years	25		p.K717M	Classical

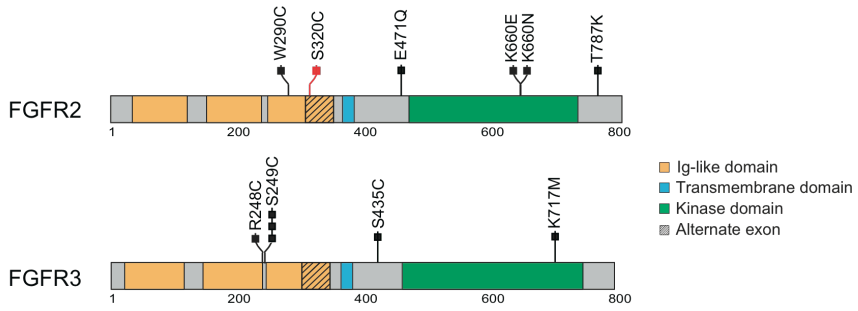

Figure 2-1. Recurrent mutations in FGFR2 and FGFR3 are observed in lung squamous cell carcinoma.

Sequencing data from The Cancer Genome Atlas (TCGA) Research Network were analyzed and recurrent missense mutations were observed along the length of the FGFR2 and FGFR3 proteins. The mutation S320C in FGFR2, in red, is located in the alternatively spliced exon in the IG-3 domain of FGFR2 IIIb; the remaining mutations are annotated to the IIIc isoform. FGFR3 mutations were tested in the IIIc isoform only; all annotations refer to that isoform.

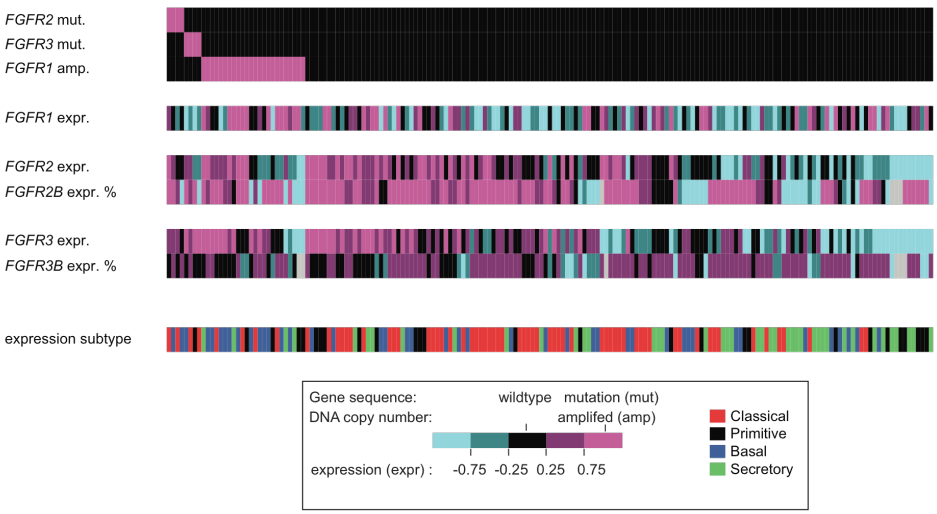

Figure 2-2. Integrated display of *FGFR* kinase alterations in the 178 lung squamous cell carcinomas reported by the TCGA Network.

Tumor samples are represented by columns and the presence of *FGFR1* amplification or *FGFR2* or *FGFR3* mutation is depicted by the shading. For each of the *FGFR* genes, relative expression is displayed. Transcript isoform usage is displayed for *FGFR2* and *FGFR3,* with higher values (pink shading) favoring expression of the IIIb isoforms. Expression subtypes as previously described (29) are shown as the bottom track. Abbreviations: mut, mutations; amp, amplified; expr, expression.

significantly enriched in the basal expression subtype (29) when compared to samples without *FGFR* kinase alteration (Fisher's Exact test on FGFR alteration and subtype; P=0.016) (Figure 2-2).

FGFR mutations co-occured with likely activating mutations in known oncogenes in three cases. LUSC-21-1078 had a high somatic mutation rate and harbored mutations in *HRAS* at codon 61 and *PDGFRA* at codon 842, both previously reported to be sites of oncogenic mutation, as well as a novel *ERBB2* E1021Q mutation (Figure 2-3). LUSC-21-1078 contained a non-canonical *KRAS* mutation G118S and LUSC-21-5485 had a previously unreported *ERBB2* mutation G1075V. *FGFR2* and *FGFR3* mutations commonly co-occurred with mutations in *TP53* (8/10) and *PIK3CA* (3/10), the latter a gene with mutations that commonly co-occur with driving oncogenes. Four of ten samples with *FGFR* mutation harbored 3q amplification of *SOX2* and two samples *CDKN2A* homozygous deletion (Figure 2-3).

FGFR2 and FGFR3 mutations drive anchorage-independent growth of NIH-3T3 cells

FGFR2 and FGFR3 mutations can promote transformation in cellular model systems (11, 27, 30). To determine whether the mutations identified in lung SqCC were oncogenic, we established NIH-3T3 cells which stably expressed each mutation to assess for anchorage-independent growth in soft agar, a commonly used cellular assay to determine the oncogenic potential of a transgene. NIH-3T3 cells stably expressing each *FGFR2* or *FGFR3* transgene were seeded in soft agar in triplicate. After three weeks, we observed colony formation in cells expressing the majority of observed FGFR2 and FGFR3 mutations (Figure 2-4A). We determined that extracellular domain mutations W290C and S320C in FGFR2, and R248C and S249C in FGFR3, significantly increased colony formation compared to wild type FGFR2 or

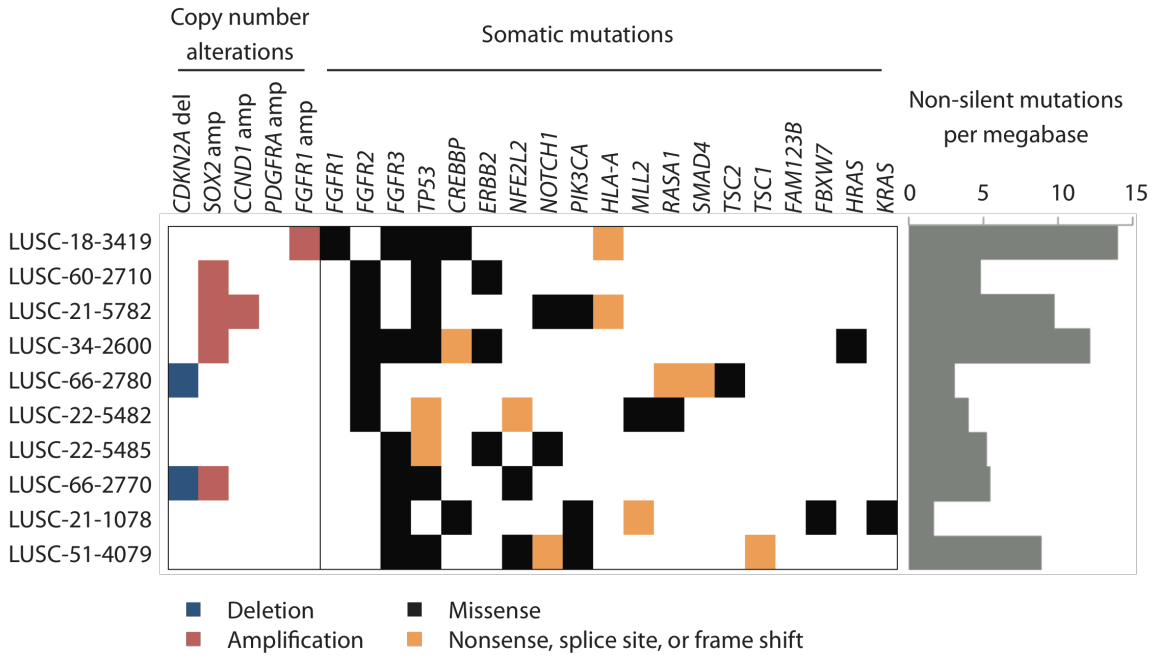

Figure 2-3. Lung squamous cell carcinoma tumors with mutations in FGFR2 or FGFR3 do not commonly co-occur with other genomic alterations, except *TP53* mutation.

TCGA samples containing FGFR2 and FGFR3 mutations underwent analysis for co-occurring somatic copy number alterations and mutations. FGFR mutations overwhelmingly co-occurred with *TP53* mutations; otherwise no obvious other recurrently co-occurring mutated genes were observed. In the left panel of SCNA events, blue indicates deletions and red indicates amplifications. In the right panel of somatic mutations, black indicates a missense point mutation and orange indicates a predicted loss-of-function nonsense, splice site, or frameshift mutation.

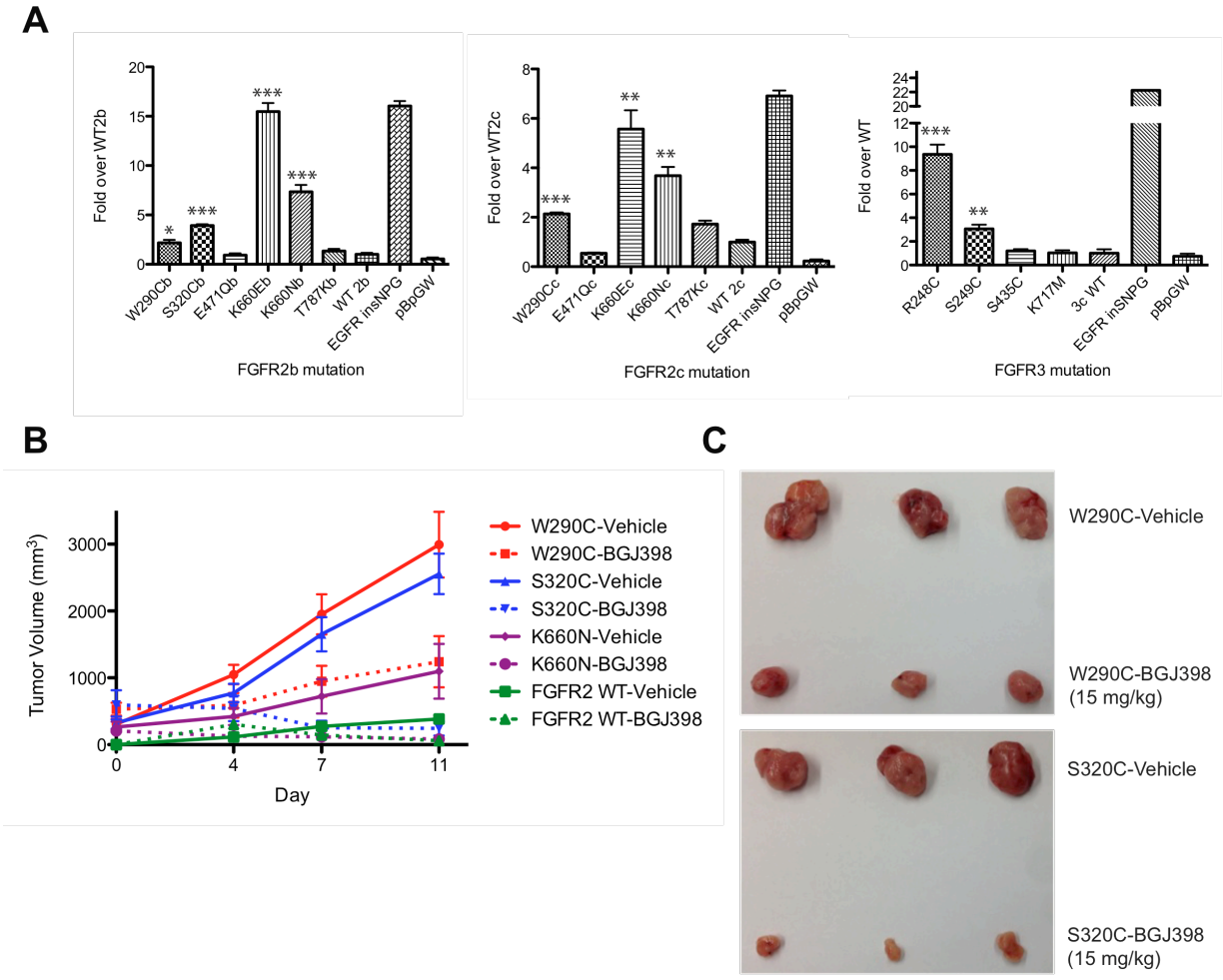

Figure 2-4. A subset of lung SqCC mutations in FGFR2 and FGFR3 are transforming in anchorage independent growth assays and xenograft assays.

(A) NIH-3T3 cells stably expressing each mutation were seeded into Select agar in triplicate at a density of 50,000 cells per well. After three weeks, each well was photographed and cells were counted. The colony formation compared to wild type was calculated for each isoform and graphed. EGFR insNPG was included as a positive control, and the pBabe-puro Gateway empty vector was included as a negative control (pBp GW). P-values were calculated with the student's t-test and significance is indicated by asterisks; * < 0.05, ** < 0.01, *** < 0.001.

Figure 2-4 continued

(B) Nude mice injected with transforming FGFR2 mutant cells from (A) developed tumors, which were then treated with BGJ398 (dashed lines) or vehicle (solid lines).

(C) Tumors were dissected from the mice for visual inspection comparing treatment with vehicle or drug. Top panel, FGFR2-W290C tumors; bottom panel, FGFR2-S320C.

FGFR3, as did kinase domain mutations K660E and K660N in *FGFR2* ($p<0.05$ by Student's t-test). In contrast, FGFR2 mutations E471Q and T787K, and FGFR3 mutations S435C and K717M did not form colonies above wild type. There was also no colony formation observed in cells expressing the empty vector, while robust formation of colonies was observed in NIH-3T3 cells expressing an activating *EGFR* insertion mutation, as expected. *FGFR2* mutations were generated in both common isoforms of *FGFR2* with similar results obtained for all assayed mutations with the exception of *FGFR2* T787K, which was very modestly transforming only in isoform IIIc (Figure 2-4A).

FGFR2 and FGFR3 mutations drive tumor formation in xenograft models

A second model of transformation was employed for ECD FGFR2 mutations due to the novelty of their characterization. NIH-3T3 cells expressing transforming FGFR2 mutations or wild type were injected into nude mice. Tumors had reached approximately 200-300 mm^3 in all mice injected with mutant cells by day 13 to begin treatment with a pan-FGFR inhibitor, BGJ398, or vehicle, with ECD mutations driving particularly strong tumor formation (Figure 2-4B, solid lines). Tumors formed by cells expressing wild type FGFR2 grew more slowly, and began treatment on day 16 (Figure 2-4B). We posit that this tumor formation in the presence of overexpressed wild type receptor may be due to the presence of ligand in the tumor stroma sufficient to activate the WT receptor.

Tumors treated with BGJ398 slowed or reversed their growth compared to vehicle (Figure 2-4B, dashed lines), so that by the end of the study, tumor burden in vehicle-treated versus BGJ398-treated mice was noticeably distinct (Figure 2-4C).

Extracellular domain mutations form ligand sensitive intermolecular disulfide bonds

A common mechanism of activation of the FGFR2 and FGFR3 kinases is through the formation of covalently bound receptor dimers (30, 31). This has been also observed in other receptor tyrosine kinases (RTKs), including members of the ErbB family (32). While wild type RTKs maintain precise extracellular structure required for ligand binding and receptor dimerization through the formation of intramolecular disulfide bonds, mutant receptors can form intermolecular disulfide dimers due through a novel cysteine residue created by the mutation itself, or through instability created by a mutated residue near a structural intramolecular disulfide bond (31). Indeed, this mechanism was previously established for the transforming *FGFR3* mutations that we have observed in lung SqCC, R248C and S249C (30).

To assess whether mutations in the extracellular domain of FGFR2 and FGFR3 lead to increased dimerization, and whether these covalent bonds could be increased by ligand stimulation, we serum starved cells in the presence of PBS for eight hours, 5 nM FGF1 and 2 μg/mL heparin for eight hours, or 5 nM FGF1 and 2 μg/mL heparin for 30 minutes, followed by washing with PBS and serum starving in the presence of PBS for the remaining 7.5 hours. Cells were lysed and we performed electrophoresis in both reducing and non-reducing conditions followed by immunoblotting for FGFR2 and FGFR3. FGFR2 ECD mutations were sufficient to drive covalent dimerization in the absence of ligand, but dimerization was increased in the presence of even 30 minutes of ligand stimulation (Figure 2-5A). In FGFR3 mutations, on the other hand, dimerization was observed but not increased under ligand-stimulation conditions compared to PBS (Figure 2-5B). As has been demonstrated previously (33), FGFR proteins typically form highly glycosylated folded protein products. While FGFR2 W290C appears to

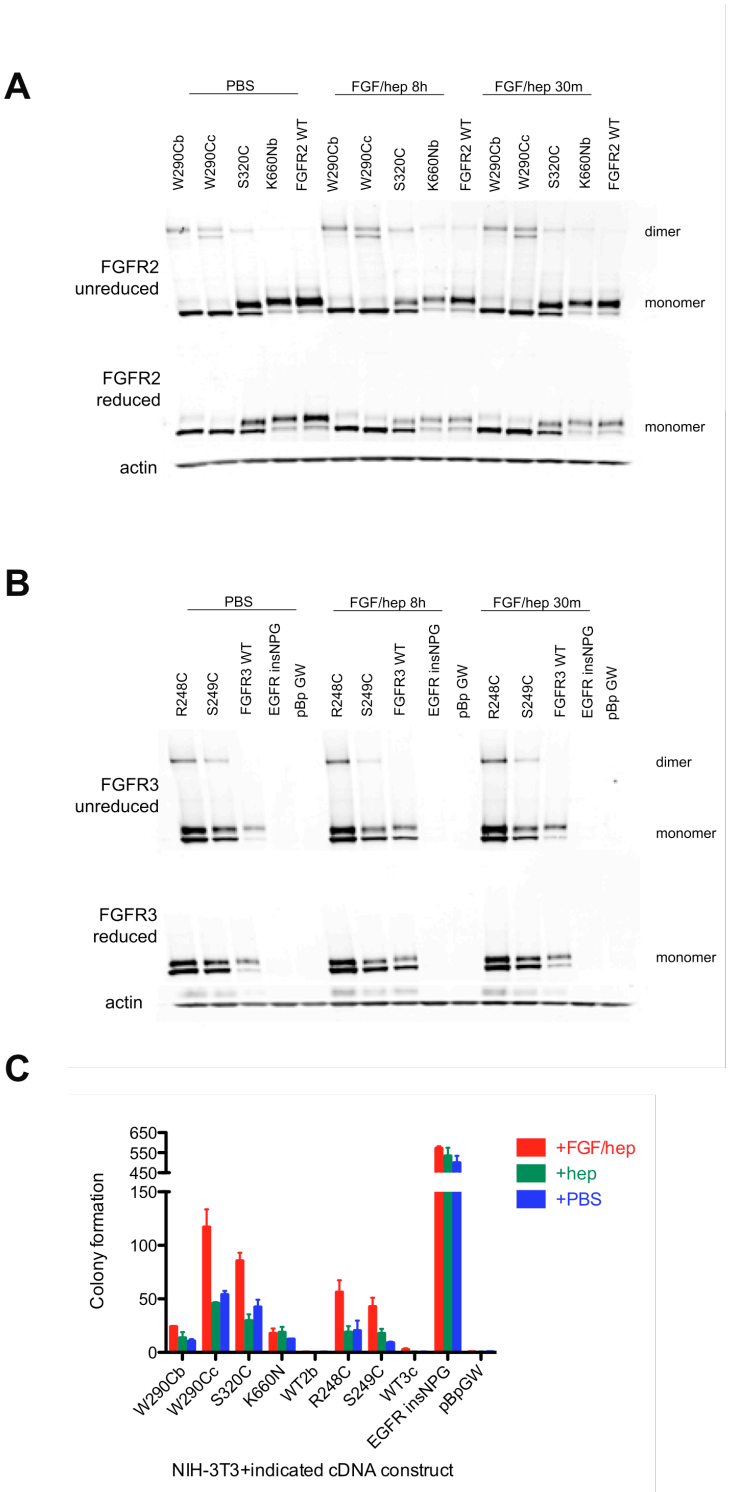

Figure 2-5. Mutations in the extracellular domains of FGFR2 and FGFR3 form covalent dimers in the absence of ligand, but are sensitive to ligand stimulation.

Figure 2-5 continued

(A) & (B) NIH-3T3 cells expressing the indicated point mutations in FGFR2 (A) or FGFR3 (B) were serum starved and stimulated with PBS or FGF1 and heparin for 8 hours, or with FGF1 and heparin for 30 minutes, washed, and then with PBS for 7.5 hours. Unreduced and reduced lysates were probed for the formation of covalently bonded receptor-dimers. Dimers formed by cells expressing FGFR2 mutations and visualized by immunoblot, could be increased by the addition of ligand (A). For cells expressing mutations in FGFR3, dimer formation was not changed when visualized by immunoblot (B) (30).

(C) Cells from (A) and (B) were seeded into Select agar as in Figure 2-4A in the presence of PBS (+PBS), heparin alone (+hep), or FGF1 and heparin (+FGF/hep) and colonies were counted after three weeks. In both FGFR2- and FGFR3-expressing cells, extracellular domain mutations segregated with increased colony formation response in the presence of FGF1 and heparin, while controls were unchanged.

undergo a glycosylation defect contributing to its lower molecular weight, this mutant form still retains the capacity to dimerize.

We then seeded the same cells into soft agar in the presence of PBS, 2 μg/mL heparin alone, or 5 nM FGF1 and 2 μg/mL heparin. After three weeks, we observed greater colony formation in response to FGF1 and heparin treatment than in heparin alone or PBS treated cells (Figure 2-5C).

FGFR2 and FGFR3-driven cellular transformation is blocked by clinically relevant FGFR inhibitors

Having established that *FGFR2* and *FGFR3* mutations in lung SqCC drive anchorage-independent growth in NIH-3T3 cells, we next asked whether this transformation could be blocked by small molecule inhibitors of FGFRs currently in clinical development. NIH-3T3 cells expressing each mutation were again seeded into soft agar in the presence or absence of the multi-kinase inhibitor AP24534 (ponatinib) (34). Ponatinib targets imatinib-resistant BCR-ABL harboring the T315I mutation in chronic myeloid leukemia (34), and has activity against FGFR family members (35). We observed that colony formation was inhibited in the presence of ponatinib in cells harboring activating *FGFR2* or *FGFR3* mutations, but not in cells harboring an activating EGFR insertion mutation (Figure 2-6A, left panel). Cells expressing different mutations demonstrated differential sensitivity to ponatinib. All extracellular domain mutations in FGFR2 and S249C in FGFR3 lost colony forming potential when exposed to 100 nM of drug, whereas kinase domain mutations lost colony formation potential at 10 nM of drug. Exceptions were FGFR2 K660E expressed in the IIIc isoform, which behaved similarly to the FGFR2 ECD mutations, and FGFR3 R248C, which had a ten-fold higher inhibitory concentration than any

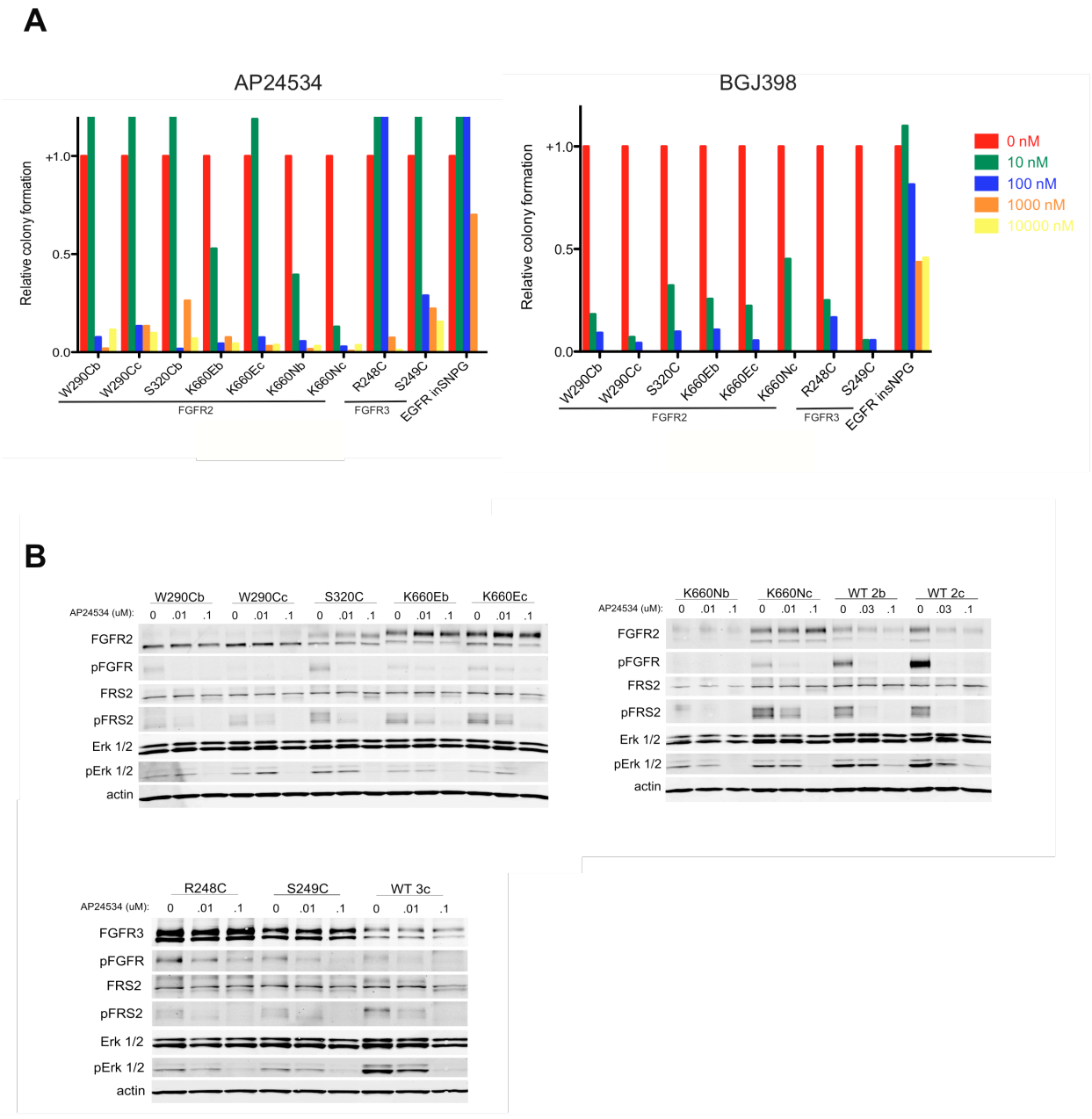

Figure 2-6. Anchorage independent colony formation and downstream signaling are abrogated in the presence of anti-FGFR inhibitors.

(A) NIH-3T3 cells expressing each transforming mutation were seeded into Select agar as in Figure 2-4A, in the presence of increasing concentrations of ponatinib (AP24534) (left panel) and BJG398 (right panel), and similar analysis was performed. For ponatinib, different mutation

Figure 2-6 continued

constructs, and also different isoforms, as in the case of K660E, exhibited a loss of colony formation on the order of 10-100 nM drug, except for FGFR3 R248C, which lost colony formation at 1 μM drug. All mutations were inhibited to greater than 50% of the DMSO control at 10 nM of drug for BGJ398.

(B) Cells were serum starved and exposed to the indicated concentrations of ponatinib for four hours and ligand stimulated for 30 minutes with FGF1, after which cells were lysed and probed for known downstream signaling molecules via immunoblot. Phosphorylation is lost by 100 nM drug in all cases except pFGFR in FGFR3-R248C-expressing cells, an observation consistent with the results of the colony formation assay in (A).

other mutation, at 1 μM. By comparison, colony formation driven by EGFR was not lost until cells were exposed to 10 μM of drug.

To determine whether ponatinib was targeting and inhibiting colony formation driven by mutant *FGFR2* and *FGFR3*, we assessed phosphorylation of several proteins in the FGFR signaling pathway by immunoblotting. As expected, levels of phospho-FGFR, phospho-FRS2, and phospho-Erk all decreased in response to increasing concentrations of ponatinib (Figure 2-6B), suggesting that colony formation was lost due to a decrease in FGFR-mediated signaling.

In order to evaluate whether ponatinib was acting by specific inhibition of FGFR kinases, and also to explore cellular response to several clinically relevant FGFR inhibitors, the NIH-3T3 assays were also performed with BGJ398, a selective FGFR kinase inhibitor (36) as well as pazopanib (GW786034) (37) and dovitinib (TKI-258) (38), two multi-kinase inhibitors with specificity for FGFR family members. Colony formation was inhibited by at least 50% in the presence of 10 nM BGJ398 for all cells expressing *FGFR* mutations, while cells expressing the activating EGFR insertion did not lose the capacity for colony formation until 1 μM BGJ398 (Figure 2-6A, right panel), and wild type phosphorylation was lost at 10 nM under ligand stimulation conditions (Figure 2-7A). Dovitinib also inhibited colony formation in cells expressing mutant FGFR compared to activated EGFR, but with less uniformity across mutations. FGFR2 ECD mutations lost 50% colony formation between 100 nM and 1 μM dovitinib. In contrast, colony formation was inhibited by 50% between 10 nM and 100 nM for FGFR2 kinase domain mutations excluding K660E IIIc, which behaved similar to the FGFR2 ECD mutations. Cells expressing FGFR3 R248C and S249C were sensitive between 10 nM and 100 nM. Again, cells transformed by mutant EGFR did not lose colony formation until exposed to 10μM drug (Figure 2-7B, left panel). Mutant EGFR-expressing cells had sustained

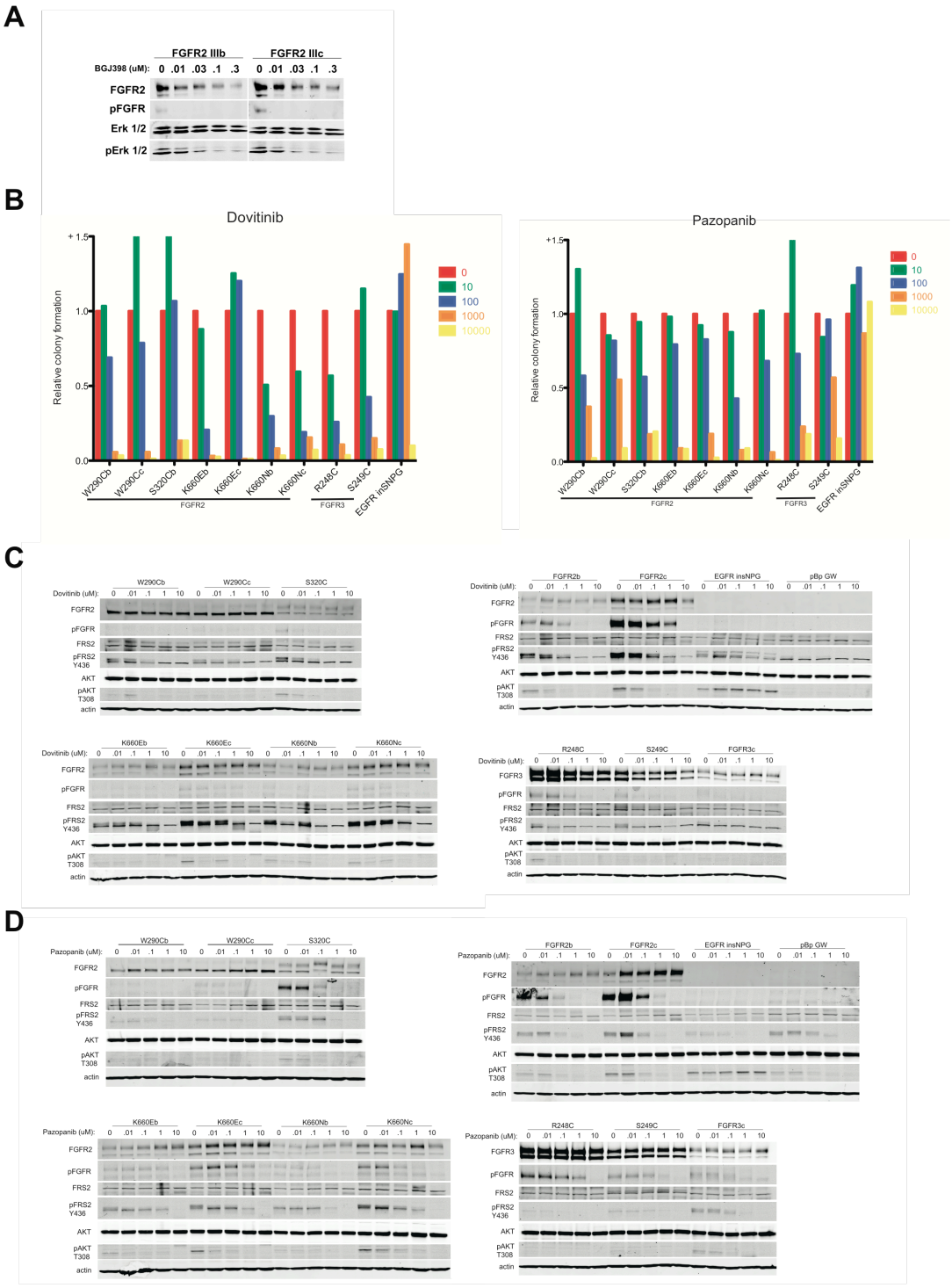

Figure 2-7. Anchorage independent colony formation and downstream signaling are abrogated in the presence of anti-FGFR inhibitors. These experiments were performed similarly to those documented in Figure 2-6.

Figure 2-7 continued

(A) NIH-3T3 cells expressing FGFR2 IIIb or IIIc wild type were serum starved in indicated concentrations of BGJ398 overnight and then stimulated with FGF1 and heparin for 30 minutes prior to lysis. FGFR-dependent phosphorylation decreased in the presence of BGJ398 as concentrations increased.

(B) NIH-3T3 cells expressing each transforming mutation were seeded into Select agar as in Figure 2-4A, in the presence of increasing concentrations of dovitinib (left panel) or pazopanib (right panel), and resulting colonies were quantified. Dovitinib demonstrated a trend similar to ponatinib, in which the extracellular domain FGFR2 and FGFR3 mutations were inhibited to 50% of control at 100-1000 nM, while kinase domain mutations lost colony formation at 10-100 nM drug except for K660E IIIc, which resembled the ECD mutational response. Pazopanib was somewhat less potent in the inhibition of colony formation due to FGFR mutations, with colony formation being inhibited to 50% of DMSO control at 100-1000 nM drug.

(C) & (D) Cells were serum starved and exposed to indicated concentrations of dovitinib (C) or pazopanib (D) for four hours and then ligand stimulated for 30 minutes with FGF1, after which cells were lysed and probed for known downstream phosphorylated signaling molecules via immunoblot. FGFR-dependent phosphorylation decreased in the presence of inhibitors as concentrations increased.

phosphorylation at AKT T308 up to 10μM dovitinib, as detected by immunoblot, while detectable AKT phosphorylation was lost by 100 nM to 1 μM dovitinib in cells expressing *FGFR* mutations (Figure 2-7C). Pazopanib similarly inhibited colony formation in cells expressing all FGFR2 and FGFR3 mutations at concentrations of 100 nM-1 μM drug, while cells expressing mutant EGFR formed colonies even in the presence of 10 μM drug (Figure 2-7B, right panel). Consistently, biochemical studies revealed sustained AKT T308 phosphorylation in mutant EGFR cells exposed to 10 μM pazopanib, while detectable AKT T308 phosphorylation was lost in mutant FGFR cells at 100 nM to 1μM pazopanib (Figure 2-7D).

In NIH-3T3 cells expressing the extracellular domain mutations of both *FGFR2* and *FGFR3* and in the kinase domain mutation *FGFR2* K660E IIIc, we observed that low concentrations of ponatinib (10 nM) conferred a growth promoting phenotype above control, which was abrogated at higher concentrations of drug (Figure 2-6A, left panel). We believe that this could be due to the multi-kinase inhibitory properties of ponatinib, which may inhibit a second kinase that could impact FGFR2 or FGFR3 signaling. This phenomenon was also observed when these experiments were performed with the two other multi-kinase inhibitors with anti-FGFR activity, pazopanib and dovitinib (Figure 2-7B), but not with BGJ398, a more selective FGFR kinase inhibitor (Figure 2-6A, right panel).

Analysis of FGFR2 and FGFR3 inhibition in IL-3 independent Ba/F3 cells

The Ba/F3 cell system is a useful *in vitro* model to assess oncogenic dependency. Expression of a transforming oncogene in this system and subsequent depletion of interleukin-3 (IL-3), on which the parental cells depend, results in cellular dependency on ongoing activity of the oncogene. To test whether cellular transformation driven by mutated *FGFR2* could be

abrogated in a second system by small molecule FGFR inhibitors and to test the relative efficacy of these compounds, we generated Ba/F3 cells expressing the *FGFR2* mutations that had demonstrated significant colony formation in the NIH-3T3 anchorage-independence assay. These cell lines were dependent on FGFR signaling in the presence of FGF and heparin, and in the absence of IL-3. Phosphorylation of the FGFR kinase domain and FRS2 were measured by immunoblot, and interestingly, cells expressing FGFR2 K660E IIIc showed a greater degree of phosphorylation of both molecules despite similar expression levels as compared to cells expressing other mutations (Figure 2-8A).

Ba/F3 cells expressing wild-type and mutated *FGFR2* transgenes were first seeded into media containing increasing concentrations of ponatinib in quadruplicate. We observed that ponatinib inhibited IL-3 independent proliferation of Ba/F3 cells expressing the FGFR mutations at about 10 nM of drug treatment, but cells expressing an EGFR activating insertion or parental Ba/F3 cells grown in the presence of IL-3 were only inhibited by 10 μM of drug (Figure 2-8B, left panel). IC_{50} values for Ba/F3 cells expressing each mutant were also calculated and plotted (Figure 2-8C, left panel). These assays were also performed on cells seeded into media containing BGJ398, and similarly, cells expressing FGFR mutations, but not the EGFR insertion or parental Ba/F3 cells, were inhibited at about 10 nM inhibitory concentrations of drug (Figure 2-8B, right panel and Figure 2-8C, right panel). Interestingly, insensitive controls in the presence of ponatinib appeared to gain a growth advantage in the presence of drug at concentrations in the range of 10-100 nM (Figure 2-8B), similar to our observations in the anchorage independence colony formation assay (Figure 2-6A, Figure 2-7B).

To further assess the potency of small molecule FGFR kinase inhibitors in the Ba/F3 system, we assembled a panel of FGFR kinase inhibitors described in the literature (Table 2-2)

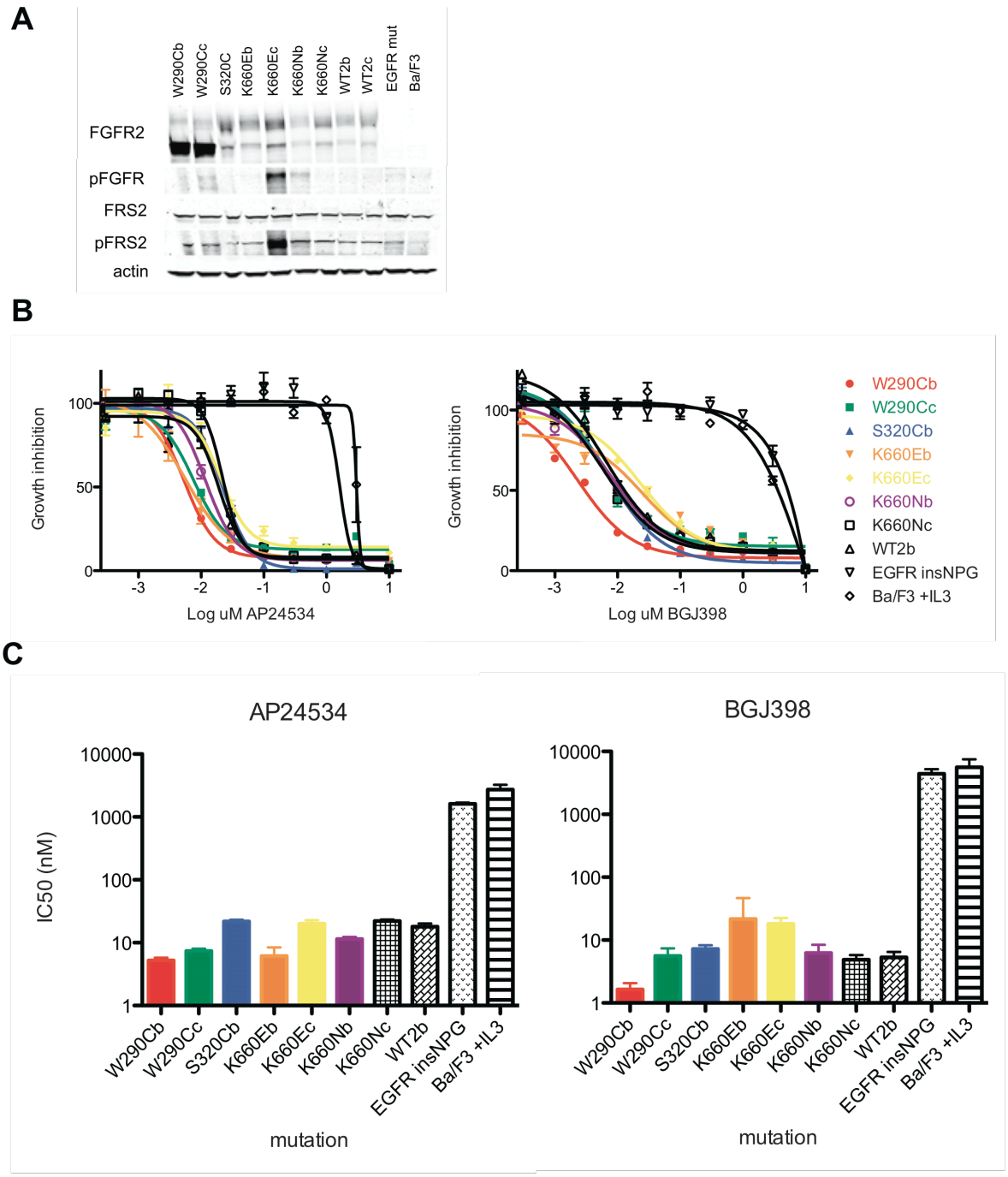

Figure 2-8. Ba/F3 cells that are dependent on FGFR2 and FGFR3 signaling are sensitive to FGFR inhibitors.

(A) Ba/F3 cells that expressed each transforming mutation were generated in the presence of IL-3, and cells dependent on FGFR signaling were isolated by exchanging IL-3 with FGF-7 or FGF-

Figure 2-8 continued

9 and heparin. These cells were lysed and probed for FGFR2 or FGFR3 expression, phospho-FGFR, FRS2, and phospho-FRS2 Y436. Actin was used as a loading control.

(B) Ba/F3 cells expressing each mutation construct were seeded into 96-well plates at a density of 5,000 cells per well, in the presence of increasing concentrations of ponatinib (left panel) or BGJ398 (right panel). After four days, proliferation was measured by adding Cell Titer Glo and assaying resulting luminescence.

(C) Individual IC_{50} values were calculated for each mutation and plotted on a log scale.

Table 2-2. Clinically relevant kinase inhibitors with activity against FGFR family members assembled for this study.

Name	Alt name	Company	Selected known targets	Reference
TKI-258	Dovitinib	Novartis	VEGFR, PDGFR, FGFRs, FLT3, KIT	38
BGJ-398		Novartis	FGFRs	36
BMS-582664	Brivanib	BMS	VEGFR, FGFRs	42
AP24534	Ponatinib	Ariad	BCR-ABL, KIT, VEGFR2, FGFR1	34, 35
E7080		Eisei	VEGFR, PDGFR, FGFRs	40
AZD2171	Cediranib	Astra Zeneca	VEGFR, FGFRs, KIT	41
AZD4547		Astra Zeneca	FGFRs	39
Pazopanib	Votrient	GSK	VEGFR, PDGFR, c-Kit	37

and tested the Ba/F3 inhibitory response in the presence of each, as with ponatinib and BGJ398. The panel included one inhibitor specific to the kinase domain of the FGFR family, AZD4547 (39), and five multi-kinase inhibitors with FGFR inhibitory potential: E7080 (40), pazopanib, dovitinib, cediranib (AZD2171) (41), and brivanib alaninate (42). Each of these inhibitors demonstrated similar trends to those seen for ponatinib and BGJ398: a multi-log increase in drug sensitivity in cells expressing FGFR mutations compared to controls (Figure 2-9). IC_{50} values for each mutation in the presence of each drug were also calculated (Figure 2-9). Strikingly, *FGFR2* K660E expressed in the IIIc isoform (in yellow) repeatedly exhibited a 5-10 fold higher IC_{50} concentrations as compared to the IIIb isoform and either isoform of the K660N mutation in the FGFR2 kinase domain (Figure 2-9). This observation was consistent with the concentrations at which anchorage independent growth observed for FGFR2 K660E IIIc was lost in the presence of several inhibitors (Figure 2-6A and Figure 2-7B).

Case report of a head and neck SqCC patient who responded to an FGFR inhibitor

We recently identified an individual with squamous cell carcinoma of the head and neck who was found to harbor a known oncogenic extracellular *FGFR2* mutation (p.P253R) in a biopsy specimen (Figure 2-10A). This mutation was initially identified in RNA sequencing data from the tumor and then confirmed by Sanger sequencing in a CLIA-certified laboratory (Figure 2-10B). *FGFR2* mutations have previously been observed at low frequencies in head and neck cancer (43, 44), and confirmed by initial reports from the TCGA for head and neck squamous cell carcinoma, where seven mutations were observed in exome sequencing data of 279 individuals as of October 1, 2012 (data obtained from the TCGA Data Coordinating Center; https://tcga-data.nci.nih.gov/tcga/). FGFR2 P253R has previously been observed in endometrial

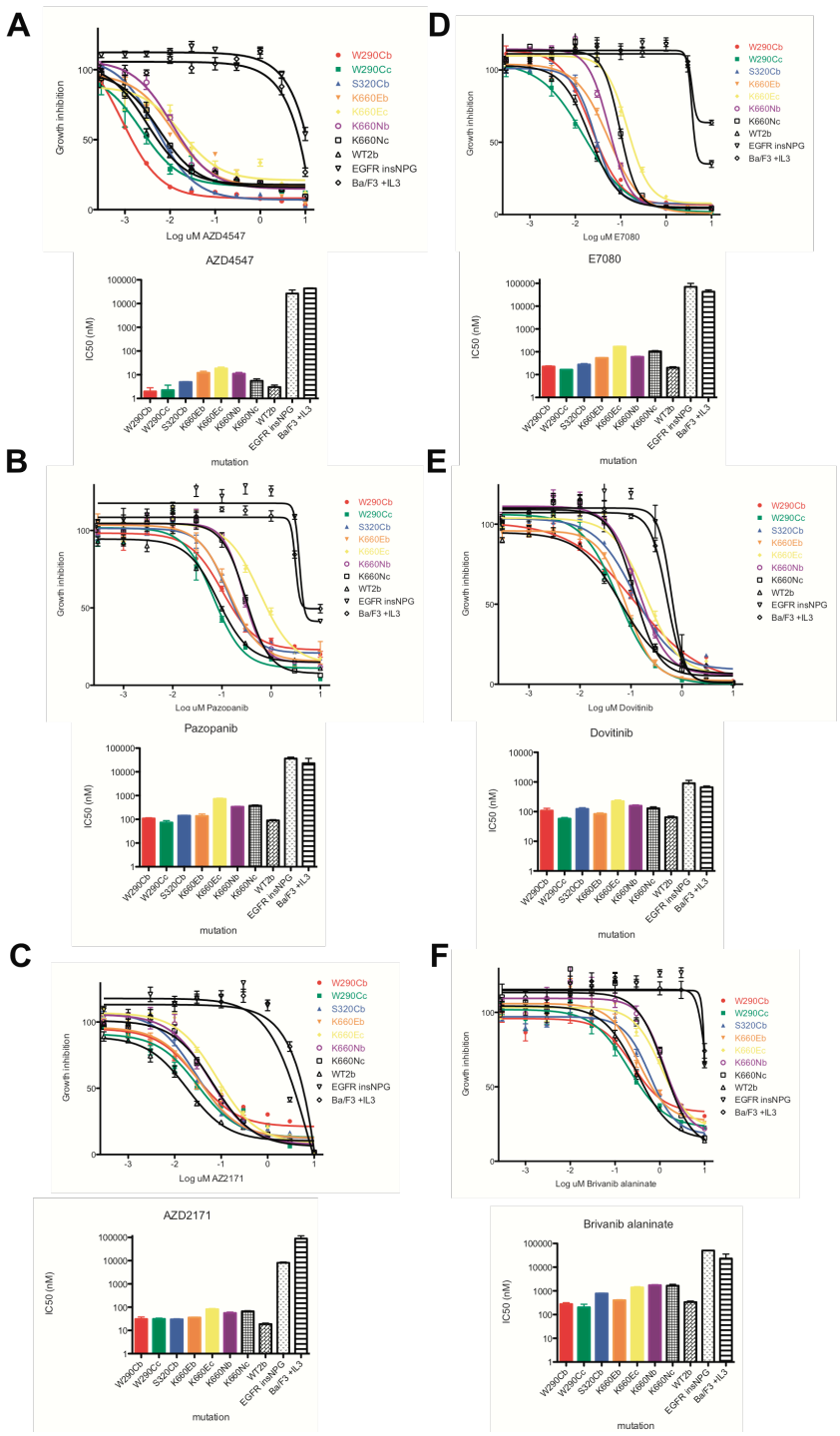

Figure 2-9. Ba/F3 cells that are dependent on FGFR2 and FGFR3 signaling are sensitive to FGFR inhibitors. These experiments were performed similarly to those documented in Figure 2-8.

Figure 2-9 continued

(A-F) Ba/F3 cells expressing each mutation construct were seeded into 96-well plates at a density of 5,000 cells per well, in the presence of increasing concentrations of the indicated drugs. After four days, proliferation was measured by adding Cell Titer Glo and assaying luminescence. Individual IC_{50} values were calculated for each mutation and plotted on a log scale (corresponding values are located below each inhibitory curve). Briefly, (A) AZD4547, a specific pan-FGFR inhibitor, demonstrates an inhibition pattern favoring ECD mutations over kinase domain mutations, and inhibits cells at about 1-10 nM drug. (B) Pazopanib and (E) dovitinib inhibit cells expressing mutations similarly, at about 100 nM drug. (C) AZ2171 and (D) E7080 inhibit cells expressing mutations similarly, at 10-100 nM drug. (F) Brivanib alaninate showed less inhibitory potential in this model, inhibiting mutation-expressing cells at 100-1000 nM drug.

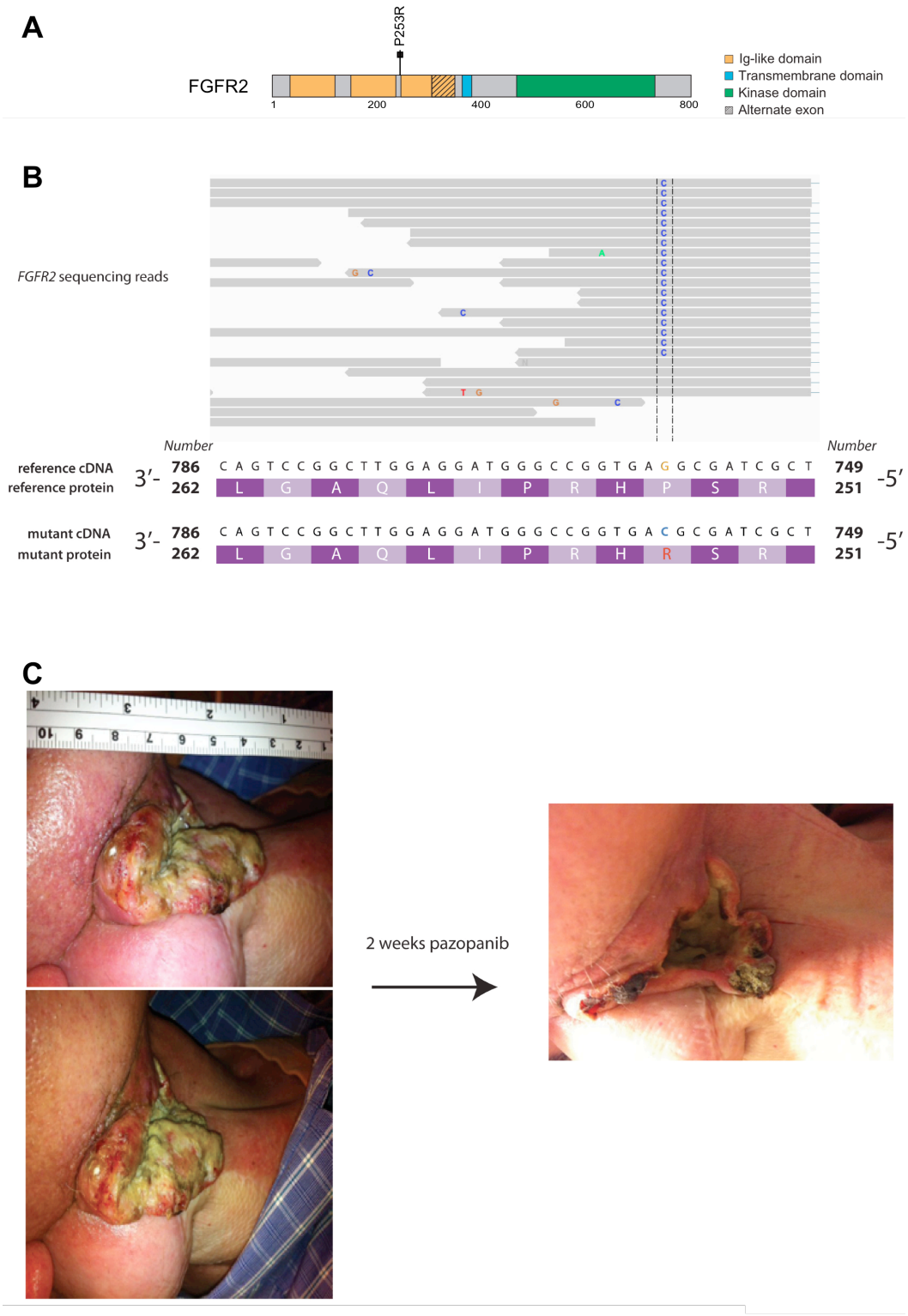

Figure 2-10. A head and neck squamous cell carcinoma patient harboring a somatic FGFR2 P253R mutation demonstrates a partial response to an FGFR inhibitor.

Figure 2-10 continued

(A) A schematic shows the location of the P253R mutation in the FGFR2 extracellular domain. (B) mRNA sequencing was performed and a somatic mutation in the *FGFR2* gene was identified, shown in the IGV viewer (http://www.broadinstitute.org/igv/). Antisense reference and mutant sequences for cDNA and protein are shown below with nucleotide and protein changes indicated.

(C) Prior to beginning treatment with pazopanib, a multi-kinase inhibitor with anti-FGFR activity, the patient exhibited large metastatic tumor growth in his left neck (left images). After a daily regimen of pazopanib for two weeks, his tumor had considerably receded (right image).

carcinoma and has been shown to be oncogenic in cellular model systems and to sensitize cells to FGFR kinase inhibitors (11). Cellular and biochemical analysis of the FGFR2 P253R mutation suggest that this event is transforming and sensitive to targeted therapies in our assays, similar to the events observed in lung SqCC (Figure 2-11).

The patient was diagnosed with locally advanced (T2N1M0, stage III) squamous cell carcinoma of the right tongue in 2008 at the age of 52. He had no history of tobacco use or alcohol abuse and was initially treated with a right hemiglossectomy, supra-omohyoid neck dissection, and free-flap reconstruction. He received post-operative radiation therapy, which completed in early 2009. He subsequently developed recurrences in the right and left neck over a period of three years and was treated with surgery, two additional courses of radiation therapy and multiple courses of chemotherapy including carboplatin, paclitaxel, cisplatin and cetuximab. In early 2012, he had further progression with biopsy proven squamous cell carcinoma in the right neck and left axilla. He unfortunately did not qualify for a clinical trial and the decision was made to treat him with pazopanib, characterized for its anti-FGFR activity above, and which has been approved by the Food and Drug Administration for other indications. He began daily treatment with 800mg pazopanib starting on April 12, 2012. At this time, he had significant gross disease in the right neck (Figure 2-10C, left panels). A follow up visit 12 days later showed a marked reduction in tumor size (Figure 2-10C, right panel). No side effects were encountered except for grade 1 fatigue. He continued on pazopanib for two months, when he presented with a right carotid hemorrhage that required emergent surgical repair. Pazopanib was discontinued at that time, and the patient remains alive as of March 15, 2013 under hospice care. This correlative observation does not definitively identify FGFR2 as the target of pazopanib, but we believe that

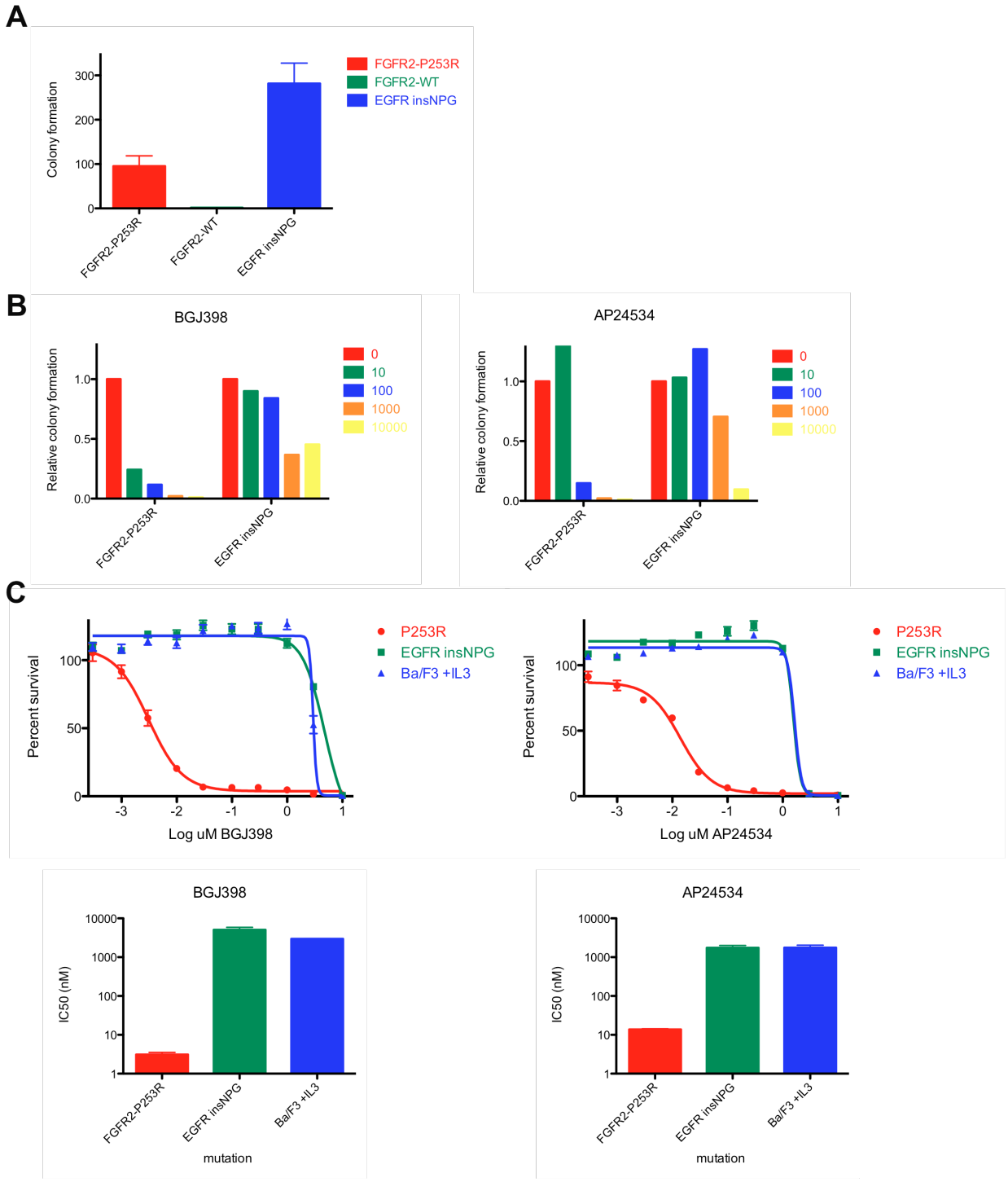

Figure 2-11. FGFR2-P253R is transforming in anchorage independent growth assays and Ba/F3 assays.

Figure 2-11 continued

(A) NIH-3T3 cells stably expressing FGFR2-P253R, FGFR2 wild type, or EGFR insNPG, were seeded into Select agar as in Figure 2-4A and subsequent colonies were counted.

(B) Anchorage independent colony formation driven by P253R is abrogated in the presence of anti-FGFR inhibitors BGJ398 or AP24534. Experiments were performed as in Figure 2-6A.

(C) Cells dependent on FGFR signaling through P253R can be targeted with anti-FGFR targeted therapies. FGFR2-P253R, EGFR insNPG, or parental Ba/F3 cells, assayed as in Figure 2-8B, show divergent responses to BGJ398 (left panel) or AP24534 (right panel). Individual IC_{50} values were calculated for each mutation and plotted on a log scale below the respective curves.

this result provides compelling rationale to continue to pursue treatment of *FGFR2*-mutated tumors with anti-FGFR targeted therapies.

DISCUSSION

Lung squamous cell carcinoma is a poorly characterized disease that leads to approximately 40,000 new deaths per year in the US. Recent large-scale genomic characterization efforts conducted by the TCGA Network have described the general landscape of genomic alterations in squamous cell lung cancer and have suggested that many tumors harbor targetable somatic alterations. One of the most provocative findings is that of recurrent *FGFR2* and *FGFR3* mutations, which are significant given that germline FGFR mutations are known to lead to craniofacial syndromes (18), that these mutations have been described in other malignancies (19), and that focal *FGFR1* amplification is known to occur in lung SqCC and appears to be a therapeutic target (16, 17). It is also of particular interest in lung cancer, given the role of *FGFR2* IIIb signaling in lung development (45, 46). This knowledge led us to generate and assay mutations harbored by both the IIIb and IIIc isoforms of *FGFR2*, as the expression levels of each isoform were varied across the samples containing mutations (Figure 2-2). In *FGFR3*, on the other hand, we generated and assayed mutations only in the IIIc isoform, as the extracellular domain mutations observed in lung SqCC have been studied in depth in both isoforms previously (47, 48) and the intracellular mutations did not map to sites of predicted functional necessity in the protein (Figure 2-12), nor did the IIIc isoform of either transform cells in our anchorage independence assay (Figure 2-4C). Isoform expression differences have the ability to vastly alter protein function in the cellular context (46, 49), and the contribution in patients harboring FGFR-mutant lung SqCC is worth pursuing in greater detail.

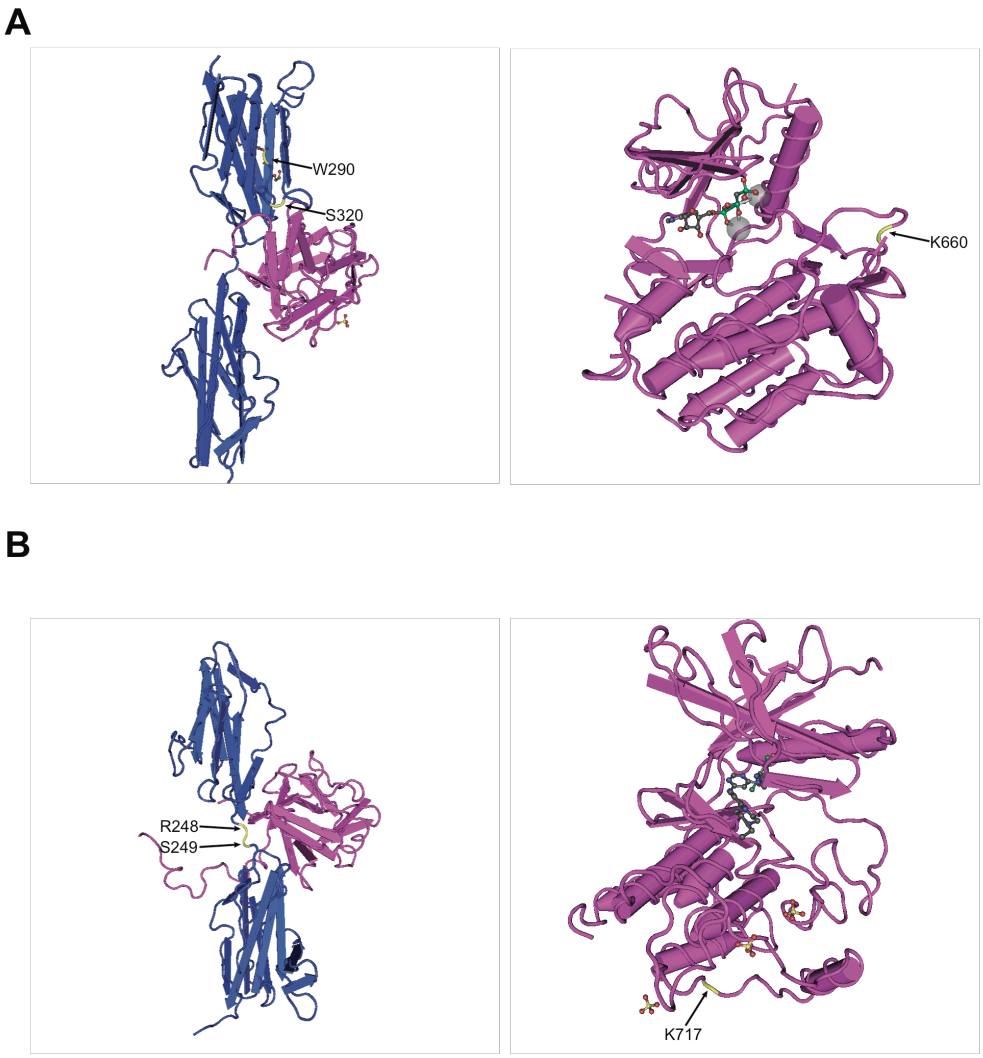

Figure 2-12. Known protein structures support mutational phenotypes.

(A) The FGFR2 IIIb ECD physical interaction with FGF10 demonstrates that W290 and S320 are integral to the maintenance of the protein structure and ligand binding (left panel, (50)). FGFR2 kinase domain interacting with ACP (an ATP analog) and Mg2+ shows that K660 falls in a somewhat unstructured region, but this residue is known to participate in a "molecular brake" region that acts as a regulatory hinge in the kinase domain (right panel, (51)). Both E471 and T787 fall outside of the two structured domains, suggesting that their functional impact is minimal.

Figure 2-12 continued

(B) FGFR3 IIIc ECD interacting with FGF1 demonstrates that R248 and S249 are located at the junction between two IG-like domains, with the high potential to regulate structure and ligand binding (left panel, (52)). FGFR3 kinase domain interacting with BGJ398 shows that K717 is located on the outside of the protein structure and far from the binding pocket, rendering it unlikely to influence function (right panel, (36)). S435 falls outside of the two structured domains, suggesting its functional impact is minimal. All structures were generated using the MMDB viewer (53).

We have confirmed that a subset of observed mutations drive transformation in NIH-3T3 cells in an anchorage independent growth assay, and that this transformation is reversible by several clinically relevant FGFR-specific and multi-kinase inhibitors. Not all *FGFR2* and *FGFR3* mutations scored as transforming in our assays, but given the very high somatic mutation rate in lung SqCC, this observation is not surprising as several mutations are likely non-functional passengers. We found that two extracellular domain mutations in *FGFR2* are able to form disulfide bonds between receptors, leading to constitutive dimers, as has been observed in other *FGFR2* ECD mutations (31) and in *FGFR3* mutations that have been described previously in urothelial carcinoma, and which we also observe here in the lung SqCC data (30). This finding is especially relevant given that the *FGFR2* W290C mutation has been observed independently in lung SqCC sequencing on two previous occasions (11, 54), demonstrating that it is a recurrent activating event in this disease. It is also possible that the glycosylation deficiency that we observed in the expressed protein harboring this mutation impacts protein function, a phenomenon with precedence in this receptor family (33). The precise functional implications rendered by this genomic event thus warrant further study.

We found that the *FGFR* mutations also exhibited sensitivity to inhibition by FGFR-specific and multi-kinase inhibitors in the Ba/F3 cell system, which models dependency on oncogenic pathways. In this case, cells were generated that were dependent on FGFR-mediated signaling, requiring expression of the introduced mutant transgene and the addition of FGF and heparin to the media, a strategy that has been adopted previously to study perturbations contributing to altered FGFR signaling (21). Many drugs in the panel of inhibitors that we tested are already approved for clinical use in other malignancies, and clinical trials are underway to test sensitivity to FGFR inhibitors in patients harboring *FGFR* amplification or mutation

(NCT01004224, NCT01457846, NCT00979134). While we cannot infer *in vivo* sensitivity to these inhibitors from our models, we do believe that this study provides a compelling rationale for extending trials of FGFR kinase inhibitors to patients with lung and head and neck SqCC harboring *FGFR2* or *FGFR3* mutations, particularly given our demonstration of *in vitro* sensitivity and demonstration of observed clinical benefit from therapy targeting FGFR alterations in a patient with an *FGFR2* P253R mutation.

This study represents one of the first functionally validated novel recurrent targets to emerge from analysis of the systematic genomic profiling of lung SqCC by the TCGA Research Network. It is our hope and expectation that findings of this nature will continue with the analysis and publication of more large genomic studies of different malignancies, and that ultimately this will lead to informed and improved clinical treatment options for patients suffering with this disease.

MATERIALS AND METHODS

Patient samples and genomic analysis

We manually reviewed *FGFR2* and *FGFR3* exome sequencing data generated by the Broad Institute Genome Characterization Center from pathologically-confirmed lung SqCC and matched normal controls as part of the TCGA research network. The TCGA research network reported on 178 of these cases (4) based on data availability at the time. Exome sequencing data were generated and analyzed at the Broad Institute using methods described previously (4). Additionally, we queried publically available sequencing data generated from 18 samples that were excluded from the initial TCGA report (as of November 2011) due to lack of available data for one or more of the other genomic platforms (mRNA, miRNA, DNA copy number, DNA

methylation). All data were de-identified and obtained in accordance with patient protection standards set by the TCGA and were obtained from the TCGA Data Portal (https://tcga-data.nci.nih.gov/tcga/).

For the individual with a clinical response to pazopanib, total RNA was extracted using the AllPrep DNA/RNA Mini Kit (Qiagen, Cat#80204). Briefly, a pea-size frozen tumor tissue was homogenized in 600µl of RLT butter using a TissueRuptor (Qiagen, Cat# 9001271) for ~30 seconds on ice. The tissue homogenate was transferred to an AllPrep spin column and total RNA purified according to the manufacturer's recommended protocol (AllPrep DNA/RNA Mini Kit, Qiagen, Cat#80204). Poly-adenylated mRNA was enriched using the Ambion MicroPoly(A)Purist kit starting from 30 µg of total RNA as an input according to the manufacturer's recommended protocol.

Illumina transcriptome sequencing libraries were prepared as previously described (55) from both mRNA and from total RNA and were subjected to 76bp paired-end sequencing on a single lane of an Illumina GAIIx sequencer. Sequencing reads were first aligned to all curated protein-coding transcripts from RefSeq (downloaded on March 1, 2009 from NCBI RefSeq human mRNA FTP site [ftp://ftp.ncbi.nih.gov/refseq/H_sapiens/mRNA_Prot/]) and were mapped back to reference human genome, hg18 as previously described (55). Potential mutations and small nucleotide polymorphisms (SNPs) were called using the Unified genotyper from the GATK tool using default settings (56).

This individual was consented for the analysis according to Institutional Protocol 94138 at the Dana-Farber Cancer Institute. The *FGFR2* P253R mutation was found in both the total RNA-seq data and mRNA-seq data, and it was confirmed from genomic DNA by Sanger

sequencing in a CLIA-certified laboratory (GeneDx, www.genedx.com). The patient was treated with pazopanib at the FDA-approved dose of 800 mg once daily.

Cell lines, antibodies, ligands, and inhibitors

NIH-3T3 cells and Ba/F3 cells were maintained as described previously (11, 21). Antibodies against FGFR2 (C-8) and FRS2 (H-91) were purchased from Santa Cruz Biotechnology, Inc. Antibodies against FGFR3 (C51F2), p-FGFR, p-FRS2 (Y436), AKT (C67E7), p-AKT (T308, 244F9), Erk 1/2 (137F5), p-Erk 1/2 (E10), and beta-actin (8H10D10) were obtained from Cell Signaling Technology, Inc.

For FGFR stimulation experiments, the FGF1 ligand was obtained from Abcam. FGF7 and FGF9 were obtained from Life Technologies. Interleukin-3 (IL-3) was purchased from VWR and heparin from StemCell Technologies, Inc.

Ponatinib (AP24534), dovitinib (TKI258), and cediranib (AZD2171) were obtained from Selleck Chemicals. Brivanib alaninate (BMS-582664) was obtained from Fischer Scientific. Pazopanib (GW786034) was obtained from Axon Medchem. AZD4547 was obtained from Active Biochem. E7080 was obtained from American Custom Chemicals Corporation. BGJ398 was a generous gift from Novartis Pharmaceuticals Corporation (Basel, CH).

Mutagenesis and cellular transfection and infection

Mutagenesis primers developed for each mutation were generated using the Agilent QuikChange Primer Design tool (www.genomics.agilent.com). *FGFR2* isoforms IIIb and IIIc, and *FGFR3* isoform IIIc were cloned into the pDONR223-Gateway entry vector and mutated by site-directed mutagenesis with the QuikChange Lightning Site-Directed Mutagenesis Kit from

Agilent Technologies. Sequence-verified constructs were cloned into the pBabe-puro Gateway expression vector and transfected into HEK-293T cells with Fugene-6 (Promega) as described previously (11). NIH-3T3 and Ba/F3 cells were infected with the resulting virus and after two days and mutation-expressing cells were selected with 2 μg/mL puromycin.

Western blot analysis and visualization of unreduced dimers

Cells were lysed in buffer containing 0.5% NP-40, 50 mM Tris pH 8, 150 mM $MgCl_2$, and phosphatase and protease inhibitors, and proteins were separated by SDS/PAGE and transferred to nitrocellulose membranes via the iBlot dry transfer system (Invitrogen). Antibody binding was detected using the fluorescence-based LI-COR Odyssey IR imaging system (LI-COR Biosciences).

To visualize receptor dimers formed by extracellular domain mutations to cysteine residues, NIH-3T3 cells expressing the appropriate mutations were serum starved for eight hours in the presence of PBS or FGF1 and heparin, as indicated in the text, washed with PBS containing 10mM iodoacetamide, and lysed in lysis buffer containing 1% Triton, 10% glycerol, 50mM Tris pH 7.4, and 10 mM iodoacetamide. Two 100 μg aliquots of each protein sample were prepared, one with reducing agent and one without. Electrophoresis was performed using 4-12% Tris-glycine SDS/PAGE gels (Invitrogen)

To confirm loss of phosphorylation of relevant kinases in the presence of inhibitor, NIH-3T3 cells expressing mutated FGFR2 or FGFR3 were washed with PBS, serum starved for four hours in the presence of indicated concentrations of inhibitor, and ligand stimulated with FGF1 for 30 minutes before lysis using western blot analysis as described above.

Soft agar colony formation assays

Two mL of 0.5% Select agar (Gibco) and media were plated to each well of a non-tissue culture-treated 6-well plate and allowed to solidify. $5x10^4$ cells were suspended in 330 µL media and mixed with 770 µL 0.5% Select agar and media, for a final concentration of 0.4% agar, and plated onto the solidified bottom layer. Plates were incubated at 37C for three weeks, photographed using QuickCapture (Logitech), and quantified via ImageJ for colony formation. Soft agar colony formation assays were performed in triplicate. Statistical comparison of colony counts was performed using the Student's T-test.

To evaluate the effect of clinical inhibitors on soft agar colony formation, the above protocol was performed with the following alteration: $5x10^4$ cells were suspended in 330 µL media plus relevant concentration of inhibitor prior to addition of 0.5% agar solution and plating.

Xenograft studies

All animal experiments were performed according to institutional guidelines regarding animal safety. Immuno-compromised mice were injected with NIH-3T3 cells stably expressing exogenous FGFR2-IIIb WT, W290C, S320C or K660N mutant isoforms. Cohorts of 7 mice were injected at 3 sites for each cell type with two million cells per site, and mice were observed until tumor volume reached approximately 200-300 mm^3. Mice were then treated with BGJ-398 at 15 mg/kg or vehicle (PEG-300) control daily for 2 weeks, and tumor size was measured during the treatment period.

Ba/F3 dependency and inhibitor studies

Ba/F3 cells expressing each mutation construct were selected in media containing IL-3 and puromycin until stable cell lines were established. To establish cells dependent on FGFR signaling, three million cells were washed twice with PBS and seeded into 2 mL of media containing FGF7 (for FGFR2 IIIb mutations) or FGF9 (for FGFR2 IIIc) and heparin. These cells were maintained until IL-3 independent cells emerged. FGFR-dependent cells were seeded into 96-well plates in 100 μL media containing FGF and heparin at a density of 5,000 cells per well. 10 μL of drug was added in quadruplicate for final concentrations of 0.3nM-10 μM in half logs, with two DMSO controls, and incubated for three or four days. 50 μL of Cell Titer Glo (Promega) was added to each well and luminescence was measured on the SpectroMax 5 imager. Percent survival compared to DMSO controls was calculated and plotted in Prism (GraphPad Software, Inc).

ACKNOWLEDGEMENTS

The authors thank Ami S. Bhatt, member of the Meyerson laboratory, Pamela M. Pollock, investigator at Queensland Institute of Technology (AUS), and David M. Ornitz, investigator at Washington University in St. Louis, for helpful discussion and technical support.

This work was supported in part by a Young Investigator Grant from the National Lung Cancer Partnership, NCI grants 1K08CA163677, and the Stephen D. and Alice Cutler Investigator Fund (P.S.H.), by Uniting Against Lung Cancer, the Lung Cancer Research Foundation, the American Lung Association, Novartis Pharmaceuticals, and NCI grant P50CA090578 (M.M.), by a Ruth L. Kirschstein National Research Service Award Individual Fellowship from the National Cancer Institute (NIH F32CA142039) (M.D.W.), and by a Canadian Institutes of Health Research Fellowship (T.J.P).

REFERENCES

1. Comprehensive molecular characterization of human colon and rectal cancer. Nature. 2012;487(7407):330-7. PMCID: 3401966.

2. Rudin CM, Durinck S, Stawiski EW, Poirier JT, Modrusan Z, Shames DS, et al. Comprehensive genomic analysis identifies SOX2 as a frequently amplified gene in small-cell lung cancer. Nat Genet. 2012.

3. Peifer M, Fernandez-Cuesta L, Sos ML, George J, Seidel D, Kasper LH, et al. Integrative genome analyses identify key somatic driver mutations of small-cell lung cancer. Nat Genet. 2012.

4. Hammerman PS, Lawrence MS, Voet D, Jing R, Cibulskis K, Sivachenko A, et al. Comprehensive genomic characterization of squamous cell lung cancers. Nature. 2012.

5. Govindan R, Ding L, Griffith M, Subramanian J, Dees ND, Kanchi KL, et al. Genomic landscape of non-small cell lung cancer in smokers and never-smokers. Cell. 2012;150(6):1121-34.

6. Imielinski M, Berger AH, Hammerman PS, Hernandez B, Pugh TJ, Hodis E, et al. Mapping the hallmarks of lung adenocarcinoma with massively parallel sequencing. Cell. 2012;150(6):1107-20.

7. Lynch TJ, Bell DW, Sordella R, Gurubhagavatula S, Okimoto RA, Brannigan BW, et al. Activating mutations in the epidermal growth factor receptor underlying responsiveness of non-small-cell lung cancer to gefitinib. The New England journal of medicine. 2004;350(21):2129-39.

8. Paez JG, Janne PA, Lee JC, Tracy S, Greulich H, Gabriel S, et al. EGFR mutations in lung cancer: correlation with clinical response to gefitinib therapy. Science. 2004;304(5676):1497-500.

9. Soda M, Choi YL, Enomoto M, Takada S, Yamashita Y, Ishikawa S, et al. Identification of the transforming EML4-ALK fusion gene in non-small-cell lung cancer. Nature. 2007;448(7153):561-6.

10. Davies H, Bignell GR, Cox C, Stephens P, Edkins S, Clegg S, et al. Mutations of the BRAF gene in human cancer. Nature. 2002;417(6892):949-54.

11. Dutt A, Salvesen HB, Chen TH, Ramos AH, Onofrio RC, Hatton C, et al. Drug-sensitive FGFR2 mutations in endometrial carcinoma. Proceedings of the National Academy of Sciences of the United States of America. 2008;105(25):8713-7. PMCID: 2438391.

12. Pollock PM, Gartside MG, Dejeza LC, Powell MA, Mallon MA, Davies H, et al. Frequent activating FGFR2 mutations in endometrial carcinomas parallel germline

mutations associated with craniosynostosis and skeletal dysplasia syndromes. Oncogene. 2007;26(50):7158-62. PMCID: 2871595.

13. Cappellen D, De Oliveira C, Ricol D, de Medina S, Bourdin J, Sastre-Garau X, et al. Frequent activating mutations of FGFR3 in human bladder and cervix carcinomas. Nat Genet. 1999;23(1):18-20.

14. Maemondo M, Inoue A, Kobayashi K, Sugawara S, Oizumi S, Isobe H, et al. Gefitinib or chemotherapy for non-small-cell lung cancer with mutated EGFR. The New England journal of medicine. 2010;362(25):2380-8.

15. Mok TS, Wu YL, Thongprasert S, Yang CH, Chu DT, Saijo N, et al. Gefitinib or carboplatin-paclitaxel in pulmonary adenocarcinoma. The New England journal of medicine. 2009;361(10):947-57.

16. Weiss J, Sos ML, Seidel D, Peifer M, Zander T, Heuckmann JM, et al. Frequent and focal FGFR1 amplification associates with therapeutically tractable FGFR1 dependency in squamous cell lung cancer. Science translational medicine. 2010;2(62):62ra93.

17. Dutt A, Ramos AH, Hammerman PS, Mermel C, Cho J, Sharifnia T, et al. Inhibitor-sensitive FGFR1 amplification in human non-small cell lung cancer. PLoS ONE. 2011;6(6):e20351. PMCID: 3110189.

18. Ornitz DM, Marie PJ. FGF signaling pathways in endochondral and intramembranous bone development and human genetic disease. Genes & development. 2002;16(12):1446-65.

19. Greulich H, Pollock PM. Targeting mutant fibroblast growth factor receptors in cancer. Trends in molecular medicine. 2011;17(5):283-92.

20. Turner N, Grose R. Fibroblast growth factor signalling: from development to cancer. Nat Rev Cancer. 2010;10(2):116-29.

21. Zhang X, Ibrahimi OA, Olsen SK, Umemori H, Mohammadi M, Ornitz DM. Receptor specificity of the fibroblast growth factor family. The complete mammalian FGF family. The Journal of biological chemistry. 2006;281(23):15694-700. PMCID: 2080618.

22. Elbauomy Elsheikh S, Green AR, Lambros MB, Turner NC, Grainge MJ, Powe D, et al. FGFR1 amplification in breast carcinomas: a chromogenic in situ hybridisation analysis. Breast cancer research : BCR. 2007;9(2):R23. PMCID: 1868920.

23. Kwabi-Addo B, Ropiquet F, Giri D, Ittmann M. Alternative splicing of fibroblast growth factor receptors in human prostate cancer. The Prostate. 2001;46(2):163-72.

24. Yan G, Fukabori Y, McBride G, Nikolaropolous S, McKeehan WL. Exon switching and activation of stromal and embryonic fibroblast growth factor (FGF)-FGF receptor genes in prostate epithelial cells accompany stromal independence and malignancy. Molecular and cellular biology. 1993;13(8):4513-22. PMCID: 360063.

25. Yu K, Herr AB, Waksman G, Ornitz DM. Loss of fibroblast growth factor receptor 2 ligand-binding specificity in Apert syndrome. Proceedings of the National Academy of Sciences of the United States of America. 2000;97(26):14536-41. PMCID: 18954.

26. Hunter DJ, Kraft P, Jacobs KB, Cox DG, Yeager M, Hankinson SE, et al. A genome-wide association study identifies alleles in FGFR2 associated with risk of sporadic postmenopausal breast cancer. Nat Genet. 2007;39(7):870-4.

27. Chesi M, Brents LA, Ely SA, Bais C, Robbiani DF, Mesri EA, et al. Activated fibroblast growth factor receptor 3 is an oncogene that contributes to tumor progression in multiple myeloma. Blood. 2001;97(3):729-36.

28. Chesi M, Nardini E, Brents LA, Schröck E, Ried T, Kuehl WM, et al. Frequent translocation t(4;14)(p16.3;q32.3) in multiple myeloma is associated with increased expression and activating mutations of fibroblast growth factor receptor 3. Nat Genet. 1997;16(3):260-4.

29. Wilkerson MD, Yin X, Hoadley KA, Liu Y, Hayward MC, Cabanski CR, et al. Lung squamous cell carcinoma mRNA expression subtypes are reproducible, clinically important, and correspond to normal cell types. Clinical cancer research : an official journal of the American Association for Cancer Research. 2010;16(19):4864-75. PMCID: 2953768.

30. d'Avis PY, Robertson SC, Meyer AN, Bardwell WM, Webster MK, Donoghue DJ. Constitutive activation of fibroblast growth factor receptor 3 by mutations responsible for the lethal skeletal dysplasia thanatophoric dysplasia type I. Cell growth & differentiation : the molecular biology journal of the American Association for Cancer Research. 1998;9(1):71-8.

31. Plotnikov AN, Hubbard SR, Schlessinger J, Mohammadi M. Crystal structures of two FGF-FGFR complexes reveal the determinants of ligand-receptor specificity. Cell. 2000;101(4):413-24.

32. Greulich H, Kaplan B, Mertins P, Chen TH, Tanaka KE, Yun CH, et al. Functional analysis of receptor tyrosine kinase mutations in lung cancer identifies oncogenic extracellular domain mutations of ERBB2. Proceedings of the National Academy of Sciences of the United States of America. 2012.

33. Gartside MG, Chen H, Ibrahimi OA, Byron SA, Curtis AV, Wellens CL, et al. Loss-of-function fibroblast growth factor receptor-2 mutations in melanoma. Molecular cancer research : MCR. 2009;7(1):41-54.

34. O'Hare T, Shakespeare WC, Zhu X, Eide CA, Rivera VM, Wang F, et al. AP24534, a pan-BCR-ABL inhibitor for chronic myeloid leukemia, potently inhibits the T315I mutant and overcomes mutation-based resistance. Cancer cell. 2009;16(5):401-12. PMCID: 2804470.

35. Gozgit JM, Wong MJ, Moran L, Wardwell S, Mohemmad QK, Narasimhan NI, et al. Ponatinib (AP24534), a multitargeted pan-FGFR inhibitor with activity in multiple FGFR-amplified or mutated cancer models. Molecular cancer therapeutics. 2012;11(3):690-9.

36. Guagnano V, Furet P, Spanka C, Bordas V, Le Douget M, Stamm C, et al. Discovery of 3-(2,6-dichloro-3,5-dimethoxy-phenyl)-1-{6-[4-(4-ethyl-piperazin-1-yl)-phenylamino]-pyrimidin-4-yl}-1-methyl-urea (NVP-BGJ398), a potent and selective inhibitor of the fibroblast growth factor receptor family of receptor tyrosine kinase. J Med Chem. 2011;54(20):7066-83.

37. Sonpavde G, Hutson TE. Pazopanib: a novel multitargeted tyrosine kinase inhibitor. Current oncology reports. 2007;9(2):115-9.

38. Renhowe PA, Pecchi S, Shafer CM, Machajewski TD, Jazan EM, Taylor C, et al. Design, structure-activity relationships and in vivo characterization of 4-amino-3-benzimidazol-2-ylhydroquinolin-2-ones: a novel class of receptor tyrosine kinase inhibitors. J Med Chem. 2009;52(2):278-92.

39. Gavine PR, Mooney L, Kilgour E, Thomas AP, Al-Kadhimi K, Beck S, et al. AZD4547: An orally bioavailable, potent and selective inhibitor of the Fibroblast Growth Factor Receptor tyrosine kinase family. Cancer Res. 2012:1-41.

40. Matsui J, Yamamoto Y, Funahashi Y, Tsuruoka A, Watanabe T, Wakabayashi T, et al. E7080, a novel inhibitor that targets multiple kinases, has potent antitumor activities against stem cell factor producing human small cell lung cancer H146, based on angiogenesis inhibition. International journal of cancer Journal international du cancer. 2008;122(3):664-71.

41. Wedge SR, Kendrew J, Hennequin LF, Valentine PJ, Barry ST, Brave SR, et al. AZD2171: a highly potent, orally bioavailable, vascular endothelial growth factor receptor-2 tyrosine kinase inhibitor for the treatment of cancer. Cancer Res. 2005;65(10):4389-400.

42. Cai Z-w, Zhang Y, Borzilleri RM, Qian L, Barbosa S, Wei D, et al. Discovery of brivanib alaninate ((S)-((R)-1-(4-(4-fluoro-2-methyl-1H-indol-5-yloxy)-5-methylpyrrolo[2,1-f][1,2,4]triazin-6-yloxy)propan-2-yl)2-aminopropanoate), a novel prodrug of dual vascular endothelial growth factor receptor-2 and fibroblast growth factor receptor-1 kinase inhibitor (BMS-540215). J Med Chem. 2008;51(6):1976-80.

43. Stransky N, Egloff AM, Tward AD, Kostic AD, Cibulskis K, Sivachenko A, et al. The mutational landscape of head and neck squamous cell carcinoma. Science. 2011;333(6046):1157-60. PMCID: 3415217.

44. Agrawal N, Frederick MJ, Pickering CR, Bettegowda C, Chang K, Li RJ, et al. Exome sequencing of head and neck squamous cell carcinoma reveals inactivating mutations in NOTCH1. Science. 2011;333(6046):1154-7. PMCID: 3162986.

45. Peters K, Werner S, Liao X, Wert S, Whitsett J, Williams L. Targeted expression of a dominant negative FGF receptor blocks branching morphogenesis and epithelial differentiation of the mouse lung. EMBO J. 1994;13(14):3296-301. PMCID: 395226.

46. De Moerlooze L, Spencer-Dene B, Revest JM, Hajihosseini M, Rosewell I, Dickson C. An important role for the IIIb isoform of fibroblast growth factor receptor 2 (FGFR2) in mesenchymal-epithelial signalling during mouse organogenesis. Development. 2000;127(3):483-92.

47. Tomlinson DC, Hurst CD, Knowles MA. Knockdown by shRNA identifies S249C mutant FGFR3 as a potential therapeutic target in bladder cancer. Oncogene. 2007;26(40):5889-99. PMCID: 2443272.

48. Bernard-Pierrot I, Brams A, Dunois-Larde C, Caillault A, Diez de Medina SG, Cappellen D, et al. Oncogenic properties of the mutated forms of fibroblast growth factor receptor 3b. Carcinogenesis. 2006;27(4):740-7.

49. Guo M, Liu W, Serra S, Asa SL, Ezzat S. FGFR2 Isoforms Support Epithelial-Stromal Interactions in Thyroid Cancer Progression. Cancer Res. 2012.

50. Yeh BK, Igarashi M, Eliseenkova AV, Plotnikov AN, Sher I, Ron D, et al. Structural basis by which alternative splicing confers specificity in fibroblast growth factor receptors. Proceedings of the National Academy of Sciences of the United States of America. 2003;100(5):2266-71. PMCID: 151329.

51. Chen H, Ma J, Li W, Eliseenkova AV, Xu C, Neubert TA, et al. A molecular brake in the kinase hinge region regulates the activity of receptor tyrosine kinases. Mol Cell. 2007;27(5):717-30. PMCID: 2094128.

52. Olsen SK, Ibrahimi OA, Raucci A, Zhang F, Eliseenkova AV, Yayon A, et al. Insights into the molecular basis for fibroblast growth factor receptor autoinhibition and ligand-binding promiscuity. Proceedings of the National Academy of Sciences of the United States of America. 2004;101(4):935-40. PMCID: 327120.

53. Madej T, Addess KJ, Fong JH, Geer LY, Geer RC, Lanczycki CJ, et al. MMDB: 3D structures and macromolecular interactions. Nucleic acids research. 2012;40(Database issue):D461-4. PMCID: 3245041.

54. Davies H, Hunter C, Smith R, Stephens P, Greenman C, Bignell G, et al. Somatic mutations of the protein kinase gene family in human lung cancer. Cancer Res. 2005;65(17):7591-5.

55. Levin JZ, Berger MF, Adiconis X, Rogov P, Melnikov A, Fennell T, et al. Targeted next-generation sequencing of a cancer transcriptome enhances detection of sequence variants and novel fusion transcripts. Genome biology. 2009;10(10):R115. PMCID: 2784330.

56. DePristo MA, Banks E, Poplin R, Garimella KV, Maguire JR, Hartl C, et al. A framework for variation discovery and genotyping using next-generation DNA sequencing data. Nat Genet. 2011;43(5):491-8. PMCID: 3083463.

CHAPTER 3

Independent mechanisms lead to acquired resistance to FGFR inhibitors in lung squamous cell carcinoma

This chapter is adapted from a manuscript in preparation.

ATTRIBUTIONS

All experiments and analyses were performed by Rachel G. Liao except as follows:

Experiments and analysis for Figure 3-2A, Table 3-1, and Table 3-3, and experiments for Figure 3-3A were performed by Paul van Hummelen and Aaron Thorner.

Experiments and analysis for Table 3-2 and experiments for Figure 3-2B were performed by Thomas E. Mullen and David J. Kwiatkowski.

Chapter 3. Independent mechanisms lead to acquired resistance to FGFR inhibitors in lung squamous cell carcinoma

SUMMARY

Genomic studies of lung squamous cell carcinoma (lung SqCC) have identified the fibroblast growth factor receptor (FGFR) kinases as the most frequently altered receptor tyrosine kinase family in this disease. Inhibitors targeting FGFRs have recently entered into clinical trials and responses to this class of drugs have been reported in patients with FGFR-driven lung SqCC. However, as with other tyrosine kinase inhibitors, acquired resistance is anticipated. Here, we describe the characterization of resistance mechanisms acquired in a non-small cell lung cancer cell line dependent on a focal *FGFR1* amplification, in response to prolonged treatment with two selective FGFR inhibitors currently in clinical trials, AZD4547 and BGJ398. We identify *MET* amplification and *NRAS* mutation as mechanisms of acquired resistance to these compounds. We also demonstrate that FGFR signaling may be maintained in a MET-dependent manner in inhibitor-resistant cells. These findings provide insight into acquired resistance to FGFR targeted therapies in lung SqCC and suggest potential clinical studies in patients whose tumors develop resistance to FGFR inhibitors.

BACKGROUND

The genomic study of human cancer has led to the discovery of many driving oncogenic kinases, resulting in the development and clinical use of specific kinase inhibitors (1-3). These inhibitors often demonstrate dramatic anti-cancer effects and modest side effects as compared to conventional chemotherapy in genomically selected tumors (4). Invariably, however, acquired resistance to these inhibitors develops, rendering tumors insensitive to inhibition of the primary driving event and often leaving patients with few treatment options (5).

Chapter 3. Independent mechanisms lead to acquired resistance to FGFR inhibitors in lung squamous cell carcinoma

In vitro studies of mechanisms of acquired resistance have been undertaken to identify therapeutic targets in resistant tumors. In many cases these studies have elucidated relevant secondary driving events that are later observed in the clinic. For example, mutagenesis screens in chronic myelogenous leukemia identified secondary mutations in the BCR-ABL translocated protein such as T315I that render the protein insensitive to first line therapies (6). These second-site mutations in BCR-ABL are found in patients resistant to therapy and have been successfully targeted with newer kinase inhibitors (7). In *EGFR*-mutant lung adenocarcinoma, both secondary mutation, often at the gatekeeper site (T790M), and MET amplification have been identified in cellular models following long-term drug treatment and were later observed in resistant patient tumors (8-10). Similarly, in *BRAF*-mutant melanoma, secondary activation of COT and other factors have been identified in screens of overexpressed kinases, and later found in patient tumors (11).

The fibroblast growth factor receptor (FGFR) kinases are a receptor tyrosine kinase (RTK) family that possess the capacity to drive oncogenesis by constitutive activation of downstream signaling pathways (12). Mutations, amplifications, and translocations in these genes leading to dependency on their downstream signaling have been described in several cancer types, and in particular, lung squamous cell carcinoma (13-18). Only recently have inhibitors targeting these proteins entered into clinical development. Currently patients are being screened for FGFR genomic alterations in their lung squamous tumors, and if identified, they can be consented to clinical trials for FGFR targeted therapies (19, 20)—a clinical success in a disease with few treatment options.

Resistance to FGFR inhibitors has recently been observed in several instances. Gastric and bladder cancer cell lines dependent on FGFR2 or FGFR3 and coexpressing MET could be

rescued with hepatocyte growth factor (HGF) stimulation in the presence of FGFR inhibition (21). A multiple myeloma cell line with overexpressed, mutant FGFR3 developed a gatekeeper mutation in the *FGFR3* gene after long-term exposure to FGFR targeted therapy (22). Three bladder cancer cell lines with mutant or translocated *FGFR3* increased expression of EGFR upon FGFR inhibition, suggesting a class-switching rescue mechanism that was not observed in FGFR1- or FGFR2-altered tumors (23).

There have been no reports to date describing mechanisms of acquired resistance to anti-FGFR therapy in lung cancer. Given that clinical responses to anti-FGFR therapy have been observed in FGFR1 amplified lung SqCC, we sought to establish potential mechanisms of acquired resistance in this setting using a cell line model. We expect resistance to develop in lung SqCC patients after prolonged treatment with FGFR inhibitors. We therefore believe that the study of resistance in a cellular context has the potential to benefit patients whose tumors have stopped responding to FGFR therapies. Here, we describe the observation of acquired resistance in FGFR1-driven lung cancer cell lines and characterize two mechanisms through which this resistance arises, providing potential new therapeutic options in tumors with acquired resistance to FGFR inhibitors.

RESULTS

Generation of cells with acquired resistance to FGFR inhibition

The cell line NCI-H2077 is a non-small cell lung cancer cell line with a focal amplification of the 8p11 locus (1.2 Mb in length), which includes the *FGFR1* gene. The cell line is genomically identical to the cell line NCI-H1581, as shown by genome fingerprinting of both lines (15), but morphologically divergent. Both lines show a high degree of sensitivity to

FGFR inhibition by kinase inhibitor treatment and FGFR1 knockdown (15, 24), indicating a dependency on FGFR1 signaling.

Over several months, populations of cells from this cell line were separately maintained in increasing concentrations of two specific, pan-FGFR small molecule inhibitors, BGJ398 (25) and AZD4547 (26), such that populations emerged that were resistant in ~5 μM of each respective drug, hereafter referred to as H2077R-BGJ and H2077R-AZD respectively (Figure 3-1). Both H2077R-BGJ and H2077R-AZD are resistant to BGJ398 and AZD4547 as well as ponatinib (Figure 3-1). Genomic DNA was isolated from the sensitive (hereafter referred to as H2077S) and resistant cells and analyzed by the Center for Cancer Genome Discovery (CCGD) at the Dana-Farber Cancer Institute (Boston, MA) and to the Partners Laboratory for Molecular Medicine (Cambridge, MA) for DNA copy number changes and acquired mutations in the resistant cells.

Resistant cell lines have upregulated MET and H2077R-AZD is sensitive to treatment with MET targeted therapy

The results of the copy number analysis from CCGD paired-end Illumina sequencing identified acquired copy number variants (CNVs) in H2077R-BGJ and H2077R-AZD (Figure 3-2A, Table 3-1). Most events were designated “CN Gain” or “CN Loss,” indicating a low-level, likely arm-length copy gain or loss. One “High Copy Gain” event was also observed in each resistant line, indicating a more focal amplification of >1 copy per cell (Table 3-1). The High Copy Gain in H2077R-AZD occurred on chromosome 7 and was made up of a low, arm-level copy gain of the q arm, in addition to a focal high copy gain, which included the known oncogene *MET* (Table 3-1, Figure 3-2A, inset). Droplet digital PCR analysis was performed on a

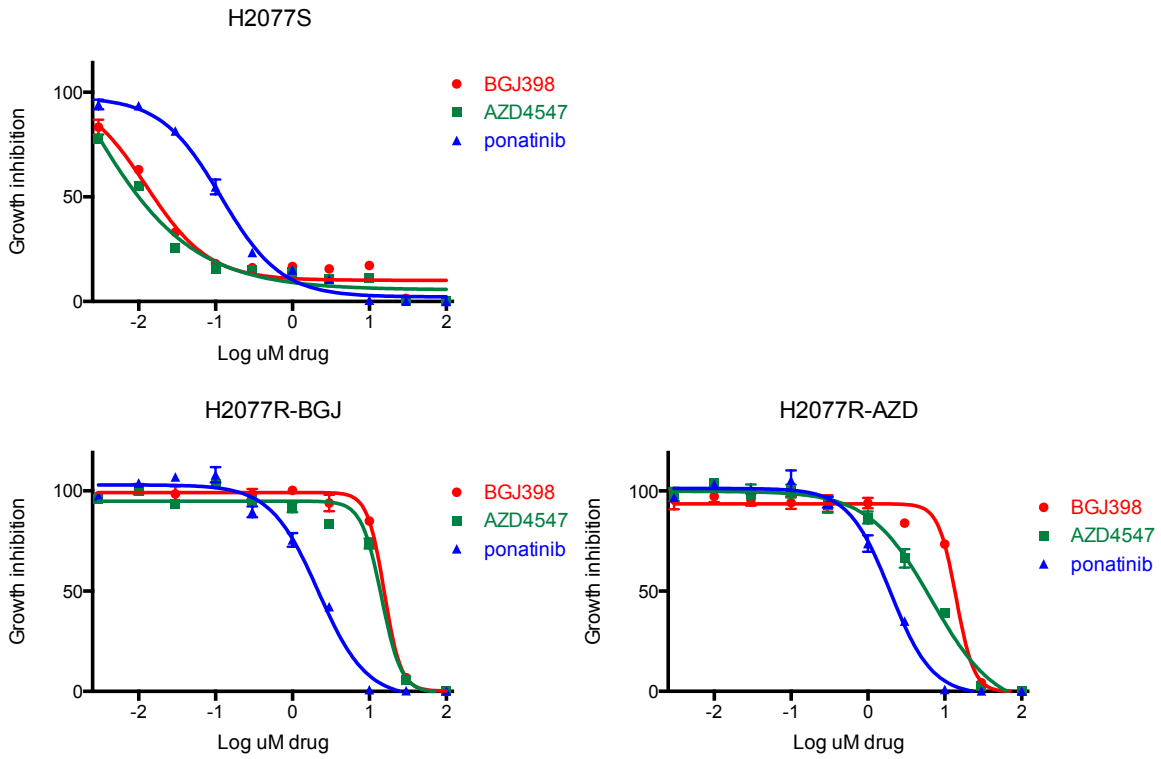

Figure 3-1. Drug treatment responses differ between sensitive and resistant cell lines.

NCI-H2077 parental cells (H2077S) are sensitive to pan-FGFR and multi-kinase small molecule inhibitors BGJ398, AZD4547, and ponatinib (top panel). NCI-H2077 cells grown over time in BGJ398 (H2077R-BGJ, left) or AZD4547 (H2077R-AZD, right) are insensitive to these small molecule inhibitors (bottom two panels).

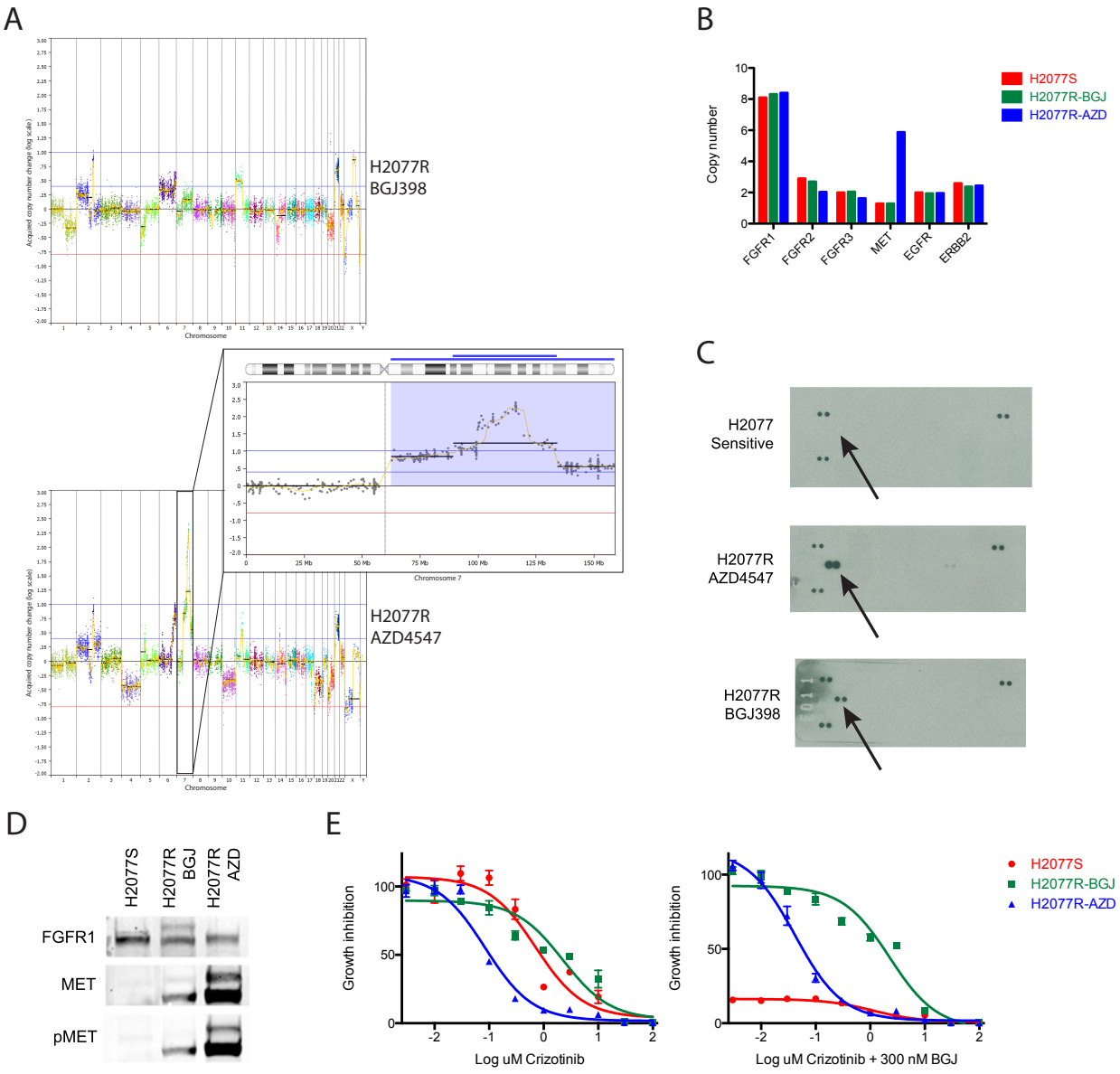

Figure 3-2. MET is expressed and phosphorylated in resistant cell lines and H2077R-AZD cells are *MET*-amplified and sensitive to MET targeted therapy.

(A) Copy number analysis by Illumina sequencing identifies a high copy gain of the *MET* locus only in H2077R-AZD cells, visualized on chromosome 7 (inset).

(B) Droplet digital PCR validates *MET* copy number as well as other known oncogenes in the three cell lines.

Figure 3-2 continued

(C) Phospho-RTK arrays (R&D Systems) incubated with lysates from H2077S, H2077R-AZD, and H2077R-BGJ cell lines show that, while sensitive cells show no measurable MET phosphorylation, resistant cells show high levels of phospho-MET (arrows), and neither resistant cell line has other obvious phospho-RTKs.

(D) Lysates from sensitive cells and resistant cells were probed for FGFR1, MET, and phospho-MET expression, demonstrating by immunoblot that both resistant lines had acquired MET expression and phosphorylation.

(E) H2077R-AZD cells are sensitive to crizotinib, an FDA-approved MET inhibitor (IC_{50} ~100 nM), while both H2077S and H2077R-BGJ have an IC_{50} >1 μM (left panel). Combination treatment of crizotinib and 300 nM BGJ398 results in an IC_{50} of about 40 nM for H2077R-AZD cells, while the IC_{50} for H2077R-BGJ cells is unchanged (right panel).

Table 3-1. Acquired statistically significant copy number gains and losses in resistant cells compared to parental sensitive cells, identified by analysis of paired-end Illumina sequencing reads.

Sample	Chromosome Region	Length	Cytoband	Event	P-value	# Genes in region
H2077R-BGJ	chr20:29,622,585-30,583,282	960698	q11.21	High Copy Gain	2.99 E-119	26
H2077R-BGJ	chr6:149,909,750-171,115,067	21205318	q25.1 - q27	CN Gain	0	131
H2077R-BGJ	chr11:0-12,369,297	12369298	p15.5 - p15.3	CN Gain	4.38 E-196	281
H2077R-BGJ	chr11:13,918,510-48,888,840	34970331	p15.2 - p11.12	CN Gain	2.18 E-188	212
H2077R-BGJ	chr11:55,207,363-67,694,795	12487433	q11 - q13.2	CN Gain	2.59 E-102	401
H2077R-BGJ	chr21:15,374,230-48,129,895	32755666	q11.2 - q22.3	CN Gain	0	288
H2077R-BGJ	chr2:157,266,024-170,987,694	13721671	q24.1 - q31.1	CN Gain	0	70
H2077R-AZD	chr6:128,377,553-171,115,067	42737515	q22.33 - q27	CN Gain	0	251
H2077R-AZD	chr7:62,585,461-89,458,102	26872642	q11.21 - q21.13	CN Gain	0	173
H2077R-AZD	chr7:89,458,102-134,228,618	44770517	q21.13 - q33	High Copy Gain	0	360
H2077R-AZD	chr7:134,228,618-159,138,663	24910046	q33 - q36.3	CN Gain	0	237
H2077R-AZD	chr11:45,911,676-48,888,840	2977165	p11.2 - p11.12	CN Gain	4.74 E-30	53
H2077R-AZD	chr11:55,207,363-67,694,795	12487433	q11 - q13.2	CN Gain	2.53 E-121	401
H2077R-AZD	chr21:15,374,230-48,129,895	32755666	q11.2 - q22.3	CN Gain	0	288
H2077R-AZD	chr2:157,266,024-170,987,694	13721671	q24.1 - q31.1	CN Gain	0	70

validation set of 13 genes (Table 3-2) and confirmed an amplification of the *MET* locus to an average of six copies per cell in H2077R-AZD cells only (Figure 3-2B). Cells were then lysed and probed for phosphorylated RTKs using a phospho-RTK array (R&D Systems) in order to assess for increased p-MET and to identify any co-occurring phosphorylation of other RTKs. Using this technique, we observed an increase of phospho-MET in both resistant cell lines compared to the sensitive cell line (Figure 3-2C). This observation was confirmed by immunoblot using the same lysates used for the phospho-RTK array, which demonstrated increase of total MET and phospho-MET in both resistant cell lines compared to H2077S, with a larger increase observed in H2077R-AZD cells (Figure 3-2D). However, when cells were treated with increasing concentrations of crizotinib, an FDA-approved inhibitor of MET activity, only H2077R-AZD cells showed sensitivity as compared to H2077S cells, indicating a divergent response between the two resistant lines based on acquired amplification status of the *HGFR* locus (Figure 3-2E, left panel). Only a slight increase in sensitivity was observed when H2077R-AZD cells were treated with crizotinib in combination with a non-lethal concentration of BGJ398, indicating a distinct resistance response from the one observed in MET-amplified lung adenocarcinoma, in which cell growth could be inhibited only under combined treatment inhibiting MET and ErbB kinases (8) (Figure 3-2E, right panel). Interestingly, no cell line responded to BKM120 (27), a selective pan-PI3K inhibitor, as a single agent or in combination with FGFR inhibitors or crizotinib, suggesting that sensitivity to MET inhibition was not being driven exclusively through the PI3K/AKT pathway (Figure 3-3).

Resistant line H2077R-BGJ has a secondary NRAS mutation and arrests upon inhibition of the MAPK pathway

Table 3-2. Droplet digital PCR validates amplification of *MET* in H2077R-AZD cells.

Thirteen genes were queried by ddPCR for raw copy number (CN) and then corrected as described in the materials and methods section.

H2077S

Gene	Negative droplets	Positive target droplets	Positive reference droplets	Total positive droplets	Raw CN	CN Corrected
AP3B1	12085	946	1890	2836	0.96	0.9
BCL2	12248	1245	1532	2777	1.61	1.4
CCND1	11879	859	1609	2468	1.03	1.2
CDK4	11914	1266	1379	2645	1.83	2.2
EGFR	11092	1346	1497	2843	1.79	2
ERBB2	12387	1283	1312	2595	1.95	2.6
FGFR1	8894	4047	1556	5603	5.85	8.1
FGFR2	15107	1127	932	2059	2.43	2.9
FGFR3	12144	1297	1514	2811	1.7	2
FGFR4	10508	2024	1292	3316	3.24	5.6
MET	10710	817	1228	2045	1.31	1.3
PDGFRA	12890	1141	1491	2632	1.51	1.3
PIK3CA	11520	545	1111	1656	0.96	0.8
RPP30	11727	1685	852	2537	4.09	4.9

H2077R-BGJ

Gene	Negative droplets	Positive target droplets	Positive reference droplets	Total positive droplets	Raw CN	CN Corrected
AP3B1	10015	2035	3548	5583	1.06	1.1
BCL2	11554	3052	3643	6695	1.63	1.5
CCND1	11257	2081	3863	5944	0.99	1.3
CDK4	8811	2958	3575	6533	1.6	2.1
EGFR	9342	3077	3731	6808	1.59	1.9
ERBB2	9208	2988	3547	6535	1.64	2.4
FGFR1	4745	7945	3810	11755	5.51	8.3
FGFR2	8780	3532	3396	6928	2.1	2.7
FGFR3	9735	2837	3432	6269	1.6	2.1
FGFR4	10191	2086	3551	5637	1.09	2.1
MET	8010	1818	2827	4645	1.21	1.3
PDGFRA	10510	2605	3372	5977	1.49	1.4
PIK3CA	9896	1523	2663	4186	1.08	1.0
RPP30	9658	3689	1939	5628	4.12	5.4

H2077R-AZD

Gene	Negative droplets	Positive target droplets	Positive reference droplets	Total positive droplets	Raw CN	CN Corrected
AP3B1	13358	2430	4356	6786	1	0.8
BCL2	12926	1867	2229	4096	1.6	1.1
CCND1	10381	1892	2630	4522	1.4	1.3
CDK4	9970	3076	2673	5749	2.4	2.3
EGFR	10071	2717	2592	5309	2.1	2.0
ERBB2	10248	2994	2714	5708	2.2	2.4
FGFR1	5271	7110	2535	9645	7.4	8.4
FGFR2	11143	2672	2600	5272	2.1	2.0
FGFR3	11300	2234	2625	4859	1.7	1.6
FGFR4	12076	2123	2886	5009	1.4	2.0
MET	5126	6428	2321	8749	7.2	5.9
PDGFRA	11204	1728	2380	4108	1.4	1.0
PIK3CA	9835	911	1292	2203	1.4	0.9
RPP30	10766	2376	1568	3944	3.1	3.1

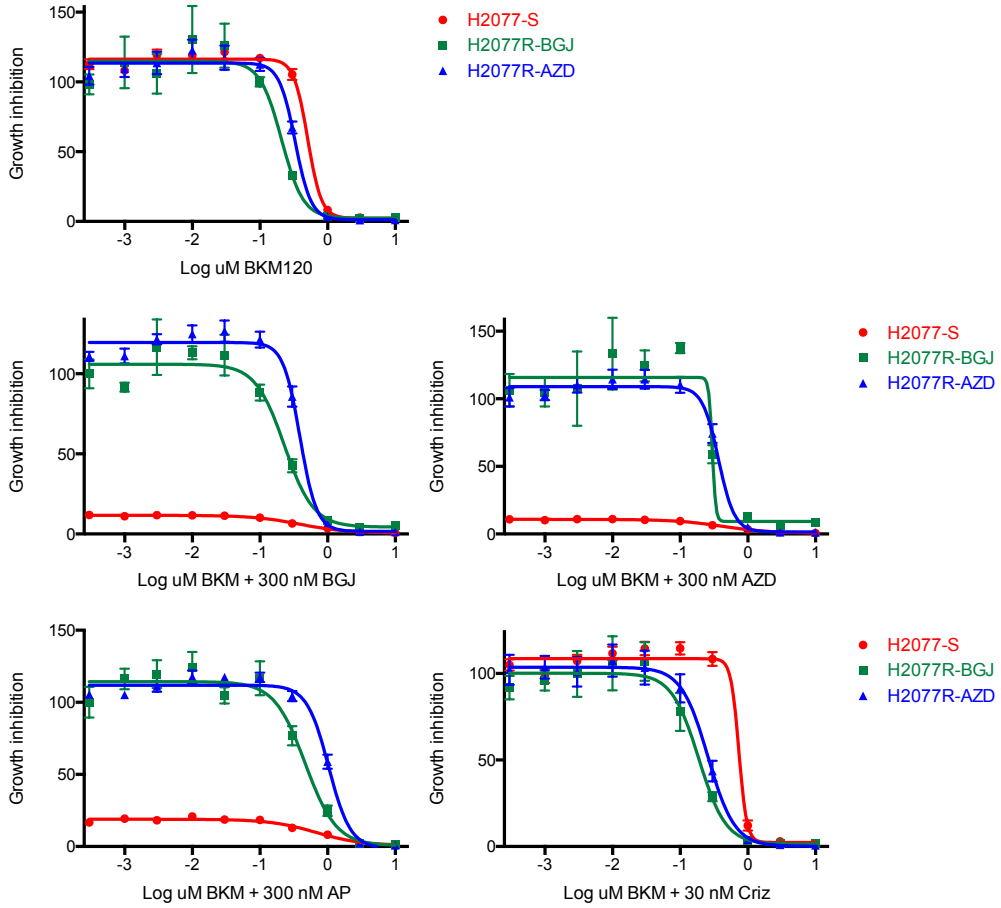

Figure 3-3. Sensitive and resistant cell lines are not inhibited by a PI3K inhibitor alone or in combination with FGFR or MET inhibitors.

BKM120, a pan-PI3K inhibitor, does not inhibit cells as a single agent (top image) or in combination with 300 nM BGJ398, AZD4547, AP24534 (ponatinib), or 30 nM crizotinib (bottom four images).

Illumina sequencing analysis identified five non-synonymous variants in each resistant line compared to the control sensitive line (Table 3-3), four of which were events in *MUC2* that were observed at the same loci in both resistant cell lines, suggestive of sequencing artifacts. One low-allelic-fraction (15.3%) novel event was observed in XPO1 in H2077R-AZD, and one NRAS Q61R mutation was identified in H2077R-BGJ at an approximate 30% allelic fraction with 148x coverage, an observation that was confirmed by a manual review of the sequencing reads (Figure 3-4A). NRAS Q61R is a known driver of cancer and a strong activator of the MAPK pathway (28). When treated with trametinib (29), a MEK inhibitor used to target MAPK pathway signaling, H2077R-BGJ cells were inhibited to a similar degree as H2077S cells, which showed a moderate sensitivity consistent with the predominance of FGFR signaling through the MAPK pathway. In contrast H2077R-AZD cells were substantially less sensitive to MEK inhibition, alone or in the presence of crizotinib, BGJ398, or AZD4547 (Figure 3-4B). No cell line was growth inhibited to zero, as would be expected with a cytotoxic effect of therapy, and indeed, previous research has shown a cytostatic effect of trametinib *in vitro* (30). We therefore treated cells with DMSO vehicle or trametinib at 5 nM and 500 nM for three days, fixed and stained with propidium iodide, and analyzed by flow cytometry to determine whether the cells treated with trametinib were predominantly in G1 phase, as would be expected if the drug had a cytostatic effect. As expected, more than 85% of H2077S and H2077R-BGJ cells were arrested in G1, with 2% or fewer cells in S phase, after treatment with 500 nM drug (Figure 3-4C, left and center panels). H2077R-AZD cells bearing *MET* amplifications, in contrast, still maintained more than 5% of cells in S phase even at 500 nM trametinib (Figure 3-4C, right panel), indicating a reduced dependence on the MAPK pathway as compared to the other cell lines. Treatment of cells with increasing concentrations of trametinib followed by lysis and

Table 3-3. Illumina sequencing of a panel of ~700 cancer and cancer-related genes reveals five acquired mutations in each resistant cell line.

Four mutations in each line are in *MUC2*, and are likely sequencing artifacts. H2077R-BGJ (R-BGJ) cells acquired an NRAS Q61R mutation and H2077R-AZD (R-AZD) cells acquired a low allelic fraction (15.3%), novel XPO1 mutation.

Gene	Protein Change	Chromosome	DNA Change (hg19)	Allelic Fraction (%)	Coverage
MUC2	L58P	11	g.1075747T>C	R-BGJ 22.6; R-AZD 43.2	75x; 44x
MUC2	E470Q	11	g.1081112G>C	R-BGJ 20; R-AZD 18.2	30x; 22x
MUC2	S562T	11	g.1081757G>C	R-BGJ 40.5; R-AZD 32.1	42x; 28x
MUC2	T1207I	11	g.1088835C>T	R-BGJ 25.4; R-AZD 56.5	71x; 46x
NRAS	Q61R	1	g.115256529A>G	R-BGJ 29.1	148x
XPO1	A377P	2	g.61721145G>C	R-AZD 15.3	131x

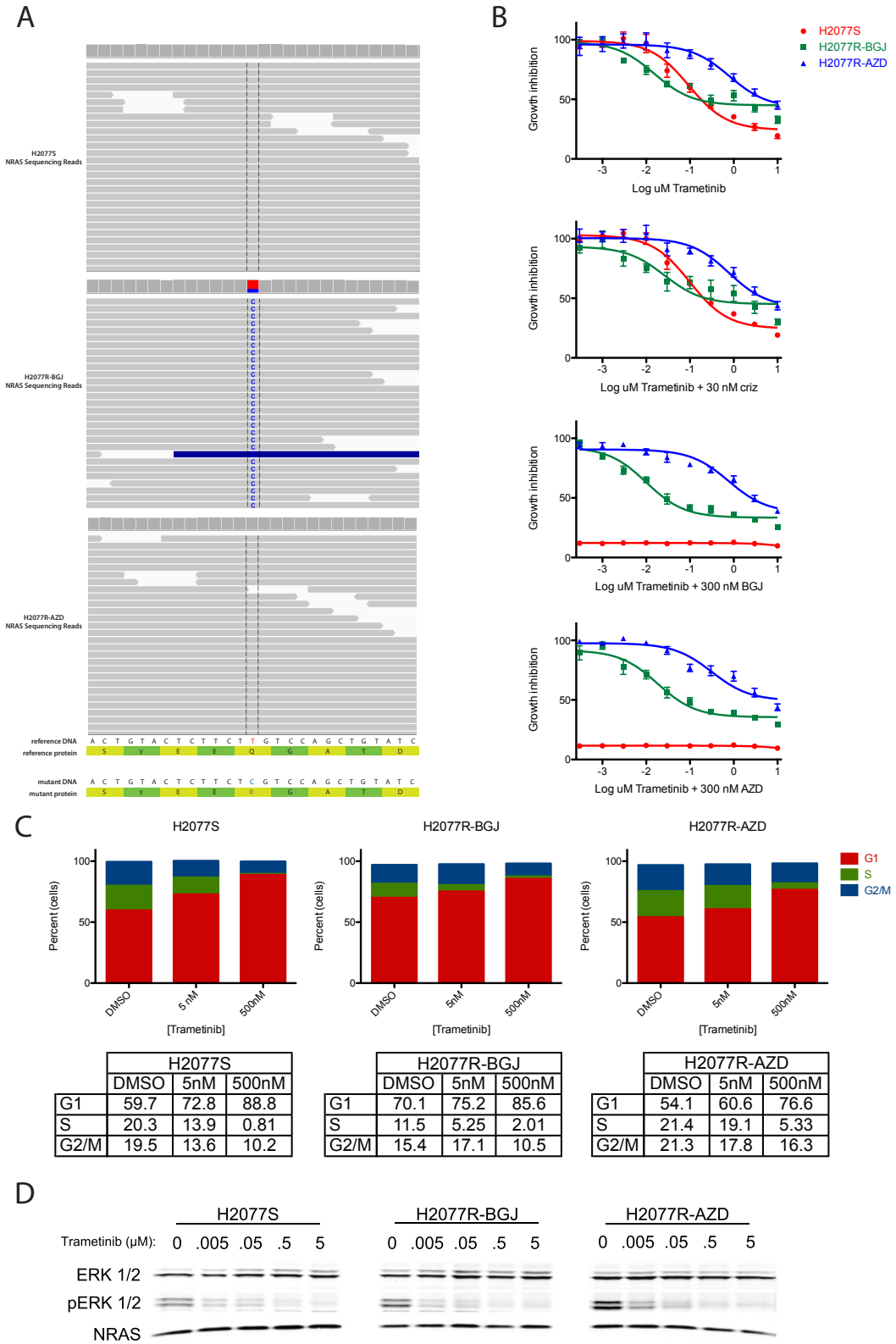

	H2077S		
	DMSO	5nM	500nM
G1	59.7	72.8	88.8
S	20.3	13.9	0.81
G2/M	19.5	13.6	10.2

	H2077R-BGJ		
	DMSO	5nM	500nM
G1	70.1	75.2	85.6
S	11.5	5.25	2.01
G2/M	15.4	17.1	10.5

	H2077R-AZD		
	DMSO	5nM	500nM
G1	54.1	60.6	76.6
S	21.4	19.1	5.33
G2/M	21.3	17.8	16.3

Figure 3-4. H2077R-BGJ cells have a secondary NRAS mutation, rendering them sensitive to inhibition of the MAPK pathway.

Figure 3-4 continued

(A) Illumina sequencing analysis of ~700 cancer and cancer-related genes in each cell line reveals a canonical NRAS Q61R mutation in H2077R-BGJ cells, present at about 30% allelic fraction (indicated by the red and blue bars over the sequencing reads). A schematic of the altered DNA and protein sequences is indicated below the three sequencing images.

(B) Trametinib, a specific MEK inhibitor used for MAPK pathway inhibition, preferentially inhibits H2077R-BGJ cells, with intermediate inhibition of H2077S cells and much less potent inhibition of H2077R-AZD cells (top panel). The observed inhibition is unchanged with combination treatments of crizotinib (second panel), BGJ398 (third panel), or AZD4547 (bottom panel).

(C) Trametinib arrests H2077R-BGJ cells in G1 at low concentrations, H2077S cells at intermediate concentrations, and H2077R-AZD cells incompletely even at higher concentrations, as measured by flow cytometry. Percentages of cells in each stage of the cell cycle after each treatment are indicated below the bar graphs.

(D) Trametinib inhibits phospho-ERK 1/2 at similar levels of drug in all three cell lines as measured by immunoblot. NRAS is expressed at similar levels in all three cell lines.

immunoblot demonstrated that MAPK activity was lost at the same concentration when all cell lines are treated with trametinib (Figure 3-4D), suggesting that unlike H2077S and H2077R-BGJ cells, H2077R-AZD cells have substantially decreased dependence on the MAPK pathway for survival.

Downstream signaling confirms MET and NRAS dependence in each respective resistant cell line and suggests a novel mechanism of MET-dependent FGFR1 activation

To biochemically confirm the results observed in the cell proliferation assays, we assessed regulation of downstream signaling in sensitive and resistant cells in the presence of BGJ398, AZD4547, and crizotinib. Cells that were treated with increasing concentrations of each drug were lysed and probed by immunoblot for phospho-MET, phospho-FRS2 (a downstream signal and readout for FGFR-dependent signaling (31)), phospho-AKT, and phospho-ERK.

Results were consistent with previous observations. MET and p-MET were upregulated in both resistant cell lines, but undetectable in sensitive parental lines, and p-MET activity was insensitive to both FGFR inhibitors (Figure 3-5A, B) but decreased at 10-100 nM to crizotinib (Figure 3-5C). p-AKT similarly was not detected in sensitive cells but was upregulated in resistant cells and showed dependence on MET signaling, consistent with the role of MET in stimulating signaling via the PI3K/AKT pathway (32).

p-ERK signaling differed between the three cell lines. p-ERK decreased at 10 nM as expected in the sensitive cell lines treated with FGFR inhibitors (Figure 3-5A, B) but not until 10 μM in crizotinib treatment (Figure 3-5C). Similarly, p-ERK was sustained in the presence of FGFR inhibitors for both H2077R-BGJ and –AZD (Figure 3-5A, B). However, under crizotinib treatment, p-ERK was lost in H2077R-AZD cells at 100 nM but sustained in –BGJ resistant cells

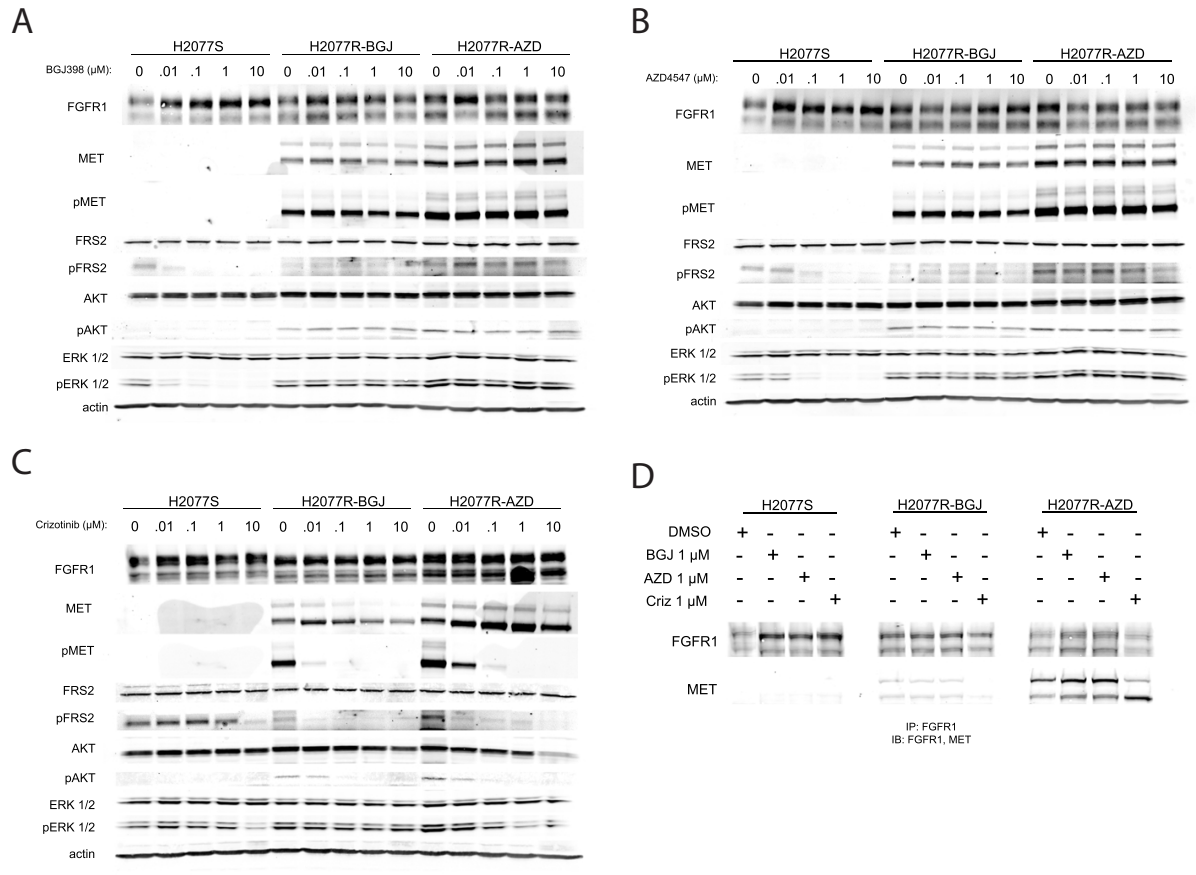

Figure 3-5. Downstream signaling demonstrates MET and NRAS dependence in each respective resistant cell line and suggests a novel mechanism for FGFR1-dependent MET activation.

(A) BGJ398 treatment alters downstream signaling of H2077S cells, but not resistant cells.

(B) AZD4547 treatment alters downstream signaling of H2077S cells but not resistant cells.

(C) Crizotinib treatment alters all downstream signaling in H2077R-AZD cells, and all signaling molecules except for p-ERK 1/2 signaling in H2077R-BGJ cells.

(D) Co-immunoprecipitation of FGFR1 and MET suggests a novel physical interaction between the two molecules, which is especially strong in H2077R-AZD cells.

through 10 μM of crizotinib; i.e., to an even greater extent than in parental cells insensitive to crizotinib treatment (Figure 3-5C). This is consistent with an *NRAS* oncogenic mutation that is a strong driver of MAPK signaling.

In contrast, H2077S cells showed loss of p-FRS2 by 100 nM of BGJ398 and AZD4547 (Figure 3-5A, B) but sustained signaling until 10 μM crizotinib (Figure 3-5C) as expected. However, we were surprised to observe that p-FRS2 signaling was restored in resistant cells, where activation was sustained during treatment with either FGFR inhibitor but lost at 10 nM crizotinib treatment (Figure 3-5A, B, C). This suggested a switch in p-FRS2 dependency to MET signaling from FGFR signaling, and was particularly strong in H2077R-AZD cells.

This switch appeared to be occurring at the receptor level. Screens for MET substrates have not identified FRS2 as a potential downstream signaling substrate for MET (33). Furthermore, we were unable to detect phospo-FGFR1 in sensitive parental cells (Figure 3-6A); however, in both resistant cell lines treated with AZD4547, p-FGFR1 is observed strongly, suggesting that phosphatase activity is being inhibited in the resistant cells no longer responsive to FGFR inhibition (Figure 3-6A, top panel). Indeed, crizotinib treatment abrogated the p-FGFR1 signal at 10 nM, suggesting that not only is FGFR1 no longer susceptible to FGFR targeted therapies, it is also dependent on MET signaling (Figure 3-6A, bottom panel).

This is consistent with previous observations of MET-driven resistance mediated through another RTK. For instance, MET amplification as a resistance mechanism in *EGFR*-mutant lung adenocarcinoma after erlotinib treatment was driven by MET-dependent activation of ErbB3 (8). In another study, HER2-positive breast cancer responses to trastuzumab were found to be dependent on MET signaling in preclinical models (34). A further report demonstrated that phosphorylation of EGFR, ErbB2, ErbB3, and RET were dependent on MET activity in several

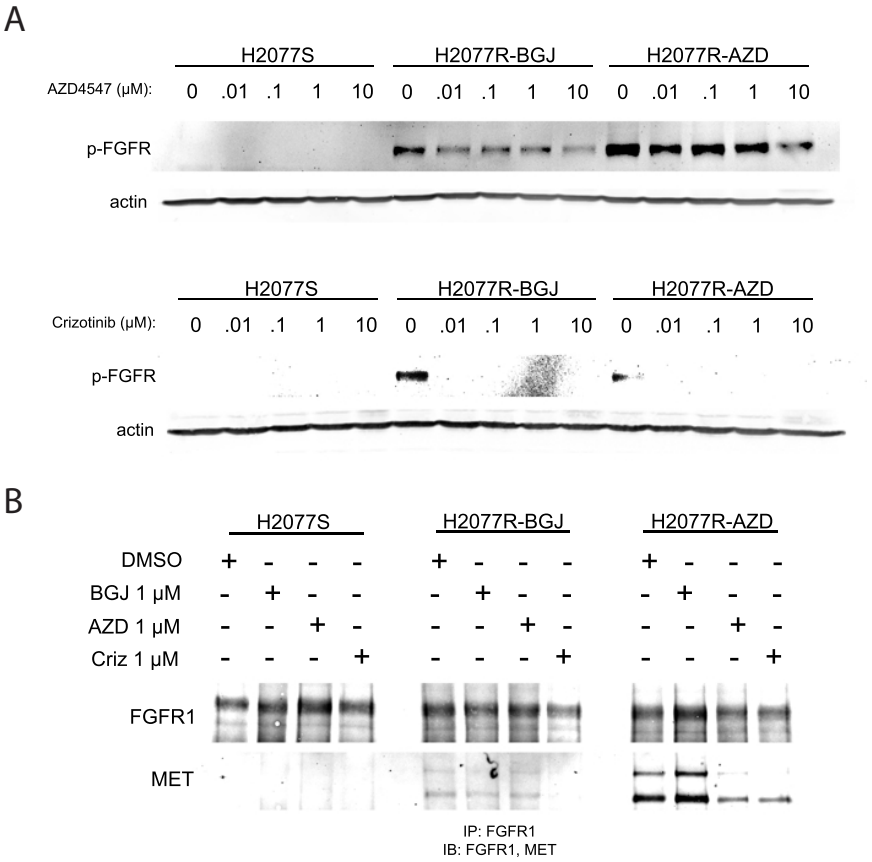

Figure 3-6. Phospho-FGFR signaling is dependent on MET signaling, possibly through a physical interaction.

(A) Resistant cells have upregulated phospho-FGFR1, which is unaffected by treatment with AZD4547 (top panel) but sensitive to crizotinib at 10 nM (bottom panel).

(B) Co-immunoprecipitation with a different anti-FGFR1 antibody from that used in Figure 3-5D demonstrates that MET and FGFR1 can interact in a manner that is not antibody specific.

lung cancer cell lines (35). No MET-associated dependency has been described for FGFR family members.

Several of these studies and others have gone on to suggest that the mechanism by which this dependency arises is through the formation of a complex, e.g., heterodimerization, between MET and the other RTK (8, 35-39). Indeed, taken together these studies suggest that MET has the capacity to activate diverse RTKs in the context of both development and oncogenesis through complex formation.

We therefore hypothesized that in MET may similarly interact with FGFR1 and is doing so in our resistant cells. We performed a coimmunoprecipitation of FGFR1 and MET in which we immunoprecipitated FGFR1 and immunoblotted for MET and FGFR1, and observed strong pulldown of MET in complex with FGFR1, particularly in H2077R-AZD cells (Figure 3-5D). Despite multiple attempts, we were unable to perform the reverse pulldown; however, we were able to repeat the FGFR1 pulldown with MET using a different antibody against FGFR1, indicating that our results are not antibody-specific (Figure 3-6B). These results are preliminary and additional work is required to clarify this relationship; however, we believe that they suggest a novel mechanism of activation of FGFR family members and further study may reveal this to be a novel mechanism of resistance to FGFR targeted therapies in resistant tumors with dependence on MET signaling.

DISCUSSION

Lung squamous cell carcinoma is a prevalent and deadly disease that until recently had few known targets and no targeted therapies available. With the completion of whole genome characterization studies of large cohorts of these tumors (16, 40), targets are being elucidated and

clinical trials are beginning for patients harboring relevant genomic events, many of which are activated kinases. One of the most promising targets at this time is alterations of FGFR kinases and multiple trials are underway of anti-FGFR therapy in this disease.

As almost universal resistance to kinase inhibitors eventually occurs in patients with solid organ cancers who respond to targeted therapies, it is of great clinical importance to elucidate resistance mechanisms *in vitro*. Here, we describe a new model of resistance to FGFR targeted therapies, which have recently been introduced in the clinic. Using a non-small cell lung cancer cell line with a focal *FGFR1* amplification and sensitive to FGFR inhibitors, NCI-H2077, we generated resistant clones in the presence of two specific, pan-FGFR inhibitors currently in clinical trials, BGJ398 and AZD4547. Contrary to our expectation that the resistant cells would develop gatekeeper mutations in *FGFR1*, we found that cells resistant to AZD4547 had acquired an amplification and upregulation of the MET protein and phospho-MET, and were sensitive to the MET inhibitor crizotinib, while cells resistant to BGJ398 had acquired a canonical NRAS Q61R mutation and were sensitive to MAPK pathway inhibition by the MEK inhibitor trametinib. Interestingly*, NRAS*-mutant cells also upregulated MET and phospho-MET levels, but were neither amplified at the *MET* locus nor sensitive to crizotinib treatment, alone or in combination with FGFR inhibitors or a MEK inhibitor.

MET is a receptor tyrosine kinase stimulated by hepatocyte growth factor (HGF) and known to influence signaling through the PI3K/AKT and MAPK pathways, among others (32). It has recently been reported that activation of either FGFRs or MET by ligand stimulation can rescue inhibition of cells dependent on MET or FGFRs, respectively (21). This is consistent with our observation that MET can act as a resistance mechanism in the context of FGFR targeted therapy; however, our model identifies an upregulation of MET, undetected in sensitive cells,

specifically in response to treatment with FGFR targeted therapies, suggesting a more complex role than simple rescue—that the expression and/or amplification of MET is itself a response to drug treatment. This is supported by the observation that both resistant cell lines had upregulated expression and phosphorylation of MET. It also suggests that initial MET expression may sustain drug-treated cells transiently, enabling long-term resistance to arise and be maintained by the eventual gain of a *MET* amplification or other stochastic event, such as secondary mutation of *NRAS*.

MET upregulation has been identified as a resistance mechanism to other therapies targeting receptor tyrosine kinases, in particular members of the ErbB family (8, 41), but unlike those cases, in which resistant cells are sensitive only upon inhibition of both MET and an ErbB family member, in our cell lines, MET inhibition alone is sufficient to inhibit cell growth. However, in these cells, we do observe MET-dependent FGFR signaling, including an increase in phospho-FGFR1 in resistant cells, and crizotinib-dependent loss of FGFR1 and FRS2 phosphorylation. FRS2 constitutively binds FGFR family members (42) and although it is known to bind other RTKs besides FGFRs, such as TrkA/B and RET (42-44), it has not been identified in screens for novel MET substrates (33), suggesting that it is unlikely that the switch in signaling is due to an association between FRS2 and MET.

Phospho-FGFR1 is not detected in sensitive parental cells, in which FGFR1 is the driving molecular alteration. This observation is likely due to the fact that normal FGFR signaling through the MAPK pathway leads to autoinhibition of receptor phosphorylation by phosphatases that are stimulated by MAPK signaling (45). This is why phospho-FRS2 is often used as a readout of FGFR signaling activity and is likely the reason that we were unable to detect p-FGFR1 in unstimulated sensitive cells. Indeed, we only observe p-FGFR1 after MET expression

arises in the resistant cells, suggesting that MET activity may be inhibiting normal phosphatase activity taking place during FGFR signaling while at the same time inhibiting the FGFR inhibitors from decreasing p-FGFR1.

These details suggest a model under which resistance emerges in NCI-H2077 cells. Under this model, normal FGFR-mediated signaling takes place in the absence of inhibition, driving oncogenic growth. During acute treatment with an FGFR tyrosine kinase inhibitor, FGFR1 activity is lost, and downstream signaling is abrogated. However, under prolonged drug treatment, MET expression is stimulated, resulting not only in activated MET, but also reinstated FGFR signaling by interaction between MET and FGFR1 and inhibition of the activity of the anti-FGFR compound. Then, this transient drug-resistant state enables cells to select for stable secondary genomic events, such as amplification or mutation, in order to maintain the resistance phenotype, as observed in both of our resistant cell lines.

Mechanisms of resistance have been identified previously after FGFR inhibitor treatment in FGFR2- or FGFR3-driven cancers including gastric, bladder, and multiple myeloma (21-23), and these studies suggest that a variety of mechanisms will be encountered in response to FGFR targeted therapy. Since FGFR1-dependent lung SqCC patients are now being treated with FGFR inhibitors in the clinic, models are required to study the resistance that will inevitably arise after prolonged drug treatment.

With this study, we therefore propose mechanisms of resistance that may arise in patients with FGFR-driven lung squamous cell carcinoma. It is our hope that these findings will improve treatment options for these patients once resistance to therapy occurs, thereby improving experience and outcomes for patients with this disease.

MATERIALS AND METHODS

Cell lines, inhibitors, and antibodies

NCI-H2077 cells were obtained from Drs. John D. Minna and Adi Gazdar, UT Southwestern Medical Center. Cells were maintained in RPMI containing 10% Fetal Bovine Serum and passaged every 3-4 days.

BGJ398, crizotinib, and ponatinib (AP24534) were purchased from Selleck. AZD4547 was purchased from Active Biochem. Trametinib was a generous gift from Dr. Cory Johannessen at The Broad Institute of Harvard and MIT (Cambridge, MA) and BKM120 was a generous gift from Dr. Mohamed Abazeed at Dana-Farber Cancer Institute (Boston, MA).

Antibodies used to detect FGFR1 by immunblot were obtained from Cell Signaling Technologies, Inc. (9740) and Santa Cruz Biotechnology, Inc. (sc-7945). Antibodies against MET (L41G3), p-MET (3077), p-FGFR (3471), p-FRS2 Y436, AKT (C67E7), p-AKT S473 (4060), ERK 1/2 (9107), p-ERK 1/2 (9101), and beta-actin (8H10D10) were obtained from Cell Signaling Technologies, Inc. Anti-FRS2 (H-91) was obtained from Santa Cruz Biotechnology, Inc.

Antibodies used for immunoprecipitation (IP) of FGFR1 are as follows. For the IP shown in Figure 3-5D, anti-FGFR1 was obtained from Santa Cruz Biotechnologies, Inc. (sc-121 AC). For the IP shown in Figure 3-6B, anti-FGFR1 was obtained from Cell Signaling Technologies, Inc. (3472).

The generation of resistant cells

NCI-H2077 cells were maintained in complete growth media at about 70% confluence. BGJ398 or AZD4547 were added to the media on one 10 cm plate of cells starting at 10 nM of

each drug. Every one to two weeks on average, when drugged cells resumed growth rates similar to parental cells, the drug concentration was increased by 50-100 nM. After about four months, resistant cells were maintained in 5 μM of each drug.

Genomic analysis of resistant cells

Genomic DNA was isolated from the sensitive and resistant cells using the DNeasy Blood and Tissue Kit (Qiagen) and sent to the Center for Cancer Genome Discovery at the Dana-Farber Cancer Institute (Boston, MA) and the Partners Laboratory for Molecular Medicine (Cambridge, MA) for analysis.

OncoPanelv2 represents a targeted sequencing strategy to simultaneously detect mutations, translocations and copy-number variations in archived clinical tumor specimen. Targeted sequencing was achieved by designing RNA baits to capture the exons of 504 genes with relevance to cancer. The bait set was augmented with specific intronic sequences to detect translocations often involved in cancer.

Sequencing libraries were prepared as described previously (46) from 100 ng of genomic DNA. Libraries were quantified by QPCR (Kapa Biosystems, Inc, Woburn, MA) and pooled in equimolar concentrations to 500 ng total and enriched for the Oncopanel_v2 baitset using the Agilent SureSelect hybrid capture kit. The enriched targeted exon libraries were again quantified by QPCR and subsequently sequenced in one lane of a Hiseq2000 sequencer (Illumina Inc, San Diego, CA) in the 2 x 100 bp pair-end mode. Sequence alignment, demultiplexing and variant calling, including single nucleotide variants (SNVs) and insertions/deletions (indels), was performed using PICARD, GATK tools, Mutect and IndeLocator as described previously (46).

Copy number analysis was performed using Nexus7.1 (BioDiscovery, Inc.) after calculating read counts using the ngCGH tool (https://github.com/seandavi/ngCGH). Copy number variants (CNVs) were called with the following BAM-ngCGH settings: significance threshold = 1E-6; max contiguous probe spacing or 1000 kbp; minimum number of probes per segment = 3. CNV gains have a log ratio >0.4 and were called high gains if >1. Single copy loss threshold was <-0.8 and large loss was <-2.

Copy number of 12 target loci (*BCL2*, *CCND1*, *CDK4*, *ERBB2*, *EGFR*, *FGFR1*, *FGFR2*, *FGFR3*, *FGFR4*, *MET*, *PDGFRA*, *PIK3CA*) was validated by droplet digital PCR (ddPCR, BioRad CX100), as described previously (47). For each target locus, two TaqMan (Life Technologies) MGB probes were used to measure the concentration of target-specific molecules relative to the concentration of reference locus molecules. *RPP30* (chr10q23) was used as the reference locus for each assay. Quantification of these concentrations provided a ratio of the target to the reference loci, and the measurement was expressed as an absolute copy number. A total of 24 ng of genomic DNA was analyzed for each target locus. To minimize aneusomy at the reference loci, the reference locus (*RPP30*) was interrogated against two additional reference loci (*AP3B1*, chr5q14; *NFAT5*, chr16q22) such that each target locus was normalized to the average concentration of the three reference loci.

Inhibitor studies for growth inhibition

Five thousand cells per well were seeded into 96-well plates in 100 µL media. 10 µL drug was added in quadruplicate for final concentrations of 0.3 nM-10 µM in half logs, or 3 nM-100 µM in half logs, with eight DMSO control wells, and incubated for four or five days. For combination inhibitor studies, the same seeding and drugging protocol was followed except that

final concentration of 30 nM or 300 nM of the second drug was also included in all wells except the DMSO controls. After incubation, 50 μL Cell Titer Glo (Promega) was added to each well and luminescence was measured on the SpectroMax 5 or the SpectroMax LM imager. Percent growth inhibition compared to DMSO controls was calculated and plotted in Prism (GraphPad Software, Inc).

Immunoblot and coimmunoprecipitation

Cells were lysed in buffer containing 0.5% NP-40, 50 mM Tris pH 8, 150 mM MgCl2, and phosphatase and protease inhibitors, and proteins were separated by SDS/PAGE and transferred to nitrocellulose membranes via the iBlot dry transfer system (Life Technologies). Antibody binding was detected using the LI-COR Odyssey IR imaging system (LI-COR Biosciences).

To confirm loss of phosphorylation of relevant kinases in the presence of inhibitor, cells were washed with PBS and serum starved overnight in the presence of indicated concentrations of inhibitor prior to lysis.

To identify potential interactions between FGFR1 and MET, on the same day as cell lysis, 500 μg protein was incubated with 30 μL (sc-121 AC) or 7 μL (3472) anti-FGFR1 antibody on a rotator overnight at 4°C. Lysates incubated with sc-121 AC were then washed four times with 500 μL cold lysis buffer, boiled with loading buffer and reducing agent, and loaded into gels as described above. Lysates incubated with anti-FGFR1 antibody #3472 were then incubated with Protein A Agarose (Life Technologies) for two hours on a rotator at 4°C, then washed, reduced, and loaded into gels as described above.

Cell cycle analysis using flow cytometry

To determine cell cycle stage after drug treatment, 300,000 cells were seeded into 10 cm plates and treated with indicated concentrations of trametinib for 72 hours. Media and cells were moved to a 15 mL tube and resuspended in 300 μL PBS. 5 mL of ice-cold 100% methanol was slowly added dropwise to each tube with constant gentle vortexing and tubes were immediately placed at -20°C and incubated overnight. Cells were then resuspended in 5 mL cold PBS and incubated on ice for one hour, after which they were resuspended in 500 μL staining solution, which consisted of 25 μg/mL propidium iodide and 50 μg/mL RNaseA in PBS, and incubated for 30 minutes at room temperature while protected from light. DNA content was measured using the FACS LSR (BD Biosciences) with the FACSDiva software and analyzed with FlowJo (Tree Star, Inc).

ACKNOWLEDGEMENTS

The authors thank Ms. Leslie Gaffney at The Broad Institute of Harvard and MIT (Cambridge, MA) for multimedia support.

REFERENCES

1. Beroukhim R, Mermel CH, Porter D, Wei G, Raychaudhuri S, Donovan J, et al. The landscape of somatic copy-number alteration across human cancers. Nature. 2010;463(7283):899-905. PMCID: 2826709.

2. Chapman MA, Lawrence MS, Keats JJ, Cibulskis K, Sougnez C, Schinzel AC, et al. Initial genome sequencing and analysis of multiple myeloma. Nature. 2011;471(7339):467-72. PMCID: 3560292.

3. Weir BA, Woo MS, Getz G, Perner S, Ding L, Beroukhim R, et al. Characterizing the cancer genome in lung adenocarcinoma. Nature. 2007;450(7171):893-8. PMCID: 2538683.

4. Stegmeier F, Warmuth M, Sellers WR, Dorsch M. Targeted cancer therapies in the twenty-first century: lessons from imatinib. Clin Pharmacol Ther. 2010;87(5):543-52.

5. Ellis LM, Hicklin DJ. Resistance to Targeted Therapies: Refining Anticancer Therapy in the Era of Molecular Oncology. Clinical cancer research : an official journal of the American Association for Cancer Research. 2009;15(24):7471-8.

6. Azam M, Latek RR, Daley GQ. Mechanisms of autoinhibition and STI-571/imatinib resistance revealed by mutagenesis of BCR-ABL. Cell. 2003;112(6):831-43.

7. Milojkovic D, Apperley J. Mechanisms of Resistance to Imatinib and Second-Generation Tyrosine Inhibitors in Chronic Myeloid Leukemia. Clinical cancer research : an official journal of the American Association for Cancer Research. 2009;15(24):7519-27.

8. Engelman JA, Zejnullahu K, Mitsudomi T, Song Y, Hyland C, Park JO, et al. MET amplification leads to gefitinib resistance in lung cancer by activating ERBB3 signaling. Science. 2007;316(5827):1039-43.

9. Kosaka T, Yatabe Y, Endoh H, Yoshida K, Hida T, Tsuboi M, et al. Analysis of epidermal growth factor receptor gene mutation in patients with non-small cell lung cancer and acquired resistance to gefitinib. Clinical cancer research : an official journal of the American Association for Cancer Research. 2006;12(19):5764-9.

10. Balak MN, Gong Y, Riely GJ, Somwar R, Li AR, Zakowski MF, et al. Novel D761Y and common secondary T790M mutations in epidermal growth factor receptor-mutant lung adenocarcinomas with acquired resistance to kinase inhibitors. Clinical cancer research : an official journal of the American Association for Cancer Research. 2006;12(21):6494-501.

11. Johannessen CM, Boehm JS, Kim SY, Thomas SR, Wardwell L, Johnson LA, et al. COT drives resistance to RAF inhibition through MAP kinase pathway reactivation. Nature. 2010;468(7326):968-72. PMCID: 3058384.

12. Turner N, Grose R. Fibroblast growth factor signalling: from development to cancer. Nat Rev Cancer. 2010;10(2):116-29.

13. Chesi M, Nardini E, Brents LA, Schrock E, Ried T, Kuehl WM, et al. Frequent translocation t(4;14)(p16.3;q32.3) in multiple myeloma is associated with increased expression and activating mutations of fibroblast growth factor receptor 3. Nat Genet. 1997;16(3):260-4.

14. Liao RG, Jung J, Tchaicha JH, Wilkerson MD, Sivachenko A, Beauchamp EM, et al. Inhibitor-sensitive FGFR2 and FGFR3 mutations in lung squamous cell carcinoma. Cancer Res. 2013.

15. Dutt A, Ramos AH, Hammerman PS, Mermel C, Cho J, Sharifnia T, et al. Inhibitor-sensitive FGFR1 amplification in human non-small cell lung cancer. PLoS ONE. 2011;6(6):e20351. PMCID: 3110189.

16. Hammerman PS, Lawrence MS, Voet D, Jing R, Cibulskis K, Sivachenko A, et al. Comprehensive genomic characterization of squamous cell lung cancers. Nature. 2012.

17. Singh D, Chan JM, Zoppoli P, Niola F, Sullivan R, Castano A, et al. Transforming fusions of FGFR and TACC genes in human glioblastoma. Science. 2012;337(6099):1231-5. PMCID: 3677224.

18. Wu YM, Su F, Kalyana-Sundaram S, Khazanov N, Ateeq B, Cao X, et al. Identification of Targetable FGFR Gene Fusions in Diverse Cancers. Cancer discovery. 2013;3(6):636-47. PMCID: 3694764.

19. Dieci MV, Arnedos M, Andre F, Soria JC. Fibroblast growth factor receptor inhibitors as a cancer treatment: from a biologic rationale to medical perspectives. Cancer discovery. 2013;3(3):264-79.

20. Greulich H, Pollock PM. Targeting mutant fibroblast growth factor receptors in cancer. Trends in molecular medicine. 2011;17(5):283-92.

21. Harbinski F, Craig VJ, Sanghavi S, Jeffery D, Liu L, Sheppard KA, et al. Rescue screens with secreted proteins reveal compensatory potential of receptor tyrosine kinases in driving cancer growth. Cancer discovery. 2012;2(10):948-59.

22. Chell V, Balmanno K, Little AS, Wilson M, Andrews S, Blockley L, et al. Tumour cell responses to new fibroblast growth factor receptor tyrosine kinase inhibitors and identification of a gatekeeper mutation in FGFR3 as a mechanism of acquired resistance. Oncogene. 2013;32(25):3059-70.

23. Herrera-Abreu MT, Pearson A, Campbell J, Shnyder SD, Knowles MA, Ashworth A, et al. Parallel RNA interference screens identify EGFR activation as an escape mechanism in FGFR3 mutant cancer. Cancer discovery. 2013.

24. Frequent and focal FGFR1 amplification associates with therapeutically tractable FGFR1 dependency in squamous cell lung cancer, (2010).

25. Guagnano V, Furet P, Spanka C, Bordas V, Le Douget M, Stamm C, et al. Discovery of 3-(2,6-dichloro-3,5-dimethoxy-phenyl)-1-{6-[4-(4-ethyl-piperazin-1-yl)-phenylamino]-pyrimidin-4-yl}-1-methyl-urea (NVP-BGJ398), a potent and selective inhibitor of the fibroblast growth factor receptor family of receptor tyrosine kinase. J Med Chem. 2011;54(20):7066-83.

26. Gavine PR, Mooney L, Kilgour E, Thomas AP, Al-Kadhimi K, Beck S, et al. AZD4547: An orally bioavailable, potent and selective inhibitor of the Fibroblast Growth Factor Receptor tyrosine kinase family. Cancer Res. 2012:1-41.

27. Maira SM, Pecchi S, Huang A, Burger M, Knapp M, Sterker D, et al. Identification and characterization of NVP-BKM120, an orally available pan-class I PI3-kinase inhibitor. Molecular cancer therapeutics. 2012;11(2):317-28.

28. Bos JL. ras oncogenes in human cancer: a review. Cancer Res. 1989;49(17):4682-9.

29. Gilmartin AG, Bleam MR, Groy A, Moss KG, Minthorn EA, Kulkarni SG, et al. GSK1120212 (JTP-74057) is an inhibitor of MEK activity and activation with favorable pharmacokinetic properties for sustained in vivo pathway inhibition. Clinical cancer research : an official journal of the American Association for Cancer Research. 2011;17(5):989-1000.

30. Watanabe M, Sowa Y, Yogosawa M, Sakai T. Novel MEK inhibitor trametinib and other retinoblastoma gene (RB)-reactivating agents enhance efficacy of 5-fluorouracil on human colon cancer cells. Cancer Sci. 2013;104(6):687-93.

31. Xu H, Lee KW, Goldfarb M. Novel recognition motif on fibroblast growth factor receptor mediates direct association and activation of SNT adapter proteins. The Journal of biological chemistry. 1998;273(29):17987-90.

32. Organ SL, Tsao MS. An overview of the c-MET signaling pathway. Ther Adv Med Oncol. 2011;3(1 Suppl):S7-S19. PMCID: 3225017.

33. Schaaf CP, Benzing J, Schmitt T, Erz DH, Tewes M, Bartram CR, et al. Novel interaction partners of the TPR/MET tyrosine kinase. FASEB J. 2005;19(2):267-9.

34. Shattuck DL, Miller JK, Carraway KL, 3rd, Sweeney C. Met receptor contributes to trastuzumab resistance of Her2-overexpressing breast cancer cells. Cancer Res. 2008;68(5):1471-7.

35. Tanizaki J, Okamoto I, Sakai K, Nakagawa K. Differential roles of trans-phosphorylated EGFR, HER2, HER3, and RET as heterodimerisation partners of MET in lung cancer with MET amplification. British journal of cancer. 2011;105(6):807-13. PMCID: 3171021.

36. Jo M, Stolz DB, Esplen JE, Dorko K, Michalopoulos GK, Strom SC. Cross-talk between epidermal growth factor receptor and c-Met signal pathways in transformed cells. The Journal of biological chemistry. 2000;275(12):8806-11.

37. Ishibe S, Karihaloo A, Ma H, Zhang J, Marlier A, Mitobe M, et al. Met and the epidermal growth factor receptor act cooperatively to regulate final nephron number and maintain collecting duct morphology. Development. 2009;136(2):337-45. PMCID: 2862758.

38. Guo A, Villen J, Kornhauser J, Lee KA, Stokes MP, Rikova K, et al. Signaling networks assembled by oncogenic EGFR and c-Met. Proceedings of the National Academy of Sciences of the United States of America. 2008;105(2):692-7. PMCID: 2206598.

39. Mueller KL, Yang ZQ, Haddad R, Ethier SP, Boerner JL. EGFR/Met association regulates EGFR TKI resistance in breast cancer. J Mol Signal. 2010;5:8. PMCID: 2911419.

40. Govindan R, Ding L, Griffith M, Subramanian J, Dees ND, Kanchi KL, et al. Genomic landscape of non-small cell lung cancer in smokers and never-smokers. Cell. 2012;150(6):1121-34. PMCID: 3656590.

41. Bardelli A, Corso S, Bertotti A, Hobor S, Valtorta E, Siravegna G, et al. Amplification of the MET Receptor Drives Resistance to Anti-EGFR Therapies in Colorectal Cancer. Cancer discovery. 2013;3(6):658-73.

42. Gotoh N. Regulation of growth factor signaling by FRS2 family docking/scaffold adaptor proteins. Cancer Sci. 2008;99(7):1319-25.

43. Kurokawa K, Iwashita T, Murakami H, Hayashi H, Kawai K, Takahashi M. Identification of SNT/FRS2 docking site on RET receptor tyrosine kinase and its role for signal transduction. Oncogene. 2001;20(16):1929-38.

44. Santoro M, Carlomagno F, Melillo RM, Fusco A. Dysfunction of the RET receptor in human cancer. Cell Mol Life Sci. 2004;61(23):2954-64.

45. Tsang M, Dawid IB. Promotion and attenuation of FGF signaling through the Ras-MAPK pathway. Sci STKE. 2004;2004(228):pe17.

46. Hettmer S, Teot LA, van Hummelen P, Macconaill L, Bronson RT, Dall'osso C, et al. Mutations in Hedgehog pathway genes in fetal rhabdomyomas. J Pathol. 2013.

47. Boettger LM, Handsaker RE, Zody MC, McCarroll SA. Structural haplotypes and recent evolution of the human 17q21.31 region. Nat Genet. 2012;44(8):881-5.

CHAPTER 4

EphA3 is significantly mutated in lung adenocarcinoma and is of unknown clinical importance

ATTRIBUTIONS

All experiments and analyses were performed by Rachel G. Liao.

Figure 4-1B is adapted from Figure S2B in the following:

Heidi Greulich[1,4,6,8], Bethany Kaplan[1,8], Philipp Mertins[8], Tzu-Hsiu Chen[8], Kumiko Tanaka[1,8], Cai-Hong Yun[9], Xiaohong Zhang[1], Se-Hoon Lee[1], Jeonghee Cho[1], Lauren Ambrogio[8], Rachel Liao[1,8], Marcin Imielinski[1,8], Shantanu Banerji[1,8], Michael S. Lawrence[8], Jinghui Zhang[10], Nam H. Pho[1,8], Sarah R. Walker[1], Wendy Winckler[8], Gad Getz[8], David Frank[1], William C. Hahn[1,2,4,8], Michael Eck[3], Jacob D. Jaffe[8], Steven A. Carr[8], Kwok-Kin Wong[1,4,6], and Matthew Meyerson[1,2,5,7,8]. (2012). Functional analysis of receptor tyrosine kinase mutations in lung cancer identifies oncogenic extracellular domain mutations of *ERBB2*. *PNAS* 109(36): 14476-81.

[1]Department of Medical Oncology,

[2]Center for Cancer Genome Discovery, and

[3]Cancer Biology, Dana-Farber Cancer Institute, Boston, MA 02115

[4]Department of Medicine and

[5]Department of Pathology, Brigham and Women's Hospital, Boston, MA 02115

[6]Department of Medicine and

[7]Department of Pathology, Harvard Medical School, Boston, MA 02115

[8]Broad Institute of Harvard and MIT, Cambridge, MA 02142

[9]Department of Biophysics, Peking University Health Science Center, Beijing 100191, China

[10]Departments of Biotechnology and Computational Biology, St. Jude Children's Research Hospital, Memphis, TN 38105

Chapter 4. EphA3 is significantly mutated in lung adenocarcinoma and is of unknown clinical importance

SUMMARY

EphA3, a member of the Eph receptor tyrosine kinase family, is a membrane-bound protein studied predominantly in the context of embryonic development. In the past several years, EphA3 and its family members have also been studied in the context of cancer formation and progression. Recently, sequencing of lung adenocarcinoma paired tumor-normal samples revealed a statistically significant number of somatic mutations in *EphA3*—11 in 188 samples. This was the first observation of *EphA3* mutations at levels above background in lung cancer, and suggested that mutations in this kinase might drive oncogenesis in lung cancer, as is the case with other significantly mutated kinases. When tested, however, we found that exogenous expression of the mutations had no measurable effect on colony forming potential in NIH-3T3 cells. Nor could we detect expression of EphA3 in cancer cell lines harboring *EphA3* mutations, as would be expected if the mutations were active. Further, ligand stimulation studies suggest that some of the observed mutations may be loss-of-function (LOF), further negating the hypothesis that these mutations drive a cancer phenotype. These observations were further supported by recent lung adenocarcinoma sequencing data in which several *EphA3* alterations occurred as nonsense, splice site, or frame shift mutations, as would be expected in a LOF context. Therefore, we conclude that, though *EphA3* is significantly mutated in lung adenocarcinoma, it does not fit the standard model for oncogenic kinases in cancer to acquire gain-of-function, driving alterations. While it is certainly possible that this LOF phenotype contributes to cancer development or maintenance as a tumor suppressor, more work is required to define its role in lung adenocarcinoma.

BACKGROUND

Chapter 4. EphA3 is significantly mutated in lung adenocarcinoma and is of unknown clinical importance

In recent years, whole genome characterization has had a pronounced effect on the way that potential cancer targets are identified. Whole genome sequencing allows an unbiased scan of the genome for cancer-associated alterations, providing a detection approach not powered solely to detect common variants in diseased populations.

This was the rationale behind a 2008 study in which 623 genes, including all tyrosine kinases, were sequenced in 188 lung adenocarcinoma tumors along with corresponding normal tissue, and somatic point mutations and copy number alterations were identified and annotated (1). In this analysis, many genes previously described as mutated in lung adenocarcinoma were observed, such as *TP53, KRAS,* and *EGFR.* Also as expected, many genes with no prior association with lung adenocarcinoma were observed containing significant alterations. One of the most significantly altered genes was the receptor tyrosine kinase (RTK) Eph receptor A3 (EphA3) (1).

The Eph receptor family is the largest family of receptor tyrosine kinases (2). They become activated by binding members of the membrane-bound ephrin *(eph-r*eceptor-*in*teracting) ligand family. There are 14 Eph receptors in mammals (including nine EphA and five EphB receptors) and eight ligands (including five ephrin-As and three ephrin-Bs) (2). Eph receptors often interact with more than one ephrin but display higher affinity for certain ephrins over others, and for the most part, EphA receptors interact with ephrin-A ligands and EphB receptors with ephrin-B ligands (3). Ligand stimulation activates morphological changes including cytoskeletal remodeling, which can ultimately lead to motility in cells expressing activated kinases (4).

Eph receptors and ephrins must be expressed by separate cells in order to stimulate activation, as expression in *cis* has been shown to abrogate activity via poorly understood

mechanisms (5). Activation mediates a bidirectional cascade of signals into both the Eph-expressing and ephrin-expressing cells (2). These signaling cascades often trigger either internalization of the activated receptor-ligand complexes to continue signaling within the cell, or proteolytic cleavage of the Eph-ephrin complex (via proteases such as ADAM10 in the case of EphA3 (6)) which leads to internalization, degradation, and down-regulation of Eph expression in the cells (2).

EphA3 encodes a 983 amino acid protein that has been well-studied for its role in embryonic development (7). It acts through both adhesive and repulsive forces to influence diverse populations of cells during axon guidance, and its loss has been shown to lead to defects in gastrulation in zebrafish (8). In the retina, EphA3 geographically directs developing ganglion cells (9); it is also required for normal cardiac development in mice (10).

Eph receptors have not been well studied in cancer, but some alterations have been identified. For example, EphA3 is overexpressed in melanoma, sarcoma, and renal cancer (11, 12) and other Eph receptors are upregulated in breast, liver, and colon cancer (13). EphA3 mutations have also been previously observed in lung cancer samples and cell lines, in both the extracellular domain (ECD) and kinase domain (14, 15).

EphA3 was significantly mutated in a 2008 survey of 188 lung adenocarcinoma samples (1). The eleven novel mutations (Table 4-1) were missense events that did not demonstrate significant clustering. Several were in functional domains; for example, one kinase domain mutation (K761N) is at a residue homologous to that of the kinase "molecular brake" in another RTK, FGFR2 (16) and is designated “probably damaging” by structural analysis (Table 4-1). We hypothesize that these mutations may drive oncogenesis in a subset of lung adenocarcinoma, and here describe preliminary data generated while testing this hypothesis.

Table 4-1. EphA3 mutations identified in lung adenocarcinoma sequencing data.

Eleven missense mutations were identified along the length of the EphA3 protein in 188 lung adenocarcinoma samples. Amino acid change is listed with Polyphen score (PBD: probably damaging; B: benign; PSD: possibly damaging) and Pfam protein domain (LBD: ligand binding domain; Cys-rich: Cysteine rich region; FN3: fibronectin type-III domain; TKD: tyrosine kinase domain).

Amino acid change	Polyphen score	Pfam domain
p.T166N	PBD	Ephrin LBD
p.G187R	PBD	Ephrin LBD
p.W250R	PBD	Cys-rich
p.M269I	B	Cys-rich
p.N379K	B	FN3
p.T393K	B	FN3
p.A435S	B	FN3
p.D446Y	B	FN3
p.D678E	B	TKD
p.R728L	PSD	TKD
p.K761N	PBD	TKD

RESULTS

EphA3 mutations are not transforming in standard cellular assays and are not expressed in *EphA3*-mutant cell lines

A common mechanism driving cancer is the aberrant activation of kinases, and in lung adenocarcinoma, receptor tyrosine kinases have frequently been implicated in oncogenesis (17-19). Altered RTKs are compelling targets for therapy, as their inhibition results in fewer side effects than conventional chemotherapy in appropriately selected tumors, and their presence can act as a biomarker predicting therapeutic response (20). We therefore sought to determine whether *EphA3* mutations were activating, enabling the potential to drive oncogenesis in lung adenocarcinoma.

Members of our group first introduced these mutations into NIH-3T3 cells and seeded them into soft agar to evaluate whether the mutations could confer anchorage-independent growth. Surprisingly, they did not (21)—even the kinase domain mutation homologous to part of the "molecular brake" in FGFR2 (16) was not transforming in this assay. We observed that 293T cells transiently transfected with *EphA3* wild type cDNA did cause rounding and blebbing in the presence of ligand—thus repeating previous work (4) and demonstrating a functional EphA3 protein product (Figure 4-1A).

Since the exogenous expression of EphA3 did not demonstrate a transformation phenotype, we sought cancer cell lines with endogenous mutant *EphA3* to determine protein function in a physiologically relevant setting. Three lung cancer cell lines, HCC15, HCC515, and NCI-H1770, have been described previously to have missense mutations in *EphA3* (14, 15) and we began testing them to determine the role of EphA3 on their growth and development and their potential as models for therapeutic development.

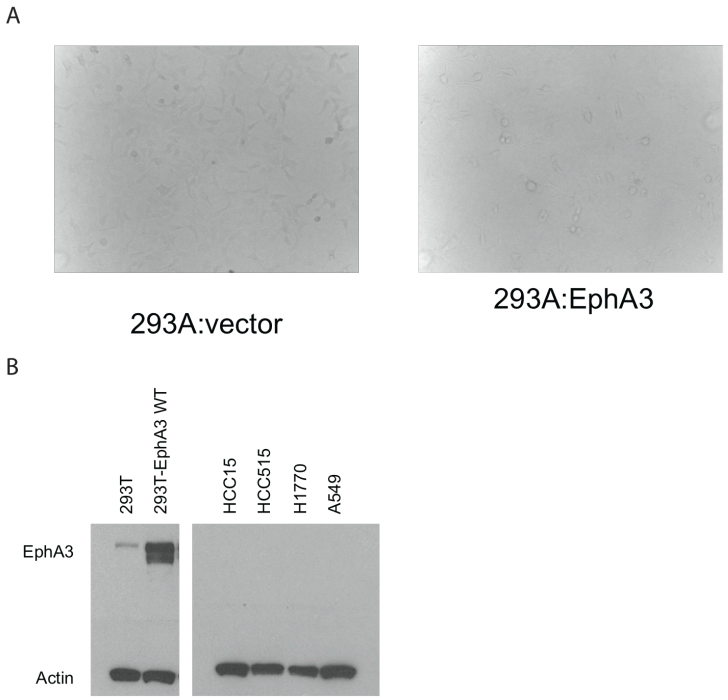

Figure 4-1. Exogenously expressed EphA3 has normal functionality, but endogenous EphA3 mutations are not expressed in lung cancer cell lines.

(A) 293A cells expressing vector control (left panel) or wild type EphA3 (right panel) were stimulated with preclustered ephrin-A5 as described previously (4). Exogenously expressed EphA3 showed a rounding and blebbing phenotype while vector control did not, consistent with prior observations.

(B) Lung cancer cell lines HCC15, HCC515, and H1770 have *EphA3* point mutations but do not express EphA3, while 293T cells transduced with exogenously expressed EphA3 readily express the protein product. Lung cancer cell line A549 has wild type EphA3 and also does not express EphA3.

However, this plan was immediately cut short when initial experiments demonstrated that none of the three cell lines expressed any detectable EphA3 (Figure 4-1B). While in transiently transfected 293T cells it was readily detectable (left panel), expression was not observed in any of the three mutant cell lines or in an *EphA3*-wild type cell line A549 (right panel). This finding further suggested that mutant EphA3 may not be functioning as a transforming oncogene.

Ligand studies suggest that some EphA3 mutations may be loss of function

Having acquired only negative readouts of EphA3 activity, we sought to identify a positive phenotype by which we could study the functional impact of EphA3. EphA3 is known to interact with a membrane-bound ligand, ephrin-A5, which stimulates EphA3 phosphorylation activity under normal developmental contexts (4). We stimulated wild type EphA3-expressing 293A cells with recombinant ephrin-A5 and were able to detect an increase in phospho-EphA3 by immunoblot with an anti-phospho-tyrosine antibody (Figure 4-2A). Due to the presence of other bands by this method (Figure 4-2A, right panel), we went on to perform immunoprecipitation for phospho-tyrosine followed by immunoblot for EphA3 to detect activated EphA3, which was cleaner (Figure 4-2B).

Having established a readout for EphA3 activation, we began to test several of the most promising candidate mutations, amino acid changes K761N in the EphA3 kinase domain and T166N and W250R in the ECD by this method. We had hypothesized that EphA3 K761N would drive greater signaling than wild type due to its homology with a molecular brake in FGFR2 (16); however, we found that its phosphorylation pattern was identical to wild type EphA3 (Figure 4-2C). In contrast, ECD mutants T166N and W250R showed decreased phosphorylation compared to wild type EphA3, suggesting that those mutations introduced a loss of ligand

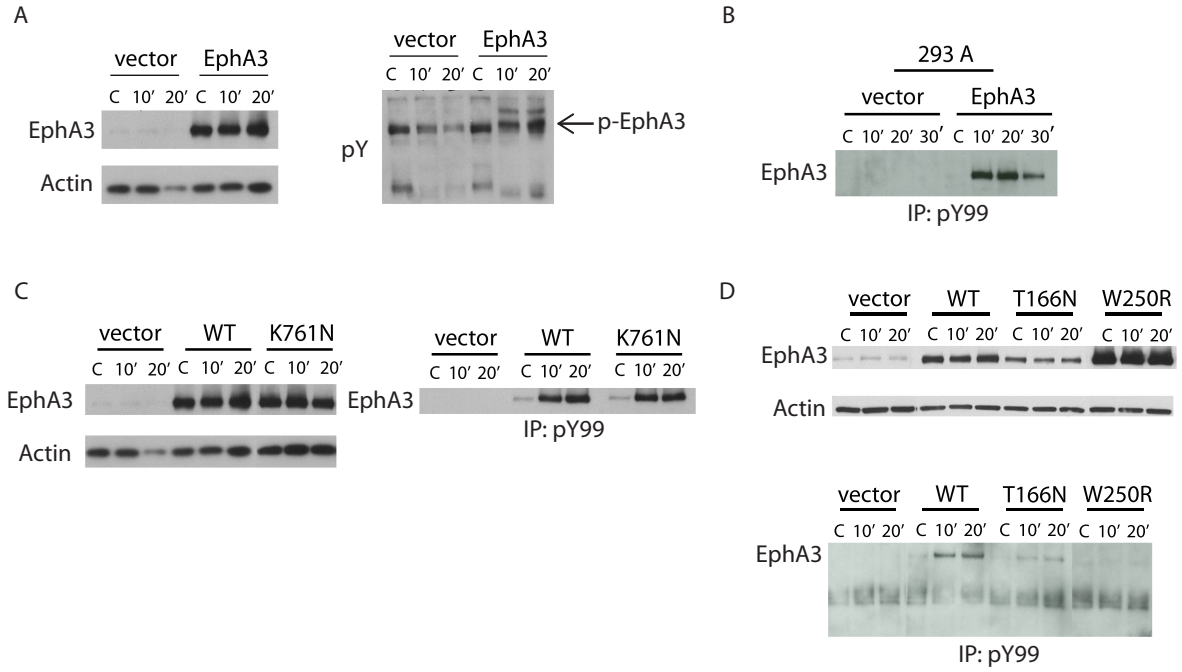

Figure 4-2. Studies of EphA3 wild type and selected mutations reveal that mutations in the extracellular domain have reduced phsophorylation upon ligand stimulation.

(A) Cells expressing vector control or wild type EphA3 were ligand stimulated for the indicated times (C: control; 10': 10 minutes; 20': 20 minutes) and probed for EphA3, actin, or phospho-tyrosine by immunoblot. Phospho-EphA3 can be identified upon ligand stimulation when immunoblotting with an anti-phospho-tyrosine antibody, but background bands are also observed (right panel; arrow, phospho-EphA3).

(B) Phospho-EphA3 can be cleanly identified by immunoprecipitating 293A-EphA3 lysates with an anti-phospho-tyrosine antibody (pY99) and immunoblotting for EphA3; activity decreases by 30 minutes after ligand stimulation.

(C) Cells expressing vector control, wild type EphA3, or the K761N kinase domain mutant show that the K761N mutant is phosphorylated to similar levels as the wild type receptor upon ligand stimulation.

Figure 4-2 continued

(D) Cells expressing vector control, wild type EphA3, or the T166N or W250R ECD mutants demonstrate that the ECD mutants have reduced phosphorylation compared to the wild type receptor upon ligand stimulation.

binding capacity (Figure 4-2D) and potentially demonstrate a more general loss-of-function phenotype due to mutations in the *EphA3* gene observed in lung adenocarcinoma.

EphA3 kinase null mutants are phosphorylated, suggesting the potential for alternative mechanisms of activation of EphA3

While performing these studies, we utilized loss-of-function kinase domain *EphA3* mutation constructs, EphA3 D746A and K653M, to control for loss of kinase activity. However, when cells transfected with these mutation constructs were stimulated with ephrin-A5, we observed phosphorylation of these supposedly "kinase dead" protein products (Figure 4-3A). This was surprising; however, a similar phenomenon was observed in the naturally non-functional EphB6 due to heterodimerization with wild type EphB1 (22). It is possible that EphA receptors might also activate non-homologous EphA receptor family members, resulting in phosphorylation of kinase null proteins.

To begin testing for other expressed EphA receptors in our system, we immunoblotted for EphA2 in 293A cells, and found it to be robustly expressed (Figure 4-3B). We also found similar phosphorylation patterns for EphA2 to what we had seen with EphA3 after ephrin-A5 stimulation (Figure 4-3C). EphA receptors are able to bind promiscuously to ephrin-A ligands, suggesting, along with our data, that EphA2 is activated by ephrin-A5 similarly to EphA3 (2). More data are required to characterize these observations in the context of EphA3 kinase null phosphorylation.

DISCUSSION

EphA3 is an RTK that was observerd to be statistically significantly mutated in a 2008

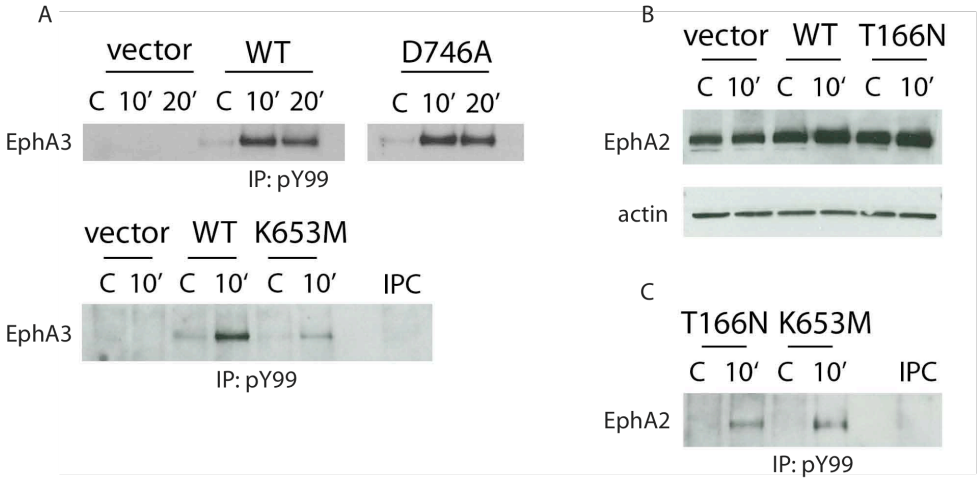

Figure 4-3. Phosphorylation of "kinase dead" exogenously expressed EphA3 mutations suggests a secondary method of phosphorylation than receptor homodimerization

(A) Cells expressing vector control, wild type EphA3 (WT), or kinase null EphA3 mutations D746A or K653M were ligand stimulated for the indicated times (C: control; 10': 10 minutes; 20': 20 minutes) and probed for phospho-tyrosine by immunoprecipitation with the pY99 antibody followed by immunoblot with an anti-EphA3 antibody. D746A shows similar phosphorylation levels to the wild type receptor under these conditions, while phosphorylation of K653M is diminished compared to WT, but still detectable. An immunoprecipitation control (IPC) was included to control for lysis buffer or antibody effects.

(B) EphA2, another EphA receptor, is robustly expressed in 293A cells irrespective of transduced vector, wild type, or EphA3 mutation construct T166N.

(C) Ligand stimulation with preclustered ephrin-A5 leads to EphA2 phosphorylation as measured by anti-phospho-tyrosine immunoprecipitation followed by immunoblot with an anti-EphA2 antibody in cells transduced with a possible loss-of-function EphA3 mutation (T166N) or a kinase null EphA3 mutation (K653M). An immunoprecipitation control (IPC) was included to control for lysis buffer or antibody effects.

sequencing report of lung adenocarcinoma (1). Our study began to determine the oncogenic potential of the *EphA3* mutations, hypothesizing that strong statistical significance of missense mutations in this RTK indicated a gain-of-function, oncogenic effect. However, our preliminary data suggest that in fact, these mutations may be causing loss-of-function, tumor suppressive effects. Indeed, this was consistent with the findings of a recent report characterizing these and other *EphA3* mutations identified in tumor sequencing projects (23). We also demonstrate an unexpected phosphorylation pattern present in kinase null EphA3 mutations and hypothesize that alternative activation methods may exist for EphA3 and other EphA family members, perhaps similar to those described previously for the EphB family (22).

Since the 2008 study in which the mutations described here were observed, further genome characterization of lung adenocarcinoma has been performed by Imielinski *et al*. (2012) (24) and The Cancer Genome Atlas (TCGA) Research Consortium (manuscript under review, data accessed using the cBioPortal for Cancer Genomics (25, 26)). These studies have provided further evidence for a loss-of-function phenotype caused by these mutations. For instance, Imielinski *et al*. identify 29 point mutations and one putative homozygous deletion of *EphA3* for a total alteration rate of 16% in 183 samples, in which four point mutations result in a nonsense or frameshift event, which along with homozygous deletion are suggestive of loss of function (report referenced in (24), data analyzed using the cBioPortal for Cancer Genomics (25, 26)). Similarly, unpublished TCGA lung adenocarcinoma sequencing data identify 22 point mutations and one homozygous deletion for an alteration rate of 10% across 229 sequenced tumors, in which three mutations result in a nonsense or frameshift event, also suggestive of loss of function (data provisional, accessed using the cBioPortal for Cancer Genomics (25, 26)). In TCGA data, five amplifications of *EphA3* were also observed.

Nonsense mutation events remain the minority in acquired genomic variants of *EphA3*, suggesting that missense mutation is instead the preferred mechanism through which receptor inactivity occurs. This is not commonly observed in RTK genes associated with cancer, but is described in the canonical case of *TP53* mutations, which are known to have dominant negative missense mutation phenotypes to drive loss of function (27). The surprising suggestion of a similar tumor suppressive role driven by missense mutation in a receptor tyrosine kinase thus warrants further study for its role in cancer.

The study of *EphA3* also provides a compelling example of how even highly statistically significant events require functional validation in order to demonstrate biological significance. As genome characterization studies continue to improve accuracy and depth of coverage, more alterations will be identified which play driving or suppressive roles, or no role at all, in cancer development and maintenance. Identifying appropriate models in which to study phenotypic outcomes of these events will further improve treatment options and care for patients diagnosed with lung adenocarcinoma and other cancers.

MATERIALS AND METHODS

Reagents

Cell lines NCI-H1770, A549, 293T, and 293A were obtained from the American Type Culture Collection (Manassas, VA). Cell lines HCC15 and HCC515 were obtained from Drs. John Minna and Adi Gazdar at UT Southwestern Medical Center, Dallas, TX. Lung cancer cell line NCI-H1770 was maintained in ACL-4 medium. Lung cancer cell lines A549, HCC15, and HCC515 were maintained in RPMI with 10% FBS added. Cell lines 293T and 293A were maintained in DMEM with 10% FBS added.

Ephrin-A5-Fc was purchased from Life Technologies. Anti-human IgG-Fc was purchased from Sigma-Aldrich. Antibodies against EphA2, EphA3, beta-actin, and phospho-tyrosine (p-Y100) were purchased from Cell Signaling Technology. Phospho-tyrosine agarose conjugate (p-Y99 AC) was purchased from Santa Cruz Biotechnology, Inc. Fugene-6 was purchased from Roche.

Cellular morphology assay

The rounding/blebbing cellular assay was performed as described previously (4). Cells were photographed on the AxioCam MRm (Carl Zeiss Microscopy).

Transfection of 293T and 293A cells

Transfections were performed when cells maintained in 6-well dishes were ~50% confluent. Six μL of Fugene-6 were diluted in 94 μL of serum-free DMEM and incubated for five minutes at room temperature, followed by the addition of 1 μg cDNA, after which the mixture was incubated for 15 minutes at room temperature. The entire mixture was then added to one well of cells in a 6-well dish, swirled gently, and incubated at 37°C for 48 hours prior to assaying gene expression and function.

Immunoblot and immunoprecipitation

Cells were lysed in buffer containing 0.5% NP-40, 50 mM Tris pH 8, 150 mM MgCl2, and phosphatase and protease inhibitors, and proteins were separated by SDS/PAGE and transferred to nitrocellulose membranes via the iBlot dry transfer system (Life Technologies). Antibody binding was detected using HRP-conjugated secondary antibodies (Cell Signaling

Technologies, Inc) reacting with the ECL western blotting substrate (Thermo Fisher Scientific, Inc.) and developed on film.

To perform phospho-tyrosine immunoprecipitation, 500 μg protein was incubated with 30 μL p-Y99 AC antibody on a rotator overnight at 4°C. Lysates were then washed four times with 500 μL cold lysis buffer, boiled with loading buffer and reducing agent, and loaded into gels as described above.

Ligand stimulation

Ligand stimulation was performed using recombinant ephrin-A5 conjugated to the Fc region of human IgG1 at the C-terminus. Ephrin-A5-Fc was clustered with anti-human IgG-Fc prior to cell stimulation by incubating a 1:10 molar ratio of ephrin-A5-Fc and anti-human IgG-Fc for 20 minutes at room temperature. Cells were stimulated by adding 10 nM preclustered ephrin-A5-Fc or anti-human IgG-Fc for indicated times and lysed for analysis.

ACKNOWLEDGEMENTS

The author thanks Heidi Greulich, Kumiko Tanaka, and Tzu-Hsiu Chen for helpful discussion and technical support.

REFERENCES

1. Ding L, Getz G, Wheeler DA, Mardis ER, McLellan MD, Cibulskis K, et al. Somatic mutations affect key pathways in lung adenocarcinoma. Nature. 2008;455(7216):1069-75. PMCID: 2694412.

2. Pasquale EB. Eph receptors and ephrins in cancer: bidirectional signalling and beyond. Nat Rev Cancer. 2010;10(3):165-80. PMCID: 2921274.

3. Flanagan JG, Vanderhaeghen P. The ephrins and Eph receptors in neural development. Annu Rev Neurosci. 1998;21:309-45.

4. Lawrenson ID, Wimmer-Kleikamp SH, Lock P, Schoenwaelder SM, Down M, Boyd AW, et al. Ephrin-A5 induces rounding, blebbing and de-adhesion of EphA3-expressing 293T and melanoma cells by CrkII and Rho-mediated signalling. J Cell Sci. 2002;115(Pt 5):1059-72.

5. Carvalho RF, Beutler M, Marler KJ, Knoll B, Becker-Barroso E, Heintzmann R, et al. Silencing of EphA3 through a cis interaction with ephrinA5. Nat Neurosci. 2006;9(3):322-30.

6. Janes PW, Saha N, Barton WA, Kolev MV, Wimmer-Kleikamp SH, Nievergall E, et al. Adam meets Eph: an ADAM substrate recognition module acts as a molecular switch for ephrin cleavage in trans. Cell. 2005;123(2):291-304.

7. Frisen J, Holmberg J, Barbacid M. Ephrins and their Eph receptors: multitalented directors of embryonic development. EMBO J. 1999;18(19):5159-65. PMCID: 1171586.

8. Oates AC, Lackmann M, Power MA, Brennan C, Down LM, Do C, et al. An early developmental role for eph-ephrin interaction during vertebrate gastrulation. Mech Dev. 1999;83(1-2):77-94.

9. Schulte D, Cepko CL. Two homeobox genes define the domain of EphA3 expression in the developing chick retina. Development. 2000;127(23):5033-45.

10. Stephen LJ, Fawkes AL, Verhoeve A, Lemke G, Brown A. A critical role for the EphA3 receptor tyrosine kinase in heart development. Dev Biol. 2007;302(1):66-79.

11. Chiari R, Hames G, Stroobant V, Texier C, Maillere B, Boon T, et al. Identification of a tumor-specific shared antigen derived from an Eph receptor and presented to CD4 T cells on HLA class II molecules. Cancer Res. 2000;60(17):4855-63.

12. Clifford N, Smith LM, Powell J, Gattenlohner S, Marx A, O'Connor R. The EphA3 receptor is expressed in a subset of rhabdomyosarcoma cell lines and suppresses cell adhesion and migration. Journal of cellular biochemistry. 2008;105(5):1250-9.

13. Dodelet VC, Pasquale EB. Eph receptors and ephrin ligands: embryogenesis to tumorigenesis. Oncogene. 2000;19(49):5614-9.

14. Davies H, Hunter C, Smith R, Stephens P, Greenman C, Bignell G, et al. Somatic mutations of the protein kinase gene family in human lung cancer. Cancer Res. 2005;65(17):7591-5.

15. Wood LD, Calhoun ES, Silliman N, Ptak J, Szabo S, Powell SM, et al. Somatic mutations of GUCY2F, EPHA3, and NTRK3 in human cancers. Hum Mutat. 2006;27(10):1060-1.

16. Chen H, Ma J, Li W, Eliseenkova AV, Xu C, Neubert TA, et al. A molecular brake in the kinase hinge region regulates the activity of receptor tyrosine kinases. Mol Cell. 2007;27(5):717-30. PMCID: 2094128.

17. Paez JG, Janne PA, Lee JC, Tracy S, Greulich H, Gabriel S, et al. EGFR mutations in lung cancer: correlation with clinical response to gefitinib therapy. Science. 2004;304(5676):1497-500.

18. Soda M, Choi YL, Enomoto M, Takada S, Yamashita Y, Ishikawa S, et al. Identification of the transforming EML4-ALK fusion gene in non-small-cell lung cancer. Nature. 2007;448(7153):561-6.

19. Greulich H, Kaplan B, Mertins P, Chen TH, Tanaka KE, Yun CH, et al. Functional analysis of receptor tyrosine kinase mutations in lung cancer identifies oncogenic extracellular domain mutations of ERBB2. Proceedings of the National Academy of Sciences of the United States of America. 2012.

20. Ellis LM, Hicklin DJ. Resistance to Targeted Therapies: Refining Anticancer Therapy in the Era of Molecular Oncology. Clinical cancer research : an official journal of the American Association for Cancer Research. 2009;15(24):7471-8.

21. Greulich H, Kaplan B, Mertins P, Chen TH, Tanaka KE, Yun CH, et al. Functional analysis of receptor tyrosine kinase mutations in lung cancer identifies oncogenic extracellular domain mutations of ERBB2. Proceedings of the National Academy of Sciences of the United States of America. 2012;109(36):14476-81.

22. Freywald A, Sharfe N, Roifman CM. The kinase-null EphB6 receptor undergoes transphosphorylation in a complex with EphB1. The Journal of biological chemistry. 2002;277(6):3823-8.

23. Lisabeth EM, Fernandez C, Pasquale EB. Cancer somatic mutations disrupt functions of the EphA3 receptor tyrosine kinase through multiple mechanisms. Biochemistry. 2012;51(7):1464-75. PMCID: 3471792.

24. Imielinski M, Berger AH, Hammerman PS, Hernandez B, Pugh TJ, Hodis E, et al. Mapping the hallmarks of lung adenocarcinoma with massively parallel sequencing. Cell. 2012;150(6):1107-20. PMCID: 3557932.

25. Cerami E, Gao J, Dogrusoz U, Gross BE, Sumer SO, Aksoy BA, et al. The cBio cancer genomics portal: an open platform for exploring multidimensional cancer genomics data. Cancer discovery. 2012;2(5):401-4.

26. Gao J, Aksoy BA, Dogrusoz U, Dresdner G, Gross B, Sumer SO, et al. Integrative analysis of complex cancer genomics and clinical profiles using the cBioPortal. Sci Signal. 2013;6(269):pl1.

27. de Vries A, Flores ER, Miranda B, Hsieh HM, van Oostrom CT, Sage J, et al. Targeted point mutations of p53 lead to dominant-negative inhibition of wild-type p53 function. Proceedings of the National Academy of Sciences of the United States of America. 2002;99(5):2948-53. PMCID: 122453.

CHAPTER 5

DISCUSSION

FGFR mutations as a druggable target in lung squamous cell carcinoma

Fibroblast Growth Factor Receptor (FGFR) alterations have been characterized previously in both germline disease (1) and cancer (2). In both contexts, alterations lead to kinase activation and sustained signaling through the FGFR pathway (3), consistent with observations of other receptor tyrosine kinases (RTKs) altered in cancer (4). Recently, the FGFR family members have been targeted by clinical small molecule inhibitors, enabling treatment options previously unrealized in patients whose tumors harbor these events (5-7). Squamous cell carcinoma of the lung has long been known as an aggressive disease for which treatment options were severely limited (8). Thus the identification of mutations in FGFR family members (Chapter 2, (9)), known to be druggable cancer targets, was an appealing topic for follow-up characterization.

The sufficient demonstration of *FGFR2* and *FGFR3* mutations as driving, targetable events in lung squamous cancer is a lofty goal. No appropriate mouse models of these tumors are available to study putative alterations (10), nor do cancer cell line models even contain the mutations, let alone exhibit dependency on mutant FGFR protein products (11). Using transgenic cell line models, we have demonstrated here that the identified mutations are both transforming (Figure 2-4A) and sensitive to inhibition by targeted therapy (Figure 2-6A, 2-8B); however, these studies occur in cellular contexts insufficient to fully model oncogenesis and treatment response. Even a clinical response to a multi-kinase inhibitor in the presence of a known activating *FGFR2* mutation (Figure 2-10) is only a correlative observation, as the driving activity of FGFR2 was not established in the tumor and the inhibitor has many targets beyond FGFR family members (12).

Thus, while the study described in Chapter 2 demonstrates that potential and actionable genomic alterations can be identified through whole genome sequencing, and their functional characterization can exert real influence over patient care (as evidenced by a clinical trial, NCT01761747, begun as a direct result of the data presented in Chapter 2), we are still far from meeting that goal. Until we develop and routinely utilize disease models that can accurately identify biomarkers of inhibitor sensitivity prior to their identification via fortuitous human tumor response, functional genomic studies such as the one described here will be an incomplete surrogate for the true demonstration of inhibitor sensitivity based on identified genomic events in human cancer.

Multiple acquired resistance mechanisms identified in *FGFR1*-amplified lung squamous cell carcinoma

Like the accurate demonstration of oncogenesis and inhibitor sensitivity described above, resistance that arises in response to inhibition is difficult to predict. *FGFR1*-amplification in lung squamous cell carcinoma was identified prior to whole genome characterization (13, 14), but phase 1 clinical trials of patients with targeted anti-FGFR therapies for this indication have only recently begun (8). A subset of patients in these studies has responded to therapy; thus, the field anticipates the occurrence of resistance.

As is known for other tumor types, resistance can arise via multiple mechanisms (15-17). In the search for resistance mechanisms in response to FGFR inhibitors, studies of bladder cancer and multiple myeloma reveal several mechanisms, which are distinct from those described arising in lung squamous cell carcinoma in Chapter 3 (18-20). Preclinical models such as these can be useful to identify clinically relevant and actionable resistance mechanisms (21-

23), but they fall short of identifying all resistance events (15) and can also identify events not observed in the clinic (24).

Our ability to predict and identify mechanisms of acquired resistance to targeted therapy remains limited, but we have also not exhausted preclinical models to identify potential resistance mechanisms. This is particularly true in contexts where targeted therapies have only recently been introduced into the clinic, as is the case with FGFR small molecule inhibitors for lung squamous cell carcinoma. It is our hope that the identification of FGFR-dependent MET activation, driven by amplification, and *NRAS* mutation will enable improved patient care, while still recognizing that more work remains to further characterize these mechanisms and to identify mechanisms that are as yet unstudied.

EphA3 **is significantly mutated in lung adenocarcinoma, and demonstrates loss-of-function characteristics**

The identification of *EphA3* as a significantly mutated receptor tyrosine kinase in lung adenocarcinoma (25) was an attractive discovery. Advances in therapy targeting driving kinases had been successful for *EGFR*-mutant lung cancer, as well as in cancers driven by other oncogenes (26-28). It came as a surprise, therefore, to find that none of these events was transforming in standard cellular assays (Chapter 4, (29)). Further study suggested a loss-of-function phenotype for several of the identified mutations (Figure 4-2), later confirmed by an independent study (29) and leading to the conclusion that tyrosine kinases may act as tumor suppressors in cancer, rather than oncogenes, and that their loss of efficacy by missense mutation has the potential to allow tumor growth to progress unchecked. This is further supported by a recent screen identifying EphA3 as a mediator of cellular senescence (30).

This observation recommends study into the intriguing field of targeting tumor suppressors for therapy. It is undoubtedly a challenge, as many tumor suppressor genes are deleted or mutated with alterations resulting in truncations (31). However, for tumor suppressors that lose function through missense mutation, targeted therapy may be an option.

This possibility has been described most extensively for *TP53*, encoding p53, which is altered in 50% or more of all cancers and is a well-studied tumor suppressor (32-34). The majority of alterations in *p53* are missense mutations that result in a dominant negative phenotype but that studies suggest can be partially overcome by restoration of wild type activity (33). Although *EphA3* mutations do not necessarily possess similar dominant negative activity, restoration of the wild type protein may similarly result in a reactivation of its tumor suppressor functions.

Genomic studies of cancer: benefits and limitations

Targetable genomic alterations and the potential for cancer treatment with few side effects

Historically, lung cancer treatment has relied on surgery, chemotherapy, and radiation, and except in early stage tumors, patient prognosis is often grim (35). Thus the technological advances made toward accurate whole-genome characterization present an opportunity to determine driving alterations that could potentially be targeted with small molecules or antibodies, thus avoiding many of the side effects common to standard therapies.

There are several limitations to current targeted treatments available. First, analysis of many factors including co-occurring events, tumor heterogeneity, and even point mutation data from tumors cannot predict with certainty which patients will respond to treatment (4). The predictive power drops further in the case of amplifications. Second, many of the “targeted”

drugs heralded by the pharmaceutical industry as silver bullets are often multi-kinase inhibitors with many protein targets at doses common in clinical therapy, with the potential for off-target effects and serious side effects (36). These drugs are often ATP-competitive and generally target either the active conformation of the kinase domain or the inactive structure. This presents difficulty due to the high homology between protein kinase domains, especially tyrosine kinase domains (36), and can result in patient toxicity even in response to "targeted" treatments (Chapter 2). Even in cases where specific drugs can target a specific protein kinase structure, some protein families, like the FGFRs, share such high structural homology that the best inhibitor of the ATP pocket of the kinase domain will still target several protein family members (37).

One solution to this issue is the development of allosteric inhibitors, which bind a non-kinase site on the protein that is unique structurally and inhibits activity via a different mechanism than inhibition of kinase activation (36). These require identification and extensive validation of the non-kinase targeted domain. Another option is monoclonal antibody therapy, which can bind the unique extracellular domain of proteins, but generally do not distinguish between mutant and wild type, nor are there common inhibitory mechanisms to exploit (38). Clearly, research toward more specific targeted therapies is needed to present patients with specific treatment options with minimal side effects.

The inverse relationship between genomic characterization of cancer and appropriate preclinical models for study

Research into targeted therapies is limited, however, by the current dearth of disease models available for appropriate preclinical study. With the explosion of genomic

characterization of cancer by The Cancer Genome Atlas and other studies, new targets with oncogenic potential have been described in large numbers, though they may require validation (9, 25, 39, 40). Existing models of disease such as those curated in the Cancer Cell Line Encyclopedia (11) have been largely exhausted of their potential to study newly identified alterations, particularly for low frequency recurrent alterations such as those identified in the FGFR family in lung squamous cell carcinoma (Chapter 2, (9)). To demonstrate the potential of these events to drive oncogenesis and respond to targeted therapy, alternative suboptimal methods, including anchorage-independent growth assays and cell proliferation assays, are employed that show standard cancer phenotypes such as transformation and dependency (Chapter 2, Figures 2-4, 2-6, 2-8). However, these assays are limited because they are able to characterize phenotypes *in vitro*, but cannot demonstrate that patients presenting with those alterations in their tumors will respond to therapy targeting them.

These limitations can be partially overcome by the generation of new models. Cancer cell lines have historically been difficult to isolate, but new methodologies have recently been identified that significantly increase the rate at which cancer cells will establish immortal cell lines in culture (41, 42). Also, genetically engineered mouse models can be generated with the capacity to model oncogenesis dependent on certain oncogenes, though often imperfectly (43, 44). Similarly, human xenografts, in which human tumors are grown in immunocompromised mice without ever growing on plastic, or mouse allografts, in which mouse-derived tumors are maintained in mice of the same genetic background with normal immune function, are of some benefit in drug studies (44, 45).

None of these models can perfectly predict human clinical response to targeted cancer therapy, but *in vitro* cancer cell line models do have predictive power to identify oncogenic

targets in human disease (11) and the various mouse models can simulate *in vivo* disease in ways not attainable in transgenic cell lines (44, 45). One might therefore suppose that more resources ought to be diverted toward generation of these models, which is reasonable but for one limitation: the extreme difficulty in acquiring patient samples. In the absence of genetically engineered mouse models, which often present major technical challenges to generate, these types of samples require the appropriate informed consent of a cancer patient and the cooperation of a surgeon who performs the biopsy or surgical removal, both of which are notoriously difficult to obtain and for which there can be little institutional structure or support. This difficulty, certainly due to the real necessity for patient privacy and protection, has nonetheless hindered the continued acquisition of human samples that may be cultured preclinically for the study of oncogenesis and susceptibility to targeted therapy for novel genomic alterations in cancer.

The limits of statistical significance and the necessity of functional validation

Large datasets derived from cancer genomes are enabling identification of many novel, recurrent, and targetable alterations *in silico*, using computational methods to deconvolute genomic events such that those occurring more frequently than expected by chance are quickly identified as positively selected and warranting further study. However, the statistical power to detect significance in these events is necessarily limited by sample size, as well as other factors such as gene length and background- and gene-specific mutation frequency (46). The reliance on statistical analysis of cancer genome data to identify targets for therapy leads to two major limitations.

The first is that the stringent criteria used to identify significant events can fail to identify truly recurrent, targetable alterations occurring at a low frequency, such as those described in

FGFR2 and *FGFR3* in Chapter 2. With larger datasets, the power to detect low-frequency alterations will increase, but rare, potentially driving events will continue to be observed in the non-significant "tail" of a graph of alterations arranged by p-value (Figure 5-1). In this sort of statistical analysis of the genomic data, a threshold of significance is set by contributing parameters including gene length and mutation frequency, and mutated genes fall above or below that threshold to indicate significance. This leaves open the possibility that mutations observed in the dataset are potentially oncogenic and actionable, but do not rise to the level of statistical significance when all criteria are included for analysis. A solution to this is to screen alterations that do not meet the criteria for statistical significance against databases such as the Catalog of Somatic Mutations in Cancer (COSMIC, (47)) and protein structure databases that predict the likelihood of functional impact of point mutations such as PolyPhen-2 (48). Screening these databases proves incomplete, however, since databases such as COSMIC can only identify previously annotated mutations in cancer, and PolyPhen-2, in addition to being only predictive, does not distinguish between gain- and loss-of-function events. Still, these tools and others can inform functional studies of genes not otherwise deemed statistically significant.

The second limitation is that identification of statistically significant genomic alterations does not necessarily predict functional relevance. This is commonly observed in the case of copy number variations in the cancer genome, where significant amplification peaks can contain many genes while few have functional impact (31). It is also observed less commonly in the case of point mutations, such as those identified in *EphA3* and described in Chapter 4. Several of these mutations were originally described as likely deleterious to protein function by an earlier version of the PolyPhen tool described above (25). Upon functional validation, our data and others suggest that the missense mutations identified in *EphA3* are in fact loss-of-function events, rather

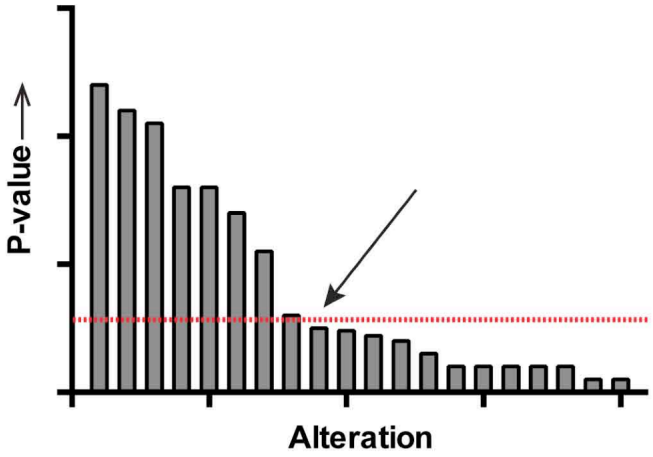

Figure 5-1. Computational analysis to identify significant oncogenic alterations in cancer genome datasets results in a "tail" of observed alterations of unknown biological significance that do not reach statistical significance.

Observed alterations arranged by p-value from most significant to least significant demonstrate that when a significance threshold is set (red dashed line), many alterations form a "tail" of events (beginning at arrow) that do not meet the level of statistical significance but may nonetheless contribute to oncogenic development or maintenance of cancer in the tumors in which the alteration was identified. This phenomenon poses a challenge for researchers seeking to identify biological contributors to oncogenesis by computational methods.

than gain-of-function, as is common for missense mutations in RTKs (Chapter 4, (29)). This unexpected observation draws particular attention to the need for comprehensive functional validation of statistically significant novel cancer genome alterations, as their function cannot be assumed *a priori*, despite suggestive data from similar proteins.

Future directions for lung squamous cell carcinoma treatment

Lung squamous cell carcinoma has historically been an aggressive disease with few treatment options beyond standard chemotherapy (8). No targeted therapies are approved and prior to TCGA analysis, no recurrent targets were known except for few low-frequency events (13, 14, 49). With the completion and publication of initial TCGA analysis, however, many putative targets have been identified (9). As described in Chapter 2, missense mutations in *FGFR2* and *FGFR3* are an exciting potential therapeutic target and have led to the initiation of a new clinical trial selecting patients with FGFR-mutated lung squamous cell carcinoma (NCI Identifier NCT01761747) as well as one of the first functional validations of a new cancer target resulting from TCGA characterization (50).

Beyond alterations in FGFR family members, other alterations that may contribute to lung squamous oncogenesis have been identified. Many of these events are currently undergoing functional validation to identify more targets in this disease. These include alterations in the PI3K/AKT pathway, such as point mutations in *PIK3CA*, *TSC1*, and *TSC2*, deletions and mutations in *PTEN*, and amplifications of *AKT3* (8, 9), suggesting a role for therapeutic targeting of this pathway in lung squamous patients. In addition, mutations in known cancer-related kinases, including *ABL1*, *ABL2*, *MET*, and *ErbB2-4* have been identified in a small percentage of cases (8, 9), suggesting that rather than a few common driving events occurring in a large

percentage of tumors, as is the case with other cancers such as melanoma (51), lung squamous cell carcinoma is a much more heterogeneous disease with many identified driving mechanisms. Thus, though numbers of cases presenting with any individual alteration are small, targeted therapeutic options exist against many of these protein products and indicate that together, a much larger number of cases may have personalized treatment options available.

Interesting non-kinase alterations are also observed in TCGA data, indicating a potential role for diverse mechanisms in oncogenesis and maintenance of this disease and possible new therapeutic vulnerabilities. Among the most altered genes in the lung squamous TCGA dataset were *NFE2L2*, *KEAP1*, and *CUL3* (8, 9), which together form a complex regulating the transcription of genes associated with the cellular response to oxidative and chemical stress (52) and, when altered, have been associated with oncogenesis and resistance to therapy in cancer (53, 54). Alterations in one of these three genes are identified in about a third of lung squamous cancers (9) and could contribute to its refractory nature. Indeed, restoration of this pathway in altered tumors has the potential to sensitize otherwise insensitive tumors to chemo- and radiotherapies and should be evaluated further in the lab and the clinic.

Future directions for FGFR studies

Known to be involved in germline craniofacial syndromes, FGFR family members have also been implicated in many types of cancers (3). They have been described as mutated in large percentages of cases in bladder cancer (55) and endometrial cancer (56, 57), translocated and mutated in multiple myeloma (58), and amplified in lung squamous (13, 14) and breast cancer (59, 60). Recently, a new transforming fusion between FGFR3 and TACC3 has been described in glioblastoma (61), bladder cancer (62), and lung squamous cancer (63), demonstrating the

need for further study into novel alterations in this protein family and a great need for therapies targeting FGFRs. Unlike some other RTKs, which have known "hotspot" mutations accounting for a large percentage of observed alterations across cancer, FGFR family members are infrequently altered at the same site across different tumor types. This requires more extensive functional validation and likely contributes to the delayed identification of FGFRs as a prominent cancer-related gene family.

Now, however, many FGFR targets are known and targeted therapies have entered the clinic (5, 7, 64). This is a great success for combined functional validation efforts and opens therapeutic options to many formerly untreatable patients. Unfortunately, resistance will undoubtedly emerge, as is observed universally in solid malignancies (65). Several mechanisms of resistance to FGFR targeted therapy have been described, in Chapter 3 and elsewhere (18-20), and like the diversity of mechanisms of activation of the FGFR signaling pathway in cancer, diverse resistance mechanisms arise in response to therapy as well. Thus in the continued study of resistance in diseases driven by alterations in these genes, we expect distinct mechanisms of resistance in different tumor types and in response to the varied targeted therapies available. The detailed and diverse research required to elucidate this expected variability will likely result in the best understanding, outcomes, and further treatment options for patients presenting with resistance to FGFR targeted therapy.

CONCLUSIONS

The genomic study of cancer has enabled the identification of putative oncogenes and tumor suppressors in many cancer types, creating the need for their functional validation as new drug targets. This need is unlikely to decrease in the near future, as genome sequencing goes

deeper, tumor heterogeneity is described, and stromal contributions to disease are better understood, and we expect that new standards for validation will be adopted to accommodate the increased number of targets that will result from these advances. We have demonstrated here the potential success of studies characterizing novel findings from cancer genome data for the development of new targets for therapy, while also providing an example indicating the need for functional validation of significant targets to inform drug development studies. We have also delved into the world of therapeutic resistance, a field increasing in its scope with every newly approved cancer drug. It is our hope that together, this work has contributed to an evidence-based defense of functional validation for putative targets in genomic studies of cancer in general, while also increasing knowledge and improving understanding specifically in the study and treatment of non-small cell lung cancer. The continuation of these types of studies in this and other cancers might then lead to the goal of all cancer research: a world in which all cancers are understandable, treatable diseases.

REFERENCES

1. Lahiry P, Torkamani A, Schork NJ, Hegele RA. Kinase mutations in human disease: interpreting genotype-phenotype relationships. Nat Rev Genet. 2010;11(1):60-74.

2. Greulich H, Pollock PM. Targeting mutant fibroblast growth factor receptors in cancer. Trends in molecular medicine. 2011;17(5):283-92.

3. Turner N, Grose R. Fibroblast growth factor signalling: from development to cancer. Nat Rev Cancer. 2010;10(2):116-29.

4. Janne PA, Gray N, Settleman J. Factors underlying sensitivity of cancers to small-molecule kinase inhibitors. Nat Rev Drug Discov. 2009;8(9):709-23.

5. AZD4547: An orally bioavailable, potent and selective inhibitor of the Fibroblast Growth Factor Receptor tyrosine kinase family, (2012).

6. Guagnano V, Furet P, Spanka C, Bordas V, Le Douget M, Stamm C, et al. Discovery of 3-(2,6-dichloro-3,5-dimethoxy-phenyl)-1-{6-[4-(4-ethyl-piperazin-1-yl)-phenylamino]-pyrimidin-4-yl}-1-methyl-urea (NVP-BGJ398), a potent and selective inhibitor of the fibroblast growth factor receptor family of receptor tyrosine kinase. J Med Chem. 2011;54(20):7066-83.

7. Guagnano V, Kauffmann A, Wohrle S, Stamm C, Ito M, Barys L, et al. FGFR genetic alterations predict for sensitivity to NVP-BGJ398, a selective pan-FGFR inhibitor. Cancer discovery. 2012;2(12):1118-33.

8. Liao RG WH, Meyerson M & Hammerman PS. Targeted therapy for squamous cell lung cancer. Lung Cancer Management. 2012;1(4):293-300.

9. Hammerman PS, Lawrence MS, Voet D, Jing R, Cibulskis K, Sivachenko A, et al. Comprehensive genomic characterization of squamous cell lung cancers. Nature. 2012.

10. You MS, Rouggly LC, You M, Wang Y. Mouse models of lung squamous cell carcinomas. Cancer Metastasis Rev. 2013;32(1-2):77-82.

11. Barretina J, Caponigro G, Stransky N, Venkatesan K, Margolin AA, Kim S, et al. The Cancer Cell Line Encyclopedia enables predictive modelling of anticancer drug sensitivity. Nature. 2012;483(7391):603-7. PMCID: 3320027.

12. Sonpavde G, Hutson TE. Pazopanib: a novel multitargeted tyrosine kinase inhibitor. Current oncology reports. 2007;9(2):115-9.

13. Dutt A, Ramos AH, Hammerman PS, Mermel C, Cho J, Sharifnia T, et al. Inhibitor-sensitive FGFR1 amplification in human non-small cell lung cancer. PLoS ONE. 2011;6(6):e20351. PMCID: 3110189.

14. Weiss J, Sos ML, Seidel D, Peifer M, Zander T, Heuckmann JM, et al. Frequent and focal FGFR1 amplification associates with therapeutically tractable FGFR1 dependency in squamous cell lung cancer. Science translational medicine. 2010;2(62):62ra93.

15. Hammerman PS, Janne PA, Johnson BE. Resistance to Epidermal Growth Factor Receptor Tyrosine Kinase Inhibitors in Non-Small Cell Lung Cancer. Clinical cancer research : an official journal of the American Association for Cancer Research. 2009;15(24):7502-9.

16. Milojkovic D, Apperley J. Mechanisms of Resistance to Imatinib and Second-Generation Tyrosine Inhibitors in Chronic Myeloid Leukemia. Clinical cancer research : an official journal of the American Association for Cancer Research. 2009;15(24):7519-27.

17. Pohlmann PR, Mayer IA, Mernaugh R. Resistance to Trastuzumab in Breast Cancer. Clinical cancer research : an official journal of the American Association for Cancer Research. 2009;15(24):7479-91. PMCID: 3471537.

18. Chell V, Balmanno K, Little AS, Wilson M, Andrews S, Blockley L, et al. Tumour cell responses to new fibroblast growth factor receptor tyrosine kinase inhibitors and identification of a gatekeeper mutation in FGFR3 as a mechanism of acquired resistance. Oncogene. 2013;32(25):3059-70.

19. Harbinski F, Craig VJ, Sanghavi S, Jeffery D, Liu L, Sheppard KA, et al. Rescue screens with secreted proteins reveal compensatory potential of receptor tyrosine kinases in driving cancer growth. Cancer discovery. 2012;2(10):948-59.

20. Herrera-Abreu MT, Pearson A, Campbell J, Shnyder SD, Knowles MA, Ashworth A, et al. Parallel RNA interference screens identify EGFR activation as an escape mechanism in FGFR3 mutant cancer. Cancer discovery. 2013.

21. Azam M, Latek RR, Daley GQ. Mechanisms of autoinhibition and STI-571/imatinib resistance revealed by mutagenesis of BCR-ABL. Cell. 2003;112(6):831-43.

22. Engelman JA, Zejnullahu K, Mitsudomi T, Song Y, Hyland C, Park JO, et al. MET amplification leads to gefitinib resistance in lung cancer by activating ERBB3 signaling. Science. 2007;316(5827):1039-43.

23. Johannessen CM, Boehm JS, Kim SY, Thomas SR, Wardwell L, Johnson LA, et al. COT drives resistance to RAF inhibition through MAP kinase pathway reactivation. Nature. 2010;468(7326):968-72. PMCID: 3058384.

24. Whittaker S, Kirk R, Hayward R, Zambon A, Viros A, Cantarino N, et al. Gatekeeper mutations mediate resistance to BRAF-targeted therapies. Science translational medicine. 2010;2(35):35ra41.

25. Ding L, Getz G, Wheeler DA, Mardis ER, McLellan MD, Cibulskis K, et al. Somatic mutations affect key pathways in lung adenocarcinoma. Nature. 2008;455(7216):1069-75. PMCID: 2694412.

26. Stegmeier F, Warmuth M, Sellers WR, Dorsch M. Targeted cancer therapies in the twenty-first century: lessons from imatinib. Clin Pharmacol Ther. 2010;87(5):543-52.

27. Paez JG, Janne PA, Lee JC, Tracy S, Greulich H, Gabriel S, et al. EGFR mutations in lung cancer: correlation with clinical response to gefitinib therapy. Science. 2004;304(5676):1497-500.

28. Lynch TJ, Bell DW, Sordella R, Gurubhagavatula S, Okimoto RA, Brannigan BW, et al. Activating mutations in the epidermal growth factor receptor underlying responsiveness of non-small-cell lung cancer to gefitinib. The New England journal of medicine. 2004;350(21):2129-39.

29. Lisabeth EM, Fernandez C, Pasquale EB. Cancer somatic mutations disrupt functions of the EphA3 receptor tyrosine kinase through multiple mechanisms. Biochemistry. 2012;51(7):1464-75. PMCID: 3471792.

30. Lahtela J, Corson LB, Hemmes A, Brauer MJ, Koopal S, Lee J, et al. A high-content cellular senescence screen identifies candidate tumor suppressors, including EPHA3. Cell Cycle. 2013;12(4):625-34. PMCID: 3594263.

31. Beroukhim R, Mermel CH, Porter D, Wei G, Raychaudhuri S, Donovan J, et al. The landscape of somatic copy-number alteration across human cancers. Nature. 2010;463(7283):899-905. PMCID: 2826709.

32. Lehmann S, Bykov VJ, Ali D, Andren O, Cherif H, Tidefelt U, et al. Targeting p53 in vivo: a first-in-human study with p53-targeting compound APR-246 in refractory hematologic malignancies and prostate cancer. Journal of clinical oncology : official journal of the American Society of Clinical Oncology. 2012;30(29):3633-9.

33. Lehmann BD, Pietenpol JA. Targeting mutant p53 in human tumors. Journal of clinical oncology : official journal of the American Society of Clinical Oncology. 2012;30(29):3648-50.

34. Stegh AH. Targeting the p53 signaling pathway in cancer therapy - the promises, challenges and perils. Expert Opin Ther Targets. 2012;16(1):67-83. PMCID: 3291789.

35. Comis RL. A brief history of the research and treatment of lung cancer from 1970 to 2003. Int J Clin Oncol. 2003;8(4):230-3.

36. Zhang J, Yang PL, Gray NS. Targeting cancer with small molecule kinase inhibitors. Nat Rev Cancer. 2009;9(1):28-39.

37. A structure-guided approach to creating covalent FGFR inhibitors, (2010).

38. Adams GP, Weiner LM. Monoclonal antibody therapy of cancer. Nat Biotechnol. 2005;23(9):1147-57.

39. Dulak AM, Schumacher S, van Lieshout J, Imamura Y, Fox C, Shim B, et al. Gastrointestinal adenocarcinomas of the esophagus, stomach and colon exhibit distinct patterns of genome instability and oncogenesis. Cancer Res. 2012.

40. Govindan R, Ding L, Griffith M, Subramanian J, Dees ND, Kanchi KL, et al. Genomic landscape of non-small cell lung cancer in smokers and never-smokers. Cell. 2012;150(6):1121-34. PMCID: 3656590.

41. Liu X, Ory V, Chapman S, Yuan H, Albanese C, Kallakury B, et al. ROCK inhibitor and feeder cells induce the conditional reprogramming of epithelial cells. The American journal of pathology. 2012;180(2):599-607. PMCID: 3349876.

42. Kondo J, Endo H, Okuyama H, Ishikawa O, Iishi H, Tsujii M, et al. Retaining cell-cell contact enables preparation and culture of spheroids composed of pure primary cancer cells from colorectal cancer. Proceedings of the National Academy of Sciences of the United States of America. 2011;108(15):6235-40. PMCID: 3076886.

43. Yin Y, Betsuyaku T, Garbow JR, Miao J, Govindan R, Ornitz DM. Rapid induction of lung adenocarcinoma by fibroblast growth factor 9 signaling through FGF receptor 3. Cancer Res. 2013.

44. Sharpless NE, Depinho RA. The mighty mouse: genetically engineered mouse models in cancer drug development. Nat Rev Drug Discov. 2006;5(9):741-54.

45. Voskoglou-Nomikos T, Pater JL, Seymour L. Clinical predictive value of the in vitro cell line, human xenograft, and mouse allograft preclinical cancer models. Clinical cancer research : an official journal of the American Association for Cancer Research. 2003;9(11):4227-39.

46. Meyerson M, Gabriel S, Getz G. Advances in understanding cancer genomes through second-generation sequencing. Nat Rev Genet. 2010;11(10):685-96.

47. Forbes SA, Bhamra G, Bamford S, Dawson E, Kok C, Clements J, et al. The Catalogue of Somatic Mutations in Cancer (COSMIC). Curr Protoc Hum Genet. 2008;Chapter 10:Unit 10 1. PMCID: 2705836.

48. Adzhubei IA, Schmidt S, Peshkin L, Ramensky VE, Gerasimova A, Bork P, et al. A method and server for predicting damaging missense mutations. Nat Methods. 2010;7(4):248-9. PMCID: 2855889.

49. Hammerman PS, Sos ML, Ramos AH, Xu C, Dutt A, Zhou W, et al. Mutations in the DDR2 kinase gene identify a novel therapeutic target in squamous cell lung cancer. Cancer discovery. 2011;1(1):78-89. PMCID: 3274752.

50. Liao RG, Jung J, Tchaicha JH, Wilkerson MD, Sivachenko A, Beauchamp EM, et al. Inhibitor-sensitive FGFR2 and FGFR3 mutations in lung squamous cell carcinoma. Cancer Res. 2013.

51. Hodis E, Watson IR, Kryukov GV, Arold ST, Imielinski M, Theurillat JP, et al. A landscape of driver mutations in melanoma. Cell. 2012;150(2):251-63. PMCID: 3600117.

52. Thimmulappa RK, Mai KH, Srisuma S, Kensler TW, Yamamoto M, Biswal S. Identification of Nrf2-regulated genes induced by the chemopreventive agent sulforaphane by oligonucleotide microarray. Cancer Res. 2002;62(18):5196-203.

53. Shibata T, Ohta T, Tong KI, Kokubu A, Odogawa R, Tsuta K, et al. Cancer related mutations in NRF2 impair its recognition by Keap1-Cul3 E3 ligase and promote malignancy. Proceedings of the National Academy of Sciences of the United States of America. 2008;105(36):13568-73. PMCID: 2533230.

54. Singh A, Bodas M, Wakabayashi N, Bunz F, Biswal S. Gain of Nrf2 function in non-small-cell lung cancer cells confers radioresistance. Antioxid Redox Signal. 2010;13(11):1627-37. PMCID: 3541552.

55. Tomlinson DC, Hurst CD, Knowles MA. Knockdown by shRNA identifies S249C mutant FGFR3 as a potential therapeutic target in bladder cancer. Oncogene. 2007;26(40):5889-99. PMCID: 2443272.

56. Drug-sensitive FGFR2 mutations in endometrial carcinoma, (2008).

57. Pollock PM, Gartside MG, Dejeza LC, Powell MA, Mallon MA, Davies H, et al. Frequent activating FGFR2 mutations in endometrial carcinomas parallel germline mutations associated with craniosynostosis and skeletal dysplasia syndromes. Oncogene. 2007;26(50):7158-62. PMCID: 2871595.

58. Chesi M, Nardini E, Brents LA, Schrock E, Ried T, Kuehl WM, et al. Frequent translocation t(4;14)(p16.3;q32.3) in multiple myeloma is associated with increased expression and activating mutations of fibroblast growth factor receptor 3. Nat Genet. 1997;16(3):260-4.

59. Luqmani YA, Graham M, Coombes RC. Expression of basic fibroblast growth factor, FGFR1 and FGFR2 in normal and malignant human breast, and comparison with other normal tissues. British journal of cancer. 1992;66(2):273-80. PMCID: 1977809.

60. Shiang CY, Qi Y, Wang B, Lazar V, Wang J, Fraser Symmans W, et al. Amplification of fibroblast growth factor receptor-1 in breast cancer and the effects of brivanib alaninate. Breast Cancer Res Treat. 2010;123(3):747-55.

61. Singh D, Chan JM, Zoppoli P, Niola F, Sullivan R, Castano A, et al. Transforming fusions of FGFR and TACC genes in human glioblastoma. Science. 2012;337(6099):1231-5. PMCID: 3677224.

62. Williams SV, Hurst CD, Knowles MA. Oncogenic FGFR3 gene fusions in bladder cancer. Hum Mol Genet. 2013;22(4):795-803. PMCID: 3554204.

63. Majewski IJ, Mittempergher L, Davidson NM, Bosma A, Willems SM, Horlings HM, et al. Identification of recurrent FGFR3 fusion genes in lung cancer through kinome-centred RNA sequencing. J Pathol. 2013;230(3):270-6.

64. Gozgit JM, Wong MJ, Moran L, Wardwell S, Mohemmad QK, Narasimhan NI, et al. Ponatinib (AP24534), a multitargeted pan-FGFR inhibitor with activity in multiple FGFR-amplified or mutated cancer models. Molecular cancer therapeutics. 2012;11(3):690-9.

65. Ellis LM, Hicklin DJ. Resistance to Targeted Therapies: Refining Anticancer Therapy in the Era of Molecular Oncology. Clinical cancer research : an official journal of the American Association for Cancer Research. 2009;15(24):7471-8.

APPENDIX

Inhibitor-sensitive FGFR2 and FGFR3 mutations in lung squamous cell carcinoma

Appendix

Published OnlineFirst June 20, 2013; DOI: 10.1158/0008-5472.CAN-12-3950

Cancer Research

Inhibitor-Sensitive FGFR2 and FGFR3 Mutations in Lung Squamous Cell Carcinoma

Rachel G. Liao, Joonil Jung, Jeremy Tchaicha, et al.

Cancer Res 2013;73:5195-5205. Published OnlineFirst June 20, 2013.

Appendix

Published OnlineFirst June 20, 2013; DOI: 10.1158/0008-5472.CAN-12-3950

Therapeutics, Targets, and Chemical Biology

Cancer Research

Inhibitor-Sensitive FGFR2 and FGFR3 Mutations in Lung Squamous Cell Carcinoma

Rachel G. Liao[1,3], Joonil Jung[3], Jeremy Tchaicha[1], Matthew D. Wilkerson[4], Andrey Sivachenko[3], Ellen M. Beauchamp[1], Qingsong Liu[2], Trevor J. Pugh[1,3], Chandra Sekhar Pedamallu[1,3], D. Neil Hayes[4], Nathanael S. Gray[2], Gad Getz[3], Kwok-Kin Wong[1], Robert I. Haddad[1], Matthew Meyerson[1,3], and Peter S. Hammerman[1,3]

Abstract

A comprehensive description of genomic alterations in lung squamous cell carcinoma (lung SCC) has recently been reported, enabling the identification of genomic events that contribute to the oncogenesis of this disease. In lung SCC, one of the most frequently altered receptor tyrosine kinase families is the fibroblast growth factor receptor (FGFR) family, with amplification or mutation observed in all four family members. Here, we describe the oncogenic nature of mutations observed in *FGFR2* and *FGFR3*, each of which are observed in 3% of samples, for a mutation rate of 6% across both genes. Using cell culture and xenograft models, we show that several of these mutations drive cellular transformation. Transformation can be reversed by small-molecule FGFR inhibitors currently being developed for clinical use. We also show that mutations in the extracellular domains of *FGFR2* lead to constitutive FGFR dimerization. In addition, we report a patient with an *FGFR2*-mutated oral SCC who responded to the multitargeted tyrosine kinase inhibitor pazopanib. These findings provide new insights into driving oncogenic events in a subset of lung squamous cancers, and recommend future clinical studies with FGFR inhibitors in patients with lung and head and neck SCC. *Cancer Res; 73(16); 5195–205. ©2013 AACR.*

Introduction

Two goals of comprehensive next-generation sequencing of cancers are to discover novel, targetable somatic alterations, and to identify new targets for which therapies already exist. Genome-scale analyses of tumors representing many cancer types have recently been completed (1–6), enabling discoveries consistent with both goals.

Historically, targetable oncogenic alterations in cancer were discovered on an individual gene basis. This was the case for cancer-causing alterations observed in several tyrosine kinases, including *EGFR* and *ALK* in lung adenocarcinoma (7–9), *FGFR2* in endometrial carcinoma (10, 11), and *FGFR3* in urothelial carcinoma (12). These studies and others have led to demonstrations of the successful application of targeted therapeutic agents and their superiority to conventional chemotherapy (13, 14).

Lung squamous cell carcinoma (lung SCC) is a prevalent and deadly disease for which no targeted therapies are approved. Recent data reported by The Cancer Genome Atlas (TCGA) lung SCC project (4) showed that the fibroblast growth factor receptor (FGFR) tyrosine kinases are one of the most frequently altered kinase families in this disease. Amplification of *FGFR1* was observed, in agreement with prior reports (15, 16). Furthermore, mutations in *FGFR2* and *FGFR3* were reported. Although the frequency of these mutations did not reach statistical significance at the cohort size examined by TCGA, several features including recurrence, prior observation in other cancer types and congenital syndromes, and lack of other dominant oncogenic alterations in tumors with *FGFR* mutations, suggested they might be driving, targetable events in a subset of patients presenting with this disease.

Germline mutations in the FGFR tyrosine kinase family were first described in craniofacial and skeletal syndromes (17). Somatic point mutations identical to those germline events have also been observed in malignancies (18). The FGFR family is made up of four active members, each containing an extracellular domain (ECD) and a cytoplasmic kinase domain. Activation is stimulated by binding FGF and heparan sulfate proteoglycan (HSPG) in the ECD, and subsequent dimerization of two receptor–ligand complexes, leading to transphosphorylation of the kinase domains. This leads to phosphorylation of

Authors' Affiliations: Departments of [1]Medical Oncology and [2]Biological Chemistry and Molecular Pharmacology, Dana-Farber Cancer Institute, Boston; [3]The Broad Institute of Harvard and MIT, Cambridge, Massachusetts; and [4]Lineberger Comprehensive Cancer Center, University of North Carolina at Chapel Hill, Chapel Hill, North Carolina

Note: Supplementary data for this article are available at Cancer Research Online (http://cancerres.aacrjournals.org/).

J. Jung, J. Tchaicha, and M.D. Wilkerson contributed equally to this work.

Corresponding Authors: Peter S. Hammerman, Department of Medical Oncology, Dana-Farber Cancer Institute, 450 Brookline Ave, Boston, MA 02215. Phone: 617-632-6335; Fax: 617-582-7880; E-mail: phammerman@partners.org; Matthew Meyerson, E-mail: Matthew_meyerson@dfci.harvard.edu; and Robert I. Haddad, E-mail: Robert_Haddad@dfci.harvard.edu

doi: 10.1158/0008-5472.CAN-12-3950

Appendix

Published OnlineFirst June 20, 2013; DOI: 10.1158/0008-5472.CAN-12-3950

binding partner FRS2 and downstream activation of Ras/MAPK and PI3K/AKT pathways (19).

The FGF family is made up of more than 20 members, all of which retain specificities for both different FGFR family members and different isoforms of each receptor (20). In addition, tissue types vary in which receptors, isoforms, and ligands are expressed, adding further levels of complexity to the system. Dysregulation can lead to oncogenesis, as has been shown with altered expression of receptors (15, 16, 21), altered isoform expression (22, 23), and altered ligand specificity (24) driven by somatic genomic events.

Aberrant FGFR signaling has been implicated in the development of several cancer types. In addition to lung SCC, *FGFR1* amplification is observed in 10% of breast cancers (21). Point mutations in *FGFR2* are observed in 12% of endometrial carcinomas (10) and mutations in *FGFR3* are observed in more than 30% of urothelial carcinomas (12). Cell lines harboring these events have shown sensitivity to inhibition by FGFR small-molecule inhibitors, and clinical trials are now testing FGFR inhibitors in patients harboring somatic events in *FGFRs* (18).

Here, we characterize *FGFR2* and *FGFR3* mutations observed in lung SCC and show the oncogenic potential of these mutations using models of transformation and dependency. We show that cells harboring these mutations are sensitive to inhibition by several FGFR and multikinase inhibitors. In addition, we report a case of a patient with an *FGFR2*-mutated oral SCC, who responded to pazopanib, an inhibitor of multiple tyrosine kinases including the FGFR family. Together, these data identify a promising new therapeutic target for patients with lung SCC and other squamous epithelial tumors.

Materials and Methods

Patient samples and genomic analysis

We manually reviewed *FGFR2* and *FGFR3* exome sequencing data generated by the TCGA research network. In addition, we queried publicly available sequencing data generated from 18 samples that were excluded from the initial TCGA report. All data were deidentified and obtained in accordance with patient protection standards set by the TCGA and were obtained from the TCGA Data Portal.

For the individual with a clinical response to pazopanib, total RNA was extracted using the AllPrep DNA/RNA Mini Kit (Qiagen; #80204). Poly-adenylated mRNA was enriched using the Ambion MicroPoly(A)Purist Kit starting from 30 μg of total RNA as an input according to the manufacturer's protocol.

Illumina transcriptome sequencing libraries were prepared as previously described (25) from mRNA and from total RNA and were subjected to 76-bp paired-end sequencing on a single lane of an Illumina GAIIx sequencer. Sequencing reads were first aligned to all curated protein-coding transcripts and were mapped back to reference human genome, hg18 as previously described (25). Potential mutations were called using the Unified genotyper from the GATK tool (26).

This individual was consented for the analysis according to Institutional Protocol 94138 at the Dana-Farber Cancer Institute (Boston, MA). The FGFR2 P253R mutation was found in both the total RNA-seq data and mRNA-seq data, and it was confirmed from genomic DNA by Sanger sequencing in a Clinical Laboratory Improvement Amendments (CLIA)–certified laboratory.

Cell lines, antibodies, ligands, and inhibitors

NIH-3T3 cells and Ba/F3 cells were obtained from the American Type Culture Collection and maintained as described previously (10, 20). Antibodies against FGFR2 (C-8) and FRS2 (H-91) were purchased from Santa Cruz Biotechnology, Inc. Antibodies against FGFR3 (C51F2), p-FGFR, p-FRS2 (Y436), AKT (C67E7), p-AKT (T308, 244F9), Erk 1/2 (137F5), p-Erk 1/2 (E10), and β-actin (8H10D10) were obtained from Cell Signaling Technology, Inc.

For FGFR stimulation experiments, the FGF1 ligand was obtained from Abcam. FGF7 and FGF9 were obtained from Life Technologies. Interleukin-3 (IL-3) was purchased from VWR and heparin from STEMCELL Technologies, Inc.

Ponatinib (AP24534), dovitinib (TKI258), and cediranib (AZD2171) were obtained from Selleck Chemicals. Brivanib alaninate (BMS-582664) was obtained from Fischer Scientific. Pazopanib (GW786034) was obtained from Axon Medchem. AZD4547 was obtained from Active Biochem. E7080 was obtained from American Custom Chemicals Corporation. BGJ398 was a gift from Novartis Pharmaceuticals Corporation.

Mutagenesis and cellular transfection and infection

Mutagenesis primers developed for each mutation were generated using the Agilent QuikChange Primer Design tool. *FGFR2* isoforms IIIb and IIIc, and *FGFR3* isoform IIIc were cloned into pDONR223 and mutated by site-directed mutagenesis with the QuikChange Lightning Site-Directed Mutagenesis Kit from Agilent Technologies. Sequence-verified constructs were cloned into pBabe-puro and transfected into HEK-293T cells with Fugene-6 (Promega) as described previously (10). NIH-3T3 and Ba/F3 cells were infected with the resulting virus and after 2 days the cells were selected with 2 μg/mL puromycin.

Western blot analysis and visualization of unreduced dimers

Cells were lysed in buffer containing 0.5% NP-40, 50 mmol/L Tris pH 8, 150 mmol/L $MgCl_2$, and phosphatase and protease inhibitors, and proteins were separated by SDS-PAGE and transferred to nitrocellulose membranes via the iBlot dry transfer system (Invitrogen). Antibody binding was detected using the LI-COR Odyssey IR imaging system (LI-COR Biosciences).

To visualize receptor dimers formed by ECD mutations to cysteine residues, NIH-3T3 cells expressing the appropriate mutations were serum-starved for 8 hours in the presence of PBS or FGF1 and heparin, washed with PBS containing 10 mmol/L iodoacetamide, and lysed in lysis buffer containing 1% Triton, 10% glycerol, 50 mmol/L Tris pH 7.4, and 10 mmol/L iodoacetamide. Two 100 μg aliquots of each protein sample were prepared, one with reducing agent and one without. Electrophoresis was carried out using 4% to 12% Tris–glycine SDS-PAGE gels (Invitrogen).

Appendix

Published OnlineFirst June 20, 2013; DOI: 10.1158/0008-5472.CAN-12-3950

To confirm loss of phosphorylation of relevant kinases in the presence of inhibitor, NIH-3T3 cells expressing mutated FGFR2 or FGFR3 were washed with PBS, serum-starved for 4 hours in the presence of indicated concentrations of inhibitor, and ligand-stimulated with FGF1 for 30 minutes before lysis.

Soft agar colony formation assays

Two milliliter of 0.5% Select agar (Gibco) and media were plated to each well of a non-tissue culture–treated 6-well plate and allowed to solidify. A total of 5×10^4 cells were suspended in 330 μL media and mixed with 770 μL 0.5% Select agar and media and then plated onto the solidified bottom layer in triplicate. Plates were incubated for 3 weeks, photographed using QuickCapture (Logitech), and quantified via ImageJ for colony formation. Statistical comparison was conducted using the Student *t* test.

To evaluate the effect of clinical inhibitors on soft agar colony formation, the above protocol was conducted with the following alteration: 5×10^4 cells were suspended in 330 μL media plus relevant inhibitor before addition of 0.5% agar solution and plating.

Xenograft studies

All animal experiments were carried out according to the institutional guidelines about animal safety. Immunocompromised mice were injected with NIH-3T3 cells stably expressing exogenous FGFR2-IIIb wild-type (WT)-, W290C-, S320C-, or K660N-mutant isoforms. Cohorts of 7 mice were injected at three sites for each cell type with 2 million cells per site, and mice were observed until tumor volume reached 200 to 300 mm^3. Mice were then treated with BGJ-398 at 15 mg/kg or vehicle (PEG-300) control daily for 2 weeks, and tumor size was measured during the treatment period.

Ba/F3 dependency and inhibitor studies

Ba/F3 cells expressing each mutation construct were selected in media containing IL-3 and puromycin. To establish cells dependent on FGFR signaling, 3 million cells were washed twice with PBS and seeded into 2 mL of media containing FGF7 (for FGFR2 IIIb) or FGF9 (for FGFR2 IIIc) and heparin. These cells were maintained until IL-3–independent cells emerged. Five thousand FGFR-dependent cells per well were seeded into 96-well plates in 100 μL media containing FGF and heparin. Ten microliter drug was added in quadruplicate for final concentrations of 0.3 nmol/L to 10 μmol/L in half logs, with two DMSO controls, and incubated for 3 or 4 days. Fifty microliter CellTiter-Glo (Promega) was added to each well and luminescence was measured on the SpectraMax 5 imager. Percentage survival compared with DMSO controls was calculated and plotted in Prism (GraphPad Software, Inc.).

Results

FGFR2 and FGFR3 are recurrently mutated in lung SCC

We analyzed whole-exome sequencing data, generated by TCGA (4), for mutations in the *FGFR2* and *FGFR3* genes. We identified five *FGFR2* and six *FGFR3* mutations in analysis of exome sequencing data of 178 tumor/normal pairs, as well as an *FGFR2* K660N mutation in a sample that was excluded from the TCGA report due to poor RNA quality (TCGA-21-1083), for a total of 12 mutations.

Patients in the reported TCGA cohort with *FGFR* mutations ($n = 10$, as one subject had two *FGFR* mutations) ranged from 58 to 81 years old with a median age of 73 years. All patients were current or former smokers with a pack-year history of 9 to 63 pack-years (median, 49). Tumors were obtained from resected specimens with a T stage of I ($n = 3$) or II ($n = 7$) and N stage of 0 ($n = 8$) or I ($n = 2$). More extensive patient data are available in Supplementary Table S1.

The observed mutations fell in both the extracellular and kinase domains of FGFR2 and FGFR3, both in codons in which mutations have been previously reported in endometrial carcinoma (10, 11) and urothelial carcinoma (12), and at novel residues (Fig. 1A). In the samples containing *FGFR2* or *FGFR3* mutations, the IIIb isoforms of each protein were overexpressed compared with the IIIc isoforms (Supplementary Fig. S1). *FGFR* kinase alterations were significantly enriched in the basal expression subtype (ref. 27; Fisher exact test; $P = 0.016$; Supplementary Fig. S1).

FGFR mutations cooccurred with mutations in known oncogenes in only 3 cases. LUSC-21-1078 had a high somatic mutation rate and harbored mutations in *HRAS* at codon 61 and *PDGFRA* at codon 842, both previously reported to be sites of oncogenic mutation, as well as a novel *ERBB2* E1021Q mutation (Fig. 1B). LUSC-21-1078 contained a noncanonical *KRAS* mutation G118S and LUSC-21-5485 had a previously unreported *ERBB2* mutation G1075V. Other samples contained no known oncogenic somatic mutations, except that *FGFR2* and *FGFR3* mutations commonly cooccurred with mutations in *TP53* (8 of 10) and *PIK3CA* (3 of 10), the latter being a gene with mutations that commonly cooccur with driving oncogenes. Four of 10 samples with *FGFR* mutation harbored 3q amplification of *SOX2* and 2 samples *CDKN2A* homozygous deletion (Fig. 1B). The presence of these events may suggest that FGFR mutations are not solely driving oncogenesis; however, due to the high heterogeneity observed in the lung SCC samples, even the presence of other known oncogenic events does not guarantee that events cooccur in cells or that subsets of tumor cells would not be sensitive to FGFR-targeted therapy.

FGFR2 and FGFR3 mutations drive anchorage-independent growth of NIH-3T3 cells

To determine whether the mutations identified in lung SCC were oncogenic, we established NIH-3T3 cells stably expressing each mutation to assess anchorage-independent growth in soft agar. We observed colony formation in cells expressing the majority of observed FGFR2 and FGFR3 mutations (Fig. 2A). We determined that ECD mutations W290C and S320C in FGFR2, and R248C and S249C in FGFR3, significantly increased colony formation compared with WT FGFR2 or FGFR3, as did kinase domain mutations K660E and K660N in *FGFR2* ($P < 0.05$ by Student *t* test). In contrast, FGFR2 mutations E471Q and T787K, and FGFR3 mutations S435C and K717M did not form colonies above WT. Robust formation of colonies was observed in NIH-3T3 cells expressing an activating *EGFR* insertion

Published OnlineFirst June 20, 2013; DOI: 10.1158/0008-5472.CAN-12-3950

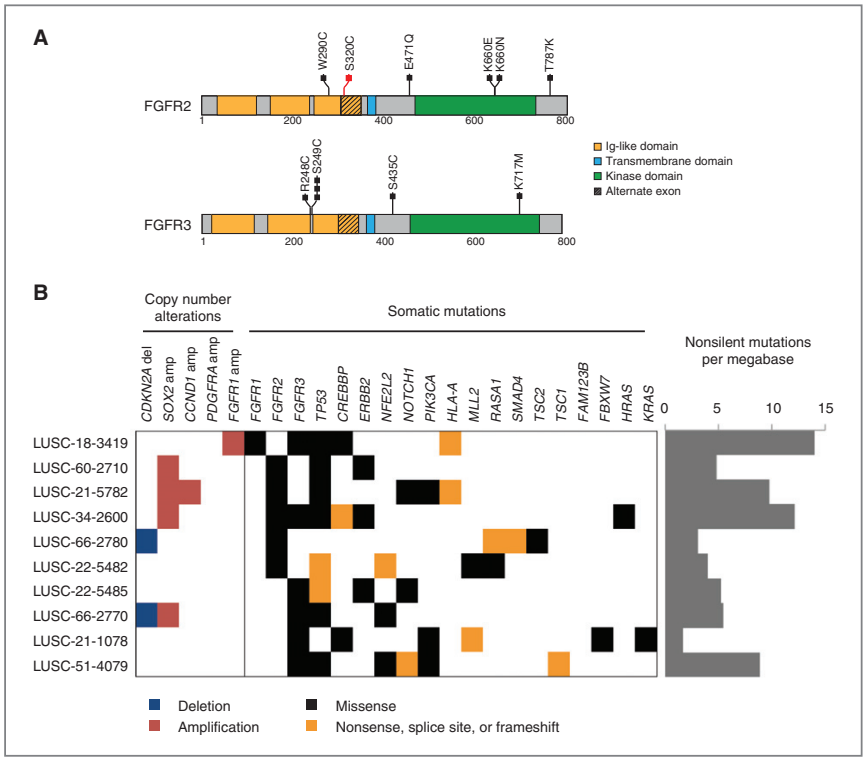

Figure 1. Recurrent mutations in FGFR2 and FGFR3 are observed in lung SCC. A, sequencing data from TCGA were analyzed and recurrent mutations were observed in FGFR2 and FGFR3. The mutation S320C in FGFR2, in red, is located in the alternatively spliced exon in the IG-3 domain of FGFR2 IIIb; the remaining mutations are annotated to the IIIc isoform. FGFR3 mutations are annotated in the IIIc isoform. B, cooccurring somatic copy number alterations and mutations in samples with mutation.

mutation. *FGFR2* mutations were generated in both common isoforms of *FGFR2* with similar results obtained for all assayed mutations with the exception of FGFR2 T787K, which was very modestly transforming only in isoform IIIc (Fig. 2A).

FGFR2 and FGFR3 mutations drive tumor formation in xenograft models

NIH-3T3 cells expressing transforming FGFR2 mutations or WT were injected into nude mice. Tumors reached approximately 200 to 300 mm^3 in all mice injected with mutant cells by day 13 and began treatment with a pan-FGFR inhibitor, BGJ398 (28), or vehicle, with ECD mutations driving particularly strong tumor formation (Fig. 2B, solid lines). Tumors formed by cells expressing WT FGFR2 grew more slowly, and began treatment on day 16 (Fig. 2B).

Tumors treated with BGJ398 slowed or reversed their growth compared with vehicle (Fig. 2B, dashed lines), so that by the end of the study, tumor burden in vehicle-treated versus BGJ398-treated mice was noticeably distinct (Fig. 2C and Supplementary Fig. S2).

Extracellular domain mutations form ligand-sensitive intermolecular disulfide bonds

A common mechanism of activation of the FGFR2 and FGFR3 kinases is through the formation of covalently bound receptor dimers (29, 30). Although WT receptor tyrosine kinases maintain extracellular structure required for ligand binding and receptor dimerization through intramolecular disulfide bonds, mutant receptors can form intermolecular disulfide dimers through a novel cysteine residue created by the mutation itself

Appendix

Published OnlineFirst June 20, 2013; DOI: 10.1158/0008-5472.CAN-12-3950

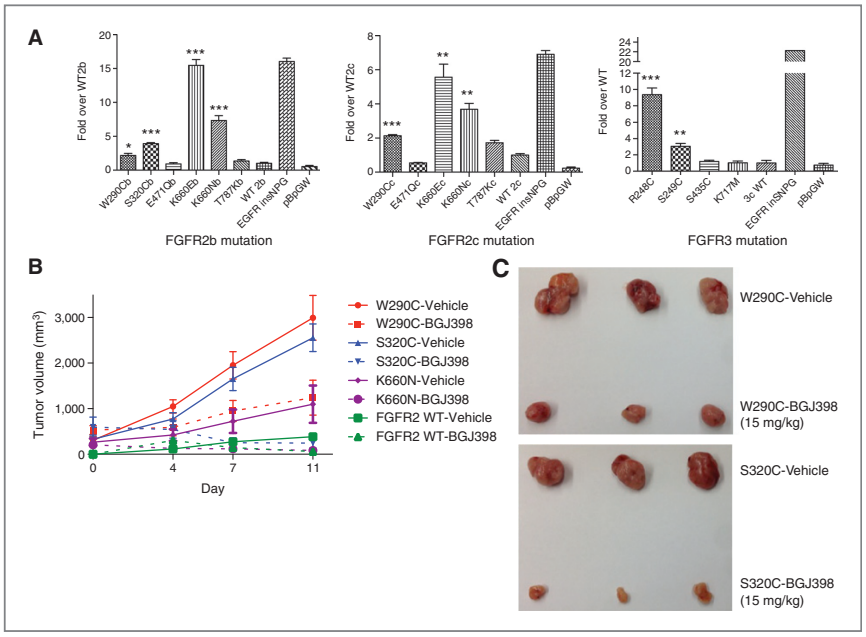

Figure 2. A subset of lung SCC mutations in FGFR2 and FGFR3 is transforming in anchorage-independent growth assays and xenograft assays. A, colony formation compared with WT in NIH-3T3 cells expressing *FGFR* mutations was calculated for each isoform and graphed. EGFR insNPG was included as a positive control, and the pBabe-puro Gateway empty vector (pBp GW) was included as a negative control. *P* values were calculated with the Student *t* test and significance is indicated by asterisks; *, $P < 0.05$; **, $P < 0.01$; ***, $P < 0.001$. B, nude mice injected with transforming FGFR2-mutant cells from A developed tumors, which were treated with BGJ398 (dashed lines) or vehicle (solid lines). C, tumors were dissected from the mice for visual inspection, comparing treatment with vehicle or drug. Top, FGFR2-W290C tumors; bottom, FGFR2-S320C. Tumor images corresponding to FGFR2-K660N and FGFR2-WT tumors are shown in Supplementary Fig. S2.

or through instability created by a mutated residue near a structural intramolecular disulfide bond (29). This mechanism was previously established for *FGFR3* mutations that we have observed in lung SCC, R248C, and S249C (30).

To assess whether mutations in the ECD of FGFR2 and FGFR3 lead to covalent dimerization, and whether dimerization could be increased by ligand stimulation, we serum-starved cells in the presence of PBS or 5 nmol/L FGF1 and 2 μg/mL heparin for 8 hours, or 5 nmol/L FGF1 and 2 μg/mL heparin for 30 minutes, followed by washing with PBS and serum-starving in the presence of PBS for the remaining 7.5 hours followed by electrophoresis in both reducing and non-reducing conditions. FGFR2 ECD mutations were sufficient to drive covalent dimerization in the absence of ligand, but dimerization was increased in the presence of even 30 minutes of ligand stimulation (Supplementary Fig. S3A). In FGFR3 mutations, on the other hand, dimerization was observed but not increased under ligand-stimulation conditions (Supplementary Fig. S3B). As has been shown previously (31), FGFR proteins typically form highly glycosylated folded protein products. Although FGFR2 W290C seems to undergo a glycosylation defect contributing to its lower molecular weight, this mutant form still retains the capacity to dimerize.

We then seeded the same cells into soft agar in the presence of PBS, 2 μg/mL heparin alone, or 5 nmol/L FGF1 and 2 μg/mL heparin. After 3 weeks, we observed greater colony formation in response to FGF1 and heparin treatment than in heparin alone or PBS-treated cells (Supplementary Fig. S3C).

FGFR2- and FGFR3-driven cellular transformation is blocked by clinically relevant FGFR inhibitors

Having established that *FGFR2* and *FGFR3* mutations in lung SCC drive anchorage-independent growth in NIH-3T3 cells, we asked whether this transformation could be blocked by small-molecule inhibitors of FGFRs. NIH-3T3 cells were seeded into soft agar in the presence or absence of the multikinase inhibitor AP24534 (ponatinib), which targets imatinib-resistant BCR-ABL (32), and has activity against FGFR family members

Published OnlineFirst June 20, 2013; DOI: 10.1158/0008-5472.CAN-12-3950

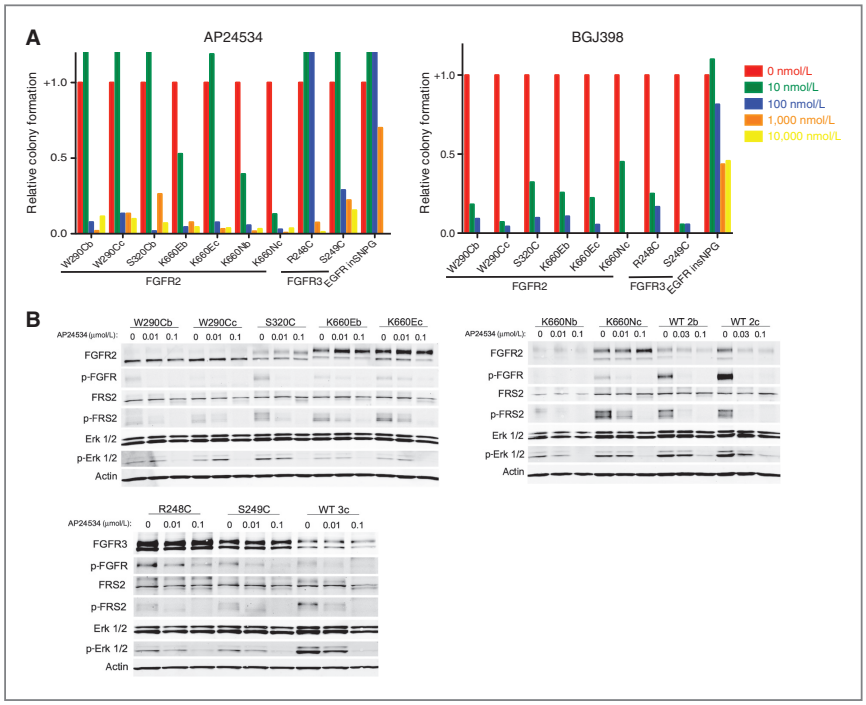

Figure 3. Anchorage-independent colony formation is abrogated in the presence of anti-FGFR inhibitors. A, NIH-3T3 cells expressing each transforming mutation were seeded in the presence of increasing concentrations of ponatinib (AP24534; left) and BJG398 (right). B, cells were serum-starved and exposed to the indicated concentrations of ponatinib for 4 hours and then ligand-stimulated for 30 minutes with FGF1, after which cells were lysed and probed via immunoblot. These experiments were carried out with several other clinical inhibitors; those results are documented in Supplementary Fig. S4.

(33). Colony formation was inhibited in the presence of ponatinib in cells harboring activating *FGFR2* or *FGFR3* mutations, but not in cells harboring an activating EGFR insertion (Fig. 3A, left). All ECD mutations in FGFR2 and S249C in FGFR3 lost colony-forming potential when exposed to 100 nmol/L of drug, whereas kinase domain mutations lost colony-forming potential at 10 nmol/L of drug. Exceptions were FGFR2 K660E expressed in the IIIc isoform, which behaved similarly to the FGFR2 ECD mutations, and FGFR3 R248C, which had a 10-fold higher inhibitory concentration than any other mutation, at 1 μmol/L. Colony formation driven by EGFR was not lost until cells were exposed to 10 μmol/L of drug.

To determine whether ponatinib was inhibiting colony formation driven by mutant *FGFR2* and *FGFR3*, we assessed phosphorylation of several proteins in the FGFR signaling pathway. Levels of phospho-FGFR, phospho-FRS2, and phospho-Erk all decreased in response to increasing concentrations of ponatinib (Fig. 3B), suggesting that colony formation was lost due to a decrease in FGFR-mediated signaling.

To evaluate whether ponatinib was acting by specific inhibition of FGFR kinases, these assays were also conducted with BGJ398, a selective FGFR kinase inhibitor (28) as well as pazopanib (GW786034; ref. 34) and dovitinib (TKI-258; ref. 35), two multikinase inhibitors with specificity for FGFR family members. Colony formation was inhibited by at least 50% in the presence of 10 nmol/L BGJ398 for all cells expressing *FGFR* mutations, whereas cells expressing the activating EGFR insertion did not lose the capacity for colony formation until 1 μmol/L BGJ398 (Fig. 3A, right), and WT phosphorylation was lost at 10 nmol/L under ligand stimulation conditions (Supplementary Fig. S4A). Dovitinib also inhibited colony formation in cells expressing mutant FGFR compared with activated EGFR, but with less uniformity across mutations. FGFR2 ECD mutations lost 50% colony formation between 100 nmol/L and

Published OnlineFirst June 20, 2013; DOI: 10.1158/0008-5472.CAN-12-3950

1 μmol/L dovitinib. In contrast, colony formation was inhibited by 50% between 10 and 100 nmol/L for FGFR2 kinase domain mutations excluding K660E IIIc, which behaved similarly to the FGFR2 ECD mutations. Cells expressing FGFR3 R248C and S249C were sensitive between 10 and 100 nmol/L. Again, cells transformed by mutant EGFR did not lose colony formation until exposed to 10 μmol/L drug (Supplementary Fig. S4B, left). Mutant EGFR-expressing cells had sustained phosphorylation at AKT T308 up to 10 μmol/L dovitinib, as detected by immunoblot, whereas detectable AKT phosphorylation was lost by 100 nmol/L to 1 μmol/L dovitinib in cells expressing *FGFR* mutations (Supplementary Fig. S4C). Pazopanib similarly inhibited colony formation in cells expressing all FGFR2 and FGFR3 mutations at concentrations of 100 nmol/L to 1 μmol/L drug, whereas cells expressing mutant EGFR formed colonies even in the presence of 10 μmol/L drug (Supplementary Fig. S4B, right). Consistently, biochemical studies revealed sustained AKT T308 phosphorylation in mutant EGFR cells exposed to 10 μmol/L pazopanib, whereas detectable AKT T308 phosphorylation was lost in mutant FGFR cells at 100 nmol/L to 1 μmol/L pazopanib (Supplementary Fig. S4D).

In NIH-3T3 cells expressing the ECD mutations of both *FGFR2* and *FGFR3* and in the kinase domain mutation *FGFR2* K660E IIIc, we observed that low concentrations of ponatinib (10 nmol/L) conferred a growth-promoting phenotype above control, which was abrogated at higher concentrations (Fig. 3A, left). This could be due to the multikinase inhibitory properties of ponatinib, which may inhibit a second kinase that could impact FGFR2 or FGFR3 signaling. This phenomenon was also observed when these experiments were carried out with the two other multikinase inhibitors with anti-FGFR activity, pazopanib and dovitinib (Supplementary Fig. S4B), but not with BGJ398, a more selective FGFR kinase inhibitor (Fig. 3A, right).

Analysis of FGFR2 and FGFR3 inhibition in IL-3–independent Ba/F3 cells

To test whether cellular transformation driven by mutated *FGFR2* could be abrogated in a second system by small-molecule FGFR inhibitors and to test the relative efficacy of these compounds, we generated Ba/F3 cells expressing the *FGFR2* mutations that had shown significant colony formation in the NIH-3T3 anchorage-independent assay. These cell lines were dependent on FGFR signaling in the presence of FGF and heparin, and in the absence of IL-3. Phosphorylation of the FGFR kinase domain and FRS2 were measured by immunoblot, and interestingly, cells expressing FGFR2 K660E IIIc showed a greater degree of phosphorylation of both molecules despite similar expression levels as compared with cells expressing other mutations (Fig. 4A).

Ba/F3 cells expressing WT and mutated *FGFR2* transgenes were first seeded into media containing increasing concentrations of ponatinib. We observed that ponatinib inhibited IL-3–independent proliferation of Ba/F3 cells expressing the FGFR mutations at about 10 nmol/L of drug treatment, but cells expressing an EGFR-activating insertion or parental Ba/F3 cells grown in the presence of IL-3 were only inhibited by 10 μmol/L of drug (Fig. 4B, left). IC_{50} values for Ba/F3 cells expressing each mutant were also calculated and plotted (Fig. 4C, left). These assays were also conducted on cells seeded into media containing BGJ398, and similarly, cells expressing FGFR mutations, but not the EGFR insertion or parental Ba/F3 cells, were inhibited at about 10 nmol/L inhibitory concentrations of drug (Fig. 4B, right and Fig. 4C, right). Interestingly, insensitive controls in the presence of ponatinib seemed to gain a growth advantage in the presence of drug at concentrations in the range of 10 to 100 nmol/L (Fig. 4B), similar to our observations in the anchorage-independent colony formation assay (Fig. 3A and Supplementary Fig. S4B).

To further assess the potency of small-molecule FGFR kinase inhibitors in the Ba/F3 system, we assembled a panel of FGFR kinase inhibitors described in the literature (refs. 28, 32–39; Supplementary Table S2) and tested the Ba/F3 inhibitory response in the presence of each. Each of these inhibitors showed similar trends to those seen for ponatinib and BGJ398: a multi-log increase in drug sensitivity in cells expressing FGFR mutations compared with controls (Supplementary Fig. S5). IC_{50} values for each mutation in the presence of each drug were also calculated (Supplementary Fig. S5). Strikingly, *FGFR2* K660E expressed in the IIIc isoform (in yellow) repeatedly exhibited a 5- to 10-fold higher IC_{50} concentration as compared with the IIIb isoform and either isoform of the K660N mutation in the FGFR2 kinase domain (Supplementary Fig. S5). This observation was consistent with the concentrations at which anchorage-independent growth observed for FGFR2 K660E IIIc was lost in the presence of several inhibitors (Fig. 3A and Supplementary Fig. S4B).

Case report of a head and neck SCC patient responding to an FGFR inhibitor

We identified an individual with SCC of the head and neck who was found to harbor an extracellular *FGFR2* mutation (p.P253R) in a biopsy specimen (Fig. 5A). This mutation was initially identified in RNA sequencing data and then confirmed by Sanger sequencing in a CLIA-certified laboratory (Fig. 5B). *FGFR2* mutations have previously been observed at low frequencies in head and neck cancer (40, 41), and confirmed by initial reports from TCGA where seven mutations were observed in exome sequencing data of 279 individuals as of October 1, 2012 (data obtained from the TCGA Data Coordinating Center). FGFR2 P253R has previously been observed in endometrial carcinoma (10). Cellular and biochemical analysis of the FGFR2 P253R mutation suggest that this event is transforming and sensitive to targeted therapies in our assays, similar to the events observed in lung SCC (Supplementary Fig. S6).

The patient was diagnosed with locally advanced (T2N1M0, stage III) SCC of the right tongue in 2008 at the age of 52 years. He had no history of tobacco use or alcohol abuse and was treated with a right hemiglossectomy and postoperative radiotherapy. He subsequently developed recurrences in the right and left neck over a period of 3 years and was treated with surgery, two additional courses of radiotherapy and multiple courses of chemotherapy including carboplatin, paclitaxel, cisplatin, and cetuximab. In 2012, he had further progression in the right neck and left axilla. He began daily treatment with 800 mg pazopanib starting on April 12, 2012. At this time, he had gross disease in the right neck (Fig. 5C, left). A follow-up

Published OnlineFirst June 20, 2013; DOI: 10.1158/0008-5472.CAN-12-3950

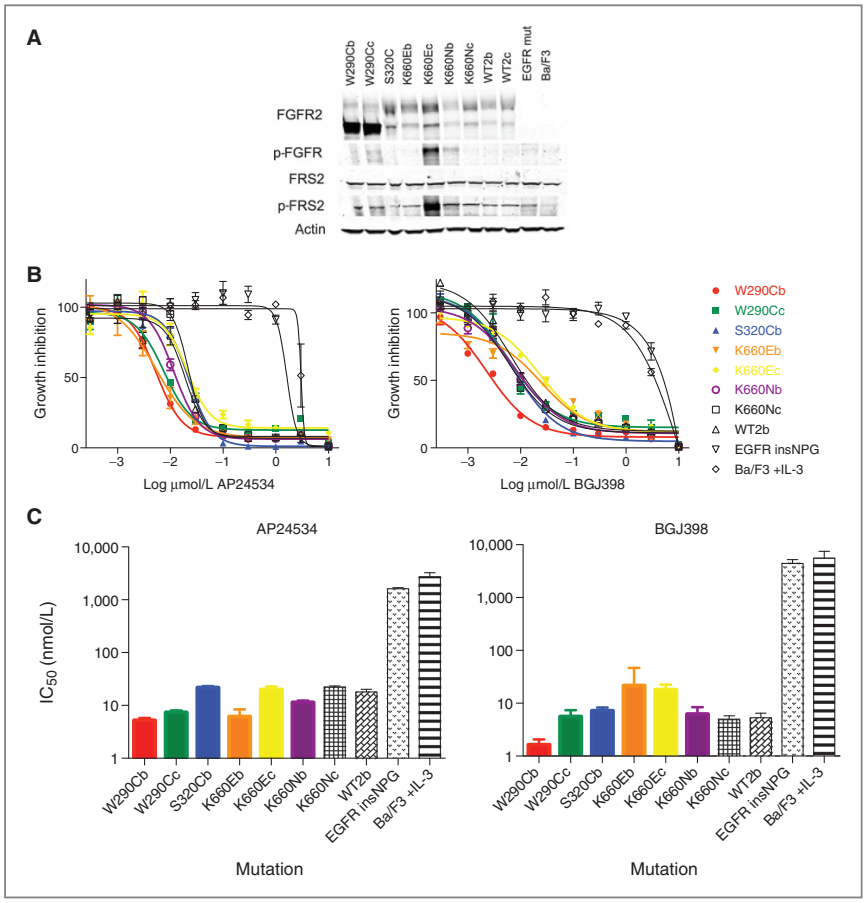

Figure 4. Ba/F3 cells dependent on FGFR signaling are sensitive to FGFR inhibitors. A, Ba/F3 cells dependent on FGFR signaling were isolated by exchanging IL-3 with FGF-7 or FGF-9 and heparin. These cells were lysed and probed for FGFR2 or FGFR3 expression, phospho-FGFR, FRS2, and phospho-FRS2 Y436. Actin was used as a loading control. B, Ba/F3 cells expressing each mutation construct were seeded into 96-well plates in the presence of increasing concentrations of ponatinib (left) or BGJ398 (right). After 4 days, proliferation was measured with CellTiter-Glo. C, IC_{50} values were calculated for each mutation. These experiments were carried out with other FGFR inhibitors; those results are documented in Supplementary Fig. S5.

visit 12 days later showed a marked reduction in tumor size (Fig. 5C, right). He continued on pazopanib for 2 months, when he presented with a right carotid hemorrhage. Pazopanib was discontinued at that time, and the patient remains alive as of March 15, 2013 under hospice care. This correlative observation does not definitively identify FGFR2 as the target of pazopanib, but we believe that this result provides compelling rationale to continue to pursue treatment of *FGFR2*-mutated tumors with anti-FGFR–targeted therapies.

Discussion

Lung SCC is a poorly characterized disease responsible for 40,000 new deaths per year in the United States. One of the most provocative findings from genomic analysis is that of

Appendix

Published OnlineFirst June 20, 2013; DOI: 10.1158/0008-5472.CAN-12-3950

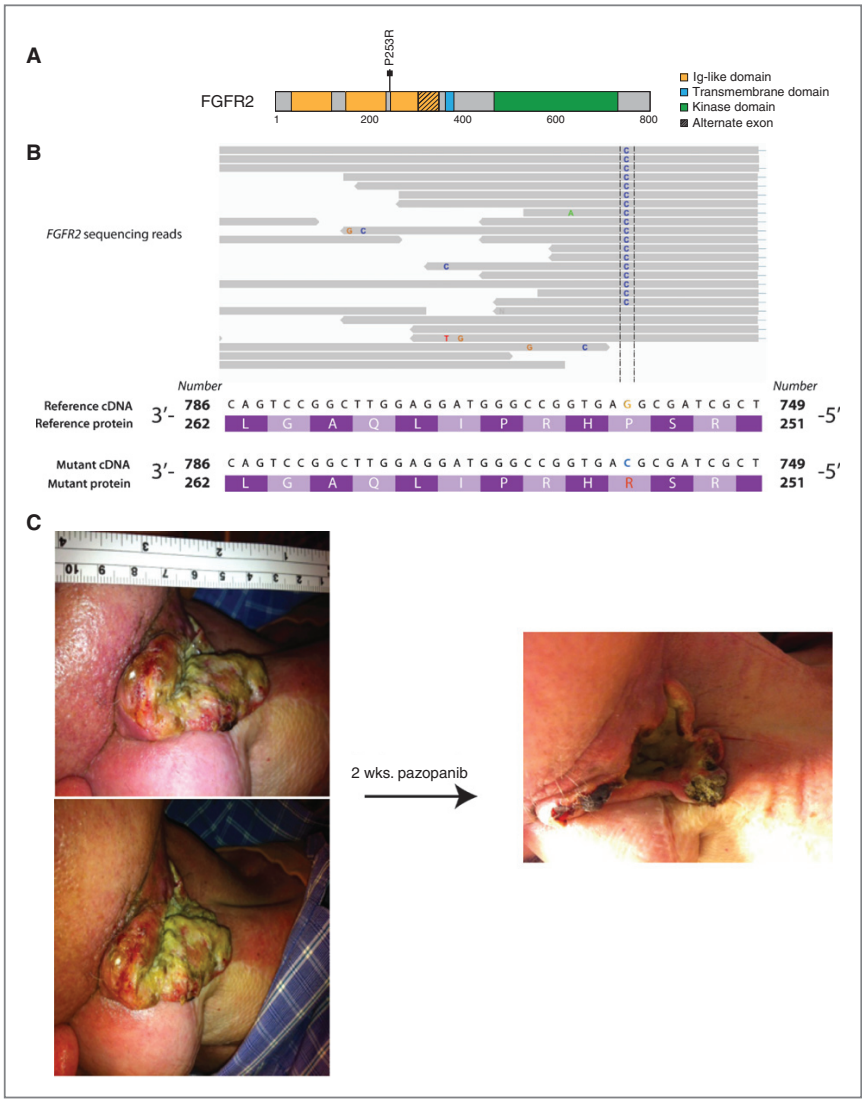

Figure 5. An oral SCC patient harboring a somatic FGFR2 P253R mutation shows a partial response to an FGFR inhibitor. A, a schematic shows the P253R mutation in the FGFR2 ECD. B, mRNA sequencing was carried out and a somatic mutation in *FGFR2* was identified, shown in the Integrative Genomics Viewer (The Broad Institute of Harvard and MIT, Cambridge, MA). C, pre- and posttreatment images from the patient.

Published OnlineFirst June 20, 2013; DOI: 10.1158/0008-5472.CAN-12-3950

recurrent *FGFR2* and *FGFR3* mutations, which are significant given that germline FGFR mutations are known to be pathogenic (17), that somatic mutations have been described in other malignancies (18), and that focal *FGFR1* amplification is known to occur in lung SCC and seems to be a therapeutic target (15, 16).

We have confirmed that a subset of observed mutations drive transformation in NIH-3T3 cells in an anchorage-independent growth assay and xenograft assays, and that this is reversible by pan-FGFR and multikinase inhibitors. Some mutations were not transforming, but given the very high somatic mutation rate in lung SCC, this observation is not surprising. We found that ECD mutations in *FGFR2* are able to form ligand-sensitive covalent receptor-dimers, as has been observed in other *FGFR2* ECD mutations (29) and in *FGFR3* mutations that have been described previously in urothelial carcinoma, and that we also observe here in the lung SCC data (30). This finding is especially relevant given that the *FGFR2* W290C mutation has been observed independently in lung SCC sequencing on two previous occasions (10, 42). It is also possible that the glycosylation deficiency that we observed in the expressed protein harboring this mutation impacts protein function, a phenomenon with precedence in this receptor family (31).

We found that the *FGFR* mutations also exhibited sensitivity to inhibition by FGFR inhibitors in the Ba/F3 system, which models dependency on oncogenic pathways. Many drugs in the panel of inhibitors that we tested are already approved for clinical use in other malignancies, and clinical trials are underway to test sensitivity to FGFR inhibitors in patients harboring *FGFR* events (NCT01004224, NCT01457846, and NCT00979134). Although we cannot infer *in vivo* sensitivity to these inhibitors from our models, we believe that this study provides a compelling rationale for extending trials of FGFR kinase inhibitors to patients with lung and oral SCC harboring *FGFR2* or *FGFR3* mutations.

This study represents one of the first functionally validated novel recurrent targets to emerge from analysis of the systematic genomic profiling of lung SCC by the TCGA Research Network. It is our expectation that these findings will continue with the publication of more genomic studies of malignancies, and that this will lead to improved treatment options for patients with this disease.

Disclosure of Potential Conflicts of Interest

M.D. Wilkerson is a consultant/advisory board member of GeneCentric. M. Meyerson has a commercial research grant from Novartis, has ownership interest (including patents) in Foundation Medicine, and is a consultant/advisory board member of Novartis and Foundation Medicine. P.S. Hammerman is a consultant/advisory board member of ARIAD. No potential conflicts of interest were disclosed by the other authors.

Authors' Contributions

Conception and design: R.G. Liao, D.N. Hayes, R.I. Haddad, M. Meyerson, P.S. Hammerman

Development of methodology: R.G. Liao, J. Jung, J. Tchaicha, D.N. Hayes, P.S. Hammerman

Acquisition of data (provided animals, acquired and managed patients, provided facilities, etc.): R.G. Liao, J. Jung, J. Tchaicha, E.M. Beauchamp, Q. Liu, D.N. Hayes, R.I. Haddad

Analysis and interpretation of data (e.g., statistical analysis, biostatistics, computational analysis): R.G. Liao, J. Jung, J. Tchaicha, M.D. Wilkerson, A. Sivachenko, Q. Liu, T.J. Pugh, C.S. Pedamallu, G. Getz, K.-K. Wong, R.I. Haddad, M. Meyerson, P.S. Hammerman

Writing, review, and/or revision of the manuscript: R.G. Liao, J. Jung, J. Tchaicha, M.D. Wilkerson, T.J. Pugh, C.S. Pedamallu, D.N. Hayes, K.-K. Wong, R.I. Haddad, M. Meyerson, P.S. Hammerman

Administrative, technical, or material support (i.e., reporting or organizing data, constructing databases): R.G. Liao, Q. Liu, T.J. Pugh, P.S. Hammerman

Study supervision: R.G. Liao, N.S. Gray, M. Meyerson, P.S. Hammerman

Acknowledgments

The authors thank Ami S. Bhatt, member of the Meyerson laboratory, Pamela M. Pollock, investigator at Queensland Institute of Technology (Brisbane, Australia), and David M. Ornitz, investigator at Washington University in St. Louis (St. Louis, MO) for helpful discussion and technical support.

Grant Support

P.S. Hammerman is a recipient of a Young Investigator Grant from the National Lung Cancer Partnership and is supported by National Cancer Institute (NCI) grants 1K08CA163677 and the Stephen D. and Alice Cutler Investigator Fund. M. Meyerson is supported by Uniting Against Lung Cancer, the Lung Cancer Research Foundation, the American Lung Association, Novartis Pharmaceuticals, and NCI grant P50CA090578. M.D. Wilkerson is supported by a Ruth L. Kirschstein National Research Service Award Individual Fellowship from the NCI (NIH F32CA142039). T.J. Pugh is supported by a Canadian Institutes of Health Research Fellowship.

The costs of publication of this article were defrayed in part by the payment of page charges. This article must therefore be hereby marked *advertisement* in accordance with 18 U.S.C. Section 1734 solely to indicate this fact.

Received October 15, 2012; revised April 16, 2013; accepted June 3, 2013; published OnlineFirst June 20, 2013.

References

1. The Cancer Genome Atlas Network. Comprehensive molecular characterization of human colon and rectal cancer. Nature 2012;487:330–7.
2. Rudin CM, Durinck S, Stawiski EW, Poirier JT, Modrusan Z, Shames DS, et al. Comprehensive genomic analysis identifies SOX2 as a frequently amplified gene in small-cell lung cancer. Nat Genet 2012;44:1111–6.
3. Peifer M, Fernandez-Cuesta L, Sos ML, George J, Seidel D, Kasper LH, et al. Integrative genome analyses identify key somatic driver mutations of small-cell lung cancer. Nat Genet 2012;44:1104–10.
4. Hammerman PS, Lawrence MS, Voet D, Jing R, Cibulskis K, Sivachenko A, et al. Comprehensive genomic characterization of squamous cell lung cancers. Nature 2012;489:519–25.
5. Govindan R, Ding L, Griffith M, Subramanian J, Dees ND, Kanchi KL, et al. Genomic landscape of non–small cell lung cancer in smokers and never-smokers. Cell 2012;150:1121–34.
6. Imielinski M, Berger AH, Hammerman PS, Hernandez B, Pugh TJ, Hodis E, et al. Mapping the hallmarks of lung adenocarcinoma with massively parallel sequencing. Cell 2012;150:1107–20.
7. Lynch TJ, Bell DW, Sordella R, Gurubhagavatula S, Okimoto RA, Brannigan BW, et al. Activating mutations in the epidermal growth factor receptor underlying responsiveness of non–small-cell lung cancer to gefitinib. N Engl J Med 2004;350:2129–39.
8. Paez JG, Janne PA, Lee JC, Tracy S, Greulich H, Gabriel S, et al. EGFR mutations in lung cancer: correlation with clinical response to gefitinib therapy. Science 2004;304:1497–500.
9. Soda M, Choi YL, Enomoto M, Takada S, Yamashita Y, Ishikawa S, et al. Identification of the transforming EML4-ALK fusion gene in non–small-cell lung cancer. Nature 2007;448:561–6.
10. Dutt A, Salvesen HB, Chen TH, Ramos AH, Onofrio RC, Hatton C, et al. Drug-sensitive FGFR2 mutations in endometrial carcinoma. Proc Natl Acad Sci U S A 2008;105:8713–7.

Appendix

Published OnlineFirst June 20, 2013; DOI: 10.1158/0008-5472.CAN-12-3950

11. Pollock PM, Gartside MG, Dejeza LC, Powell MA, Mallon MA, Davies H, et al. Frequent activating FGFR2 mutations in endometrial carcinomas parallel germline mutations associated with craniosynostosis and skeletal dysplasia syndromes. Oncogene 2007;26:7158–62.
12. Cappellen D, De Oliveira C, Ricol D, de Medina S, Bourdin J, Sastre-Garau X, et al. Frequent activating mutations of FGFR3 in human bladder and cervix carcinomas. Nat Genet 1999;23:18–20.
13. Maemondo M, Inoue A, Kobayashi K, Sugawara S, Oizumi S, Isobe H, et al. Gefitinib or chemotherapy for non–small-cell lung cancer with mutated EGFR. N Engl J Med 2010;362:2380–8.
14. Mok TS, Wu YL, Thongprasert S, Yang CH, Chu DT, Saijo N, et al. Gefitinib or carboplatin-paclitaxel in pulmonary adenocarcinoma. N Engl J Med 2009;361:947–57.
15. Weiss J, Sos ML, Seidel D, Peifer M, Zander T, Heuckmann JM, et al. Frequent and focal FGFR1 amplification associates with therapeutically tractable FGFR1 dependency in squamous cell lung cancer. Sci Transl Med 2010;2:62ra93.
16. Dutt A, Ramos AH, Hammerman PS, Mermel C, Cho J, Sharifnia T, et al. Inhibitor-sensitive FGFR1 amplification in human non–small cell lung cancer. PLoS ONE 2011;6:e20351.
17. Ornitz DM, Marie PJ. FGF signaling pathways in endochondral and intramembranous bone development and human genetic disease. Genes Dev 2002;16:1446–65.
18. Greulich H, Pollock PM. Targeting mutant fibroblast growth factor receptors in cancer. Trends Mol Med 2011;17:283–92.
19. Turner N, Grose R. Fibroblast growth factor signalling: from development to cancer. Nat Rev Cancer 2010;10:116–29.
20. Zhang X, Ibrahimi OA, Olsen SK, Umemori H, Mohammadi M, Ornitz DM. Receptor specificity of the fibroblast growth factor family. The complete mammalian FGF family. J Biol Chem 2006;281:15694–700.
21. Elbauomy Elsheikh S, Green AR, Lambros MB, Turner NC, Grainge MJ, Powe D, et al. FGFR1 amplification in breast carcinomas: a chromogenic *in situ* hybridisation analysis. Breast Cancer Res 2007;9:R23.
22. Kwabi-Addo B, Ropiquet F, Giri D, Ittmann M. Alternative splicing of fibroblast growth factor receptors in human prostate cancer. Prostate 2001;46:163–72.
23. Yan G, Fukabori Y, McBride G, Nikolaropolous S, McKeehan WL. Exon switching and activation of stromal and embryonic fibroblast growth factor (FGF)-FGF receptor genes in prostate epithelial cells accompany stromal independence and malignancy. Mol Cell Biol 1993;13:4513–22.
24. Yu K, Herr AB, Waksman G, Ornitz DM. Loss of fibroblast growth factor receptor 2 ligand-binding specificity in Apert syndrome. Proc Natl Acad Sci U S A 2000;97:14536–41.
25. Levin JZ, Berger MF, Adiconis X, Rogov P, Melnikov A, Fennell T, et al. Targeted next-generation sequencing of a cancer transcriptome enhances detection of sequence variants and novel fusion transcripts. Genome Biol 2009;10:R115.
26. DePristo MA, Banks E, Poplin R, Garimella KV, Maguire JR, Hartl C, et al. A framework for variation discovery and genotyping using next-generation DNA sequencing data. Nat Genet 2011;43:491–8.
27. Wilkerson MD, Yin X, Hoadley KA, Liu Y, Hayward MC, Cabanski CR, et al. Lung squamous cell carcinoma mRNA expression subtypes are reproducible, clinically important, and correspond to normal cell types. Clin Cancer Res 2010;16:4864–75.
28. Guagnano V, Furet P, Spanka C, Bordas V, Le Douget M, Stamm C, et al. Discovery of 3-(2,6-dichloro-3,5-dimethoxy-phenyl)-1-{6-[4-(4-ethyl-piperazin-1-yl)-phenylamino]-pyrimidin-4-yl}-1-methyl-urea (NVP-BGJ398), a potent and selective inhibitor of the fibroblast growth factor receptor family of receptor tyrosine kinase. J Med Chem 2011;54:7066–83.
29. Plotnikov AN, Hubbard SR, Schlessinger J, Mohammadi M. Crystal structures of two FGF–FGFR complexes reveal the determinants of ligand-receptor specificity. Cell 2000;101:413–24.
30. d'Avis PY, Robertson SC, Meyer AN, Bardwell WM, Webster MK, Donoghue DJ. Constitutive activation of fibroblast growth factor receptor 3 by mutations responsible for the lethal skeletal dysplasia thanatophoric dysplasia type I. Cell Growth Differ 1998;9:71–8.
31. Gartside MG, Chen H, Ibrahimi OA, Byron SA, Curtis AV, Wellens CL, et al. Loss-of-function fibroblast growth factor receptor-2 mutations in melanoma. Mol Cancer Res 2009;7:41–54.
32. O'Hare T, Shakespeare WC, Zhu X, Eide CA, Rivera VM, Wang F, et al. AP24534, a pan-BCR-ABL inhibitor for chronic myeloid leukemia, potently inhibits the T315I mutant and overcomes mutation-based resistance. Cancer Cell 2009;16:401–12.
33. Gozgit JM, Wong MJ, Moran L, Wardwell S, Mohemmad QK, Narasimhan NI, et al. Ponatinib (AP24534), a multitargeted pan-FGFR inhibitor with activity in multiple FGFR-amplified or mutated cancer models. Mol Cancer Ther 2012;11:690–9.
34. Sonpavde G, Hutson TE. Pazopanib: a novel multitargeted tyrosine kinase inhibitor. Curr Oncol Rep 2007;9:115–9.
35. Renhowe PA, Pecchi S, Shafer CM, Machajewski TD, Jazan EM, Taylor C, et al. Design, structure-activity relationships and *in vivo* characterization of 4-amino-3-benzimidazol-2-ylhydroquinolin-2-ones: a novel class of receptor tyrosine kinase inhibitors. J Med Chem 2009;52:278–92.
36. Cai Z-W, Zhang Y, Borzilleri RM, Qian L, Barbosa S, Wei D, et al. Discovery of brivanib alaninate ((S)-((R)-1-(4-(4-fluoro-2-methyl-1H-indol-5-yloxy)-5-methylpyrrolo[2,1-f][1,2,4]triazin-6-yloxy)propan-2-yl)2-aminopropanoate), a novel prodrug of dual vascular endothelial growth factor receptor-2 and fibroblast growth factor receptor-1 kinase inhibitor (BMS-540215). J Med Chem 2008;51:1976–80.
37. Gavine PR, Mooney L, Kilgour E, Thomas AP, Al-Kadhimi K, Beck S, et al. AZD4547: an orally bioavailable, potent and selective inhibitor of the fibroblast growth factor receptor tyrosine kinase family. Cancer Res 2012;72:2045–56.
38. Matsui J, Yamamoto Y, Funahashi Y, Tsuruoka A, Watanabe T, Wakabayashi T, et al. E7080, a novel inhibitor that targets multiple kinases, has potent antitumor activities against stem cell factor producing human small cell lung cancer H146, based on angiogenesis inhibition. Int J Cancer 2008;122:664–71.
39. Wedge SR, Kendrew J, Hennequin LF, Valentine PJ, Barry ST, Brave SR, et al. AZD2171: a highly potent, orally bioavailable, vascular endothelial growth factor receptor-2 tyrosine kinase inhibitor for the treatment of cancer. Cancer Res 2005;65:4389–400.
40. Stransky N, Egloff AM, Tward AD, Kostic AD, Cibulskis K, Sivachenko A, et al. The mutational landscape of head and neck squamous cell carcinoma. Science 2011;333:1157–60.
41. Agrawal N, Frederick MJ, Pickering CR, Bettegowda C, Chang K, Li RJ, et al. Exome sequencing of head and neck squamous cell carcinoma reveals inactivating mutations in NOTCH1. Science 2011;333:1154–7.
42. Davies H, Hunter C, Smith R, Stephens P, Greenman C, Bignell G, et al. Somatic mutations of the protein kinase gene family in human lung cancer. Cancer Res 2005;65:7591–5.